IMPACT OF CLIMATE CHANGE ON SOIL WATER AVAILABILITY AND MAIZE WATER NEEDS IN KESEM SUBBASIN, MIDDLE AWASH, ETHIOPIA

MSc THESIS

NEGASH TESSEMA ROBA

AUGUST 2017
HARAMAYA UNIVERSITY, HARAMAYA

Impact of Climate Change on Soil Water Availability and Maize Water Needs in Kesem Subbasin, Middle Awash, Ethiopia

A Thesis Submitted through the School of Water Resources and Environmental Engineering to the Postgraduate Programs Directorate HARAMAYA UNIVERSITY

In Partial Fulfillment of the Requirements for the Degree of

MASTER OF SCIENCE IN IRRIGATION ENGINEERING

Negash Tessema Roba

August 2017
Haramaya University, Haramaya

APPROVAL SHEET
Postgraduate Programs Directorate

We hereby certify that we have read and evaluated this Thesis titled "***Impact of Climate Change on Soil Water Availability and Maize Water Needs in Kesem Subbasin, Middle Awash, Ethiopia***" prepared under our guidance by *Negash Tessema Roba*. We recommended that it be submitted as fulfilling the thesis requirement.

Asfaw Kebede (PhD)	----------	----------
Major Advisor	Signature	Date
Shimelis Berhanu (MSc)	----------	----------
Co-Advisor	Signature	Date

As members of the Board of Examiners of the MSc Thesis Open Defense Examination, we certify that we have read and evaluated the Thesis prepared by *Negash Tessema Roba* and examined the candidate. We recommended that the Thesis be accepted as fulfilling the Thesis requirement for the degree of Master of Science in Irrigation Engineering.

----------	----------	----------
Chairman	Signature	Date
----------	----------	----------
Internal Examiner	Signature	Date
----------	----------	----------
External Examiner	Signature	Date

Final approval and acceptance of the thesis is contingent up on the submission of the final copy of the thesis to the Council of Graduate Studies (CGS) through the candidate's department or Haramaya Institute of Technology Graduate Committee (HIGC).

DEDICATION

This manuscript is dedicated to the memory of my father **Tessema Roba Haro**; he passed away without seeing my victory.

STATEMENT OF THE AUTHOR

By my signature below, I declare and affirm that this Thesis is my own work. I have followed all ethical and technical principles of scholarship in the preparation, data collection, data analysis and compilation of this Thesis. Any scholarly matter that is included in the thesis has been given recognition through citation.

This Thesis is submitted in partial fulfillment of the requirements for an MSc degree at Haramaya University. The Thesis is deposited in the Haramaya University Library and is made available to borrowers under rules of the Library. I solemnly declare that this Thesis has not been submitted to any other institution anywhere for the award of any academic degree, diploma or certificate.

Brief quotations from this Thesis may be made without special permission provided that accurate and complete acknowledgement of source is made. Requests for permission for extended quotation from or reproduction of this Thesis in whole or in part may be granted by the Dean of the Haramaya Institute of Technology when in his or her judgment the proposed use of the material is in the interest of scholarship. In all other instances, however, permissions must be obtained from the author of the Thesis.

Name: Negash Tessema Roba Signature: ----------

Date: August 18, 2017

School/Department: Water Resources and Environmental Engineering/Irrigation Engineering

BIOGRAPHICAL SKETCH

The author was born in Shirka Woreda, Arsi Zone of Oromia Regional State, Ethiopia in June 10, 1990. He began his education at Hella Abba Bilo elementary school and his secondary school at Shirka secondary school. Later he moved to Bekoji high school to complete his secondary education in June 2010. After finishing high school, he joined Adama Science and Technology University (ASTU) in October 16, 2010 and graduated with Bachelor of Science Degree in Agricultural Engineering in June 29, 2014.

Thereafter graduating from Adama Science and Technology University, he joined and served as assistance lecturer in Samara University, Ethiopia. After serving for one year, he joined Haramaya University postgraduate program to pursue his Master of Science degree in Irrigation Engineering.

ACKNOWLEDGMENTS

I take the advantage of this special occasion to express my immense gratitude to my advisors Dr. Asfaw Kebede and Mr. Shimelis Berhanu for their scientific guidance, constructive advice, encouragement, suggestions, priceless comments and friendly approach throughout my course of study. My first advisor; Dr. Asfaw taught me how to react positively to comments in research and publication and he made me free to work independently on my research activity. He was so understood person and it is not an exaggeration to say 'working with Dr. Asfaw is like working with a real and caring father'.

I would like to express my pleasure to the Samara University for giving me in country scholarship to pursue my study; and granting me the research fund through Haramaya University. My gratitude also goes to the Ministry of Water, Irrigation and Electricity, particularly for staff members under the Department of Hydrology and GIS and National Metrological Agency (NMA) for providing hydrological and metrological data for free.

It gives me great enjoyment to thanks my friends, staff and colleagues at Samara University; Dame Yadeta, Bikila Assefa, Birke Beharu, Alemu Habebe, and Essa Abiso. I also thanks to my friends at Haramaya University; Mishamo Haile, Negash Bedaso, Lemessa Muleta and Derese Abi for their sincere friendship. I have special thanks to Abiy Gebremichael (PhD candidate) at Haramaya University for his valuable shore up.

I am forever grateful to my parents and brothers; Asnake, Genene, Bereket, Meberatu and sisters; Desta, Birke and Shewaye for their support and encouraging me in all my way of the study time. Eternally, I would like to forward the leading and loving thanks to my helpful girlfriend Sifan Abebe for her never ending concern, support and encouragement.

Above all I thank the almighty GOD for his mercy and grace upon me during all my works and in all my life.

ACRONYMS AND ABBREVIATIONS

AGNPS	Agricultural Non-Point Source
AGCM	Atmospheric General Circulation Model
AOGCM	Atmosphere-Ocean General Circulation Models
Arc SWAT	The Arc GIS Integrated SWAT Hydrological Model
ARS	Agricultural Research Service
CLUE-S	Conversion on land use and its effect on small region
CMIP5	Coupled Model Inter-comparison Project Phase 5
CORDEX	Coordinated Regional Climate Downscaling Experiment
CROPWAT	Crop Water Assessment Tool
CSA	Central Statistical Agency
CWN	Crop Water Needs
DEM	Digital Elevation Model
DOY	Day of the year (1 for Jan1; and 365 for Dec 31)
ETO	Reference Evapotranspiration
ETC	Crop Evapotranspiration
FAO	Food and Agricultural Organization of the United Nations
FAR	Five Assessment Report
GCM	General Circulation Model
GIS	Geographic Information System
GPS	Geographic Positioning System
GUI	Graphical User Interface
HRU	Hydrological Response Units
IPCC	International Panel on Climate Change
ITCZ	Inter Tropical Convergence Zone
K_C	Crop coefficient
KML	Keyhole Markup Language

LULC	Land Use/ Land Cover
m.a.s.l	meters above sea level

ACRONYMS AND ABBREVIATIONS (*CONTINUED*)

MoWIE	Ministry of Water, Irrigation and Electricity
MRS	Mean Relative Sensitivity
NAPA	National Adaptation Program of Action
NAS	National Academy of Sciences
NCEP	National Centre for Environmental Prediction
NMA	National Meteorological Agency, Ethiopia
NRC	National Research Council
PET	Potential Evapotranspiration
RCA	Regional Climate for Africa
RCM	Regional Climate Model
RCP	Representative Concentration Pathways
SDSM	Statistical Downscaling Model
SNHT	Standard Normal Homogeneity Test
SRTM	Shatter Rader Topographic Mission
SWA	Soil Water Availability
SWAT	Soil and Water Assessment Tool
TAR-WGII	Third Assessment Report, Working group two on impact assessment
TGCIA	Task Group on Scenarios for Climate and Impact Assessment
UNEP	United Nations Environment Program
UNFCCC	United Nations Framework Convention on Climate Change
USDA	United States Department of Agriculture
WCRP	World Climate Research Program
WGEN	Weather Generator
WMO	World Meteorological Organization

TABLE OF CONTENTS

TABLE OF CONTENTS (*CONTINUED*)

TABLE OF CONTENTS (*CONTINUED*)

LIST OF TABLES

Table **Page**

LIST OF FIGURES

Figure

Page

LIST OF FIGURES (*CONTINUED*)

LIST OF TABLES IN THE APPENDIX

Appendix Table

Page

LIST OF FIGURES IN THE APPENDIX

Appendix Figure
Page

IMPACT OF CLIMATE CHANGE ON SOIL WATER AVAILABILITY AND MAIZE WATER NEEDS IN KESEM SUBBASIN, MIDDLE AWASH, ETHIOPIA

ABSTRACT

Nowadays the sign of climate change and its impact is revealing on different natural and synthetic systems. Accordingly, this study strives to quantify the climatic change impact of the study area, the likely change of rainfall and temperatures from the base period by near and mid future century using ensemble of CORDEX Africa RCM model output under two alternative scenarios, and the corresponding possible implications of those changes on soil water availability and crop water needs of Maize in Kesem subbasin, middle Awash, Ethiopia. Based on the result obtained from the bias corrected of future scenarios, the rainfall was projected to be increased by 2020s and 2050s for RCP4.5 and RCP8.5 scenarios. Concerning seasonal change, it was projected that Kiremt rain would likely to be increased by about 1.8% by 2020s and 20% by 2050s for RCP4.5 scenario and 6% by 2020s and 21.73% by 2050s for RCP8.5 scenario. The mean maximum temperature was predicted to be from +0.95 to 1.98^{o}C by 2020s and 2050s for RCP4.5 and +1.38 to 2.83^{o}C by 2020s and 2050s for RCP8.5 scenario respectively. Minimum temperature also predicted for the future period. Accordingly, it will be increased from 1.04 to 3.02^{o}C by 2020s and 2050s for RCP4.5 scenario. In case of RCP8.5 scenario the corresponding increase of minimum temperature would be from 0.03 to 5.13^{o}C by 2020s and 2050s. Beside climate change, land use/cover data were used as input of SWAT in baseline scenario with climate change on soil water availability and shows increasing trend in Agricultural land, bare land, settlement and decreasing in shrub and Acacia land in the sub basin. The LULC was simulated using CLUE-S model to project the land use changes under current baseline scenarios and revealed an increase in Agricultural land and decline in Acacia and shrub land. The calibrated SWAT model was used for nine years of baseline period and performed well for simulation of monthly stream flow. Statistical model performance measure, R^2 of 0.84 and E_{NS} of 0.78 for monthly calibration and R^2 of 0.78 and E_{NS} of 0.73 for monthly validation respectively, indicated well to very good performance of the model simulation. After an intensive model calibration and validation for sensitive flow parameters, comparison of monthly simulated soil water in baseline period shows increasing trend by about 3.6mm and decreasing by -0.95mm for 1984-1998 and 1999-2013 years respectively. Relative to base period, the soil water availability in the kiremt season reduced by 6.02% and 5.22% for RCP4.5 and 2.21% and 2.36% for RCP8.5 respectively for first and second fifteen years of 2020s. For reliable Maize production in terms of water demand, determination of onset, offset and LGP is crucial and assessed using INSTAT climate guide. Anchored in the bias corrected future climate scenarios, ET_O and CWN were estimated. Overall, 0.04, 1.02% for RCP4.5 of 2020s and 2050s and 21.24, 24.29% change in ET_O for RCP8.5 of 2020s and 2050s were predicted from base period. Crop water need have been predicted to increase by 8.16% and 10.39% for RCP4.5 and by 9.45% and 10.94% for RCP8.5 scenarios of 2020s and 2050s from the base

period for the same level of production. The study investigate that due to combined effect of projected variation in rainfall and temperature and then affect soil water availability there will be increment of Maize water needs in Kesem subbasin.

Key words: Climate Change, RCM, SWA, SWAT model, Awash basin, Kesem subbasin.

1. INTRODUCTION

The world has awaken to the reality that climate shows alarming signs of changing more rapidly and dramatically than at any time in recorded history (FAO, 2011). Climate change may be due to natural or external forcing, or to the persistent anthropogenic changes in the composition of the atmosphere or in land use (Chipindu, 2009). It is one of the more imperative issues that attract the attention of scientists and policy makers.

Projected twenty first century changes in temperature and precipitation patterns due to climate change may alter the availability of water leading to new challenges for agriculture in many regions throughout the world (Hunt and Watkiss, 2011). The potential impact of climate change on the ability to meet future demands for agriculture and satisfy other competing goals for surface water supplies is an issue of importance in many regions (Brekke *et al*., 2009).

Climate change will reduce water availability, hydropower potential and changing seasonality of flows in many regions. For instance, the average annual global surface air temperature have increased by about 0.6^{o}c while sea level has risen by 10-25 cm over the last hundred fifty years and these increases have been partially attributed to the accumulation of greenhouse gases in the atmosphere (IPCC, 2010). According to the fifth assessment report (AR5) of the IPCC, the global surface temperatures at the end of the twenty-first century (2090–2099) are projected to increase higher than 4°C, in the range of 1.8 to 4°C relative to 1980 – 1999 and sea-level rise for these same emission scenarios ranged from 48 to 59cm (IPCC, 2013).

The drastic change of climate and sea level rise in a short span of time impacts on many socio-economic sectors like; low-lying areas and coastal wetlands, agricultural production, water supplies, human health and terrestrial and aquatic ecosystems (Thornton *et al*., 2009; Corner *et al.,* 2012). Africa has been identified as one part of world most vulnerable to climate change impacts. The negative consequences of climate change in Africa episode as frequent floods, droughts and shift in marginal agricultural systems (Collier *et al*., 2008). Sub-Saharan Africa (SSA) is arguably the most vulnerable region to many unpleasant effects of climate

change due to a very high dependence on rain-fed agriculture (World Bank, 2015). Ethiopia is among the most vulnerable countries in SSA due to its great reliance on climate vulnerable economy (Conway and Schipper, 2011). This is due to its low level of economic development, heavy dependence on rain-fed agriculture and high population growth (Eshetu *et al.,* 2014). In the country, research on Awash basin indicated that 20% decrease in rainfall in the basin coupled with a 2°C increase in temperature would result in a 41% decrease in the annual runoff (Kinfe, 1999). Sahilu and Nigussie (2015) point out that in the rift valley of Ethiopia minimum and maximum temperature increase by 2^{o}c monthly and rainfall change shows increasing trend using CORDEX Africa RCM under both RCP4.5 and 8.5 scenarios.

In Awash basin, minimum temperatures have increased slightly faster than maximum or mean temperatures (Boko *et al.*, 2007) which can intensify water needs by crop for sustainable growth and yield. Water needs by crop are affected by climatic parameters and hence, crop water needs vary from year to year and so do water availability. Some of these climatic variables are changing due to global warming (IPCC, 2011) and on the other hand, they present great spatial and temporal variability. The latter reason has made them inadequate for indicating soil water consumption by plants, which is an essential parameter for assessing water availability. Thus, soil water content measurements are thought to be more useful in the assessment of crop water needs (Vera *et al*., 2009), even though soil properties also vary in time and space. Therefore, monitoring soil water content may be helpful to obtain more accurate soil water balance.

In the context of this research, the study inspects the impacts of climate change on soil water availability and maize water needs. In climate impact assessments, climate models, both global and regional, are the primary tools that aid in our understanding of many processes that govern the climate system (Jeremy *et al*., 2007). GCMs are the vital resource used to perform climate change experiments regionally, globally and very fine scale up to point climate pattern; but they have main drawbacks because of their course resolution. This is one source of uncertainty in GCM-based simulations of future climate (IPCC, 2011). RCM is a climate model of higher resolution than a global climate model and provide quality data at point scale (Laprise, 2008).

Therefore due to its high resolution and quality data of point scale, RCM model which archive from CORDEX Africa data base was used for this impact studies.

In line with climate model, hydrological model were used to simulate soil water availability in the sub basin. To predict reliable quantity and rate of water yield, watershed hydrological model are often used. To do this, the applicability of hydrological models has been evaluated under different condition by different researchers in different part of the world. For example Matamoros *et al*. (2005) tests SWAT and AGNPS model to evaluate their potential applicability under data scarcity and the result reveals as SWAT model with less basin sub division shows to be more accurate than AGNPS model. Similarly Borah and Bera (2003) evaluated the mathematical bases of eleven leading watershed scale hydrologic and nonpoint source models and they conclude that as SWAT model was promising model for long term continuous simulation in Agricultural watershed. Another author, Shimelis (2008) evaluated the applicability of SWAT model to examine the influence of topography, land use, soil and climatic condition on stream flow, soil erosion and sediment yield and concluded that SWAT model performed to be adequately accurate. It was also proved by Easton *et al*. (2010) as SWAT model was applicable to the entire Blue Nile country.

Thus, among all hydrological models, SWAT model was selected for this study being it was promising model for simulation predominately in Agricultural watershed. Therefore this study was assessed the extent of soil water availability by considering future Land use/cover change via CLUE-S model with the aid of SWAT model. Concomitantly, in the current world, scholars are competing to develop water balance models to estimate crop water needs in the past decade like CROPWAT window (version 4.0, 7.0 and 8.0), ARCU, WOFOST and DSSAT. CROPWAT model was used as a tool for assessing crop water needs for its simplicity and easy to use, and linked to less intense data requirements than other dynamic models. Therefore, for this research work CROPWAT 8.0 which developed by FAO, 1998 was used for its reliability, accuracy and modified based on the penman-Monteith method than version 4.0 and 7.0; for example Eid *et al.* (2006).

In Ethiopia, specifically in middle Awash Maize (Zea mays L.) is one of the major food crops, both in terms of area coverage and overall amount of production (CSA, 2011). Its production in terms of water needs will be changed in regular crop planting times, length of growing season, and shifts in suitable crop types by climate change (Jiang *et al.,* 2009). Also climate change exacerbates failure in maize productivity due to water stress (Eid *et al.,* 2006). Therefore, since it is potential food crop in the subbasin, for this study Maize crop was selected.

In Awash River basin, water resources availability is only 10 to 20% of Ethiopia water resource whereas the population in this basin is over 60% of the country's population due to diverse climate change influences on hydrological cycle and its water balance terms and livelihood activities of the farming community (MoWIE, 2013). Kesem subbasin is one of the vulnerable areas to climate change impacts in Awash River basin. In the subbasin, hydrological and cropping systems are characterized by erratic and low productivity due to unpredictable rainfall. The capacity of these systems to support local food security and water availability depends largely on the seasonal patterns of rainfall, which vary strongly between years (Belete and Semu, 2013). The variability of seasonal rainfall exacerbates natural resource degradation and natural disasters due to rainfall patterns and rain fed farming (NMA, 2012). The main problem of availability of water resources and crop production in the sub basin is uneven distribution of the rainfall, planting date, choice of variety and dates of onset/cessation for farmers to deal with the effects of climate variability and change are far-reaching.

Therefore, local perspectives can be combined with scientific climate scenarios to draw policy recommendations for future estimation strategies. Future climate change impact assessment researches conducted so far in the study area are limited. Most of it focuses on water resource availability and planning, water resource and extreme events, policy responses to climate change assessment in the entire basin (for example, Kinfe, 1999; Mosello *et al*., 2015; Tiruneh *et al*., 2013) leaving out the estimation of soil water availability and crop water needs in subbasin level. Therefore, to fill this gap, this study gives clue as the first baseline and future

climate change impact on soil water availability and maize water needs in Kesem subbasin, paid attention to climate change implication in the study area.

To know and manage future implication, planner and policy maker need an understanding of past and current climate change impact and adaptation strategies. This information in combination with projected impact of climate change is a key to prioritize measures to address and prepare for policy maker and planner for adaptation options in the study area. Thus, quantitative scientific evidence on soil water availability and Maize water needs and its future availability is vital for policy makers, farmers and planners to formulate the adaptation options in order to increase moisture content, crop yield and address food insecurity with the growing population under the changing future climate. However, such quantitative information together with various possible scenarios has not been well documented in the study area.

The analysis of current and future climate change impact on soil water availability and maize water needs will assist policy makers, donors, project managers, non-governmental organizations (NGOs) and other development practitioners to deliver right policy and programs in required areas on time. As a result, this study provides valuable data and baseline information in order to develop sustainable adaptation mechanisms and strategies to the response of the rising climate change and variability in the study area.

Thus, the study set out to throw light upon the following important questions.

- How much will the soil water availability likely change in the future and in what trend, compared to the baseline period?
- How much will the Maize water needs likely change in the future and in what trend, compared to the baseline period?

Based on the key research questions formulated, the main objective of the research is to assess the likely changes of soil water availability and Maize water needs in the middle Awash; Kesem subbasin under changing climate scenarios. Specifically, this research mainly focuses on the following specific objectives:

- To assess soil water availability under current and future climate change scenarios in the middle Awash; Kesem subbasin.

- To determine Maize water needs under changing climate scenarios in the Middle Awash; Kesem subbasin.

-

2. LITERATURE REVIEW

2.1. Overview of Climate Change

Scholars look in many places to find intimations about climate change to examine historical records, collect measurements, and observe trends in temperature and precipitation weather patterns, sea level, and other features of the environment. Because there are so many evidences from all over the world that the climate is changing from time to time, it's known that climate change is already happening today and it has been enforcing so many problems.

According to IPCC (2013) climate change can be defined as a change in the state of the climate that can be identified by their change and variability of its properties, and that persists for an extended period, typically decades or longer. It refers to any change in climate over time, whether due to natural variability or human activity (NRC, 2010). So one way of detecting such an influence is through long-term changes in mean conditions, preferably guided by climate model studies as to which variables and how they should change. This requires long averages to overcome the effects of natural variability, and for quantities such as global temperatures (Santer *et al*., 2011).

Changes in certain extremes, such as higher temperatures and increases in heavy rains and droughts are likely with climate change (IPCC, 2013; Trenberth, 2011). In the United States, extremes of high temperatures have been occurring at a rate of twice those of cold extremes (Meehl *et al*., 2009), and this has accelerated considerably since June 2010 to a factor of 2.7, and in the summer of 2011 to a factor of over 8.

Observational evidence from all continents and most oceans shows that many natural systems are being affected by regional climate changes, particularly temperature increases. As climate varies or changes because of human and other induced drivers including the chain from greenhouse gas (GHG) emissions to atmospheric concentrations, it alters precipitation amount, intensity, frequency, and type (Trenberth, 2011). Warming accelerates land-surface drying as

heat goes into evaporation of moisture and this increases the potential incidence and severity of droughts, which has been observed in many places worldwide (Dai, 2011). Scientists are repeatedly asked about increasing climate change events especially change in global surface temperature. Different climate researcher are given similar answer to this question for instance (Trenberth, 2012) gave a short answer to this question on his study 'framing the way to relate climate extremes to climate change' as; all weather events are affected by climate change because the environment in which they occur is warmer and moister than it used to be.

The general change in global climate is very fast from time to time this include the change in global temperature always shows an increasing trend over the globe and the rise in sea level due to melting ice for the past time frame (IPCC, 2013). The linear warming trend over the 50 years from 1956 to 2005 is 0.130 (0.10 to 0.16) ^{o}C per decade which is nearly twice that for the 100 years from 1906 to 2005. Rising temperatures also will cause shifts in crop growing seasons which affects food security (UNFCCC, 2007). Global average sea level rose at an average rate of 1.8 [1.3 to 2.3] mm per year over 1961 to 2003 and at an average rate of about 3.1 (2.4 to 3.8) mm per year from 1993 to 2003 (IPCC, 2007). There is very high confidence, based on more evidence from a wider range of studies, that recent warming is strongly affecting hydrology, ecosystem and water availability (Laprise, 2008).

The IPCC Fifth Assessment Report (AR5) concluded that most of the observed increase in global average temperature since the mid-20th century is very likely due to the observed increase in anthropogenic greenhouse gas concentrations. As it was very well know carbon dioxide (CO_2) is the most important anthropogenic GHG. The annual emissions have grown between 1970 and 2004 by about 80%, from 21 to 38 giga tones (Gt), and represented 77% of total anthropogenic GHG emissions in 2004. The rate of growth of CO_2-eq emissions was much higher during the recent 10-year period of 1995-2004 (0.92 $GtCO_2$-eq per year) than during the previous period of 1970-1994 (0.43 $GtCO_2$-eq per year) (IPCC, 2013).

2.2. Climate Models

2.2.1. General circulation model (GCM)

Climate models, both global and regional, are the primary tools that aid in our understanding of many processes that govern the climate system (Jeremy *et al*., 2007). Climate is one of the most challenging geophysical systems to be simulated because of the number of interacting components and the wide range of time and spatial scales of relevant processes and their complexity (Laprise, 2008). Global climate models also known as general circulation models (GCMs) are the most complex of climate models, since they attempt to represent the main components of the climate system in three dimensions.

According to IPCC (2011), GCMs are the vital resource used to perform climate change experiments regionally, globally and very fine scale up to point climate pattern from which climate change scenarios are derived; but they have main drawbacks because of their course resolution. Most of the time they lack producing of current climate trend including the most important statistical parameters like mean and variance.

GCMs depict the climate using a three dimensional grid over the globe, typically having a horizontal resolution of between 250 and 600 km, 10 to 20 vertical layers in the atmosphere and sometimes as many as 30 layers in the oceans (IPCC, 2011). Their resolution is thus quite coarse relative to the scale of exposure units in most impact assessments. Moreover; many physical processes, such as those related to clouds, also occur at smaller scales and cannot be properly modeled. Instead, their known properties must be averaged over the larger scale in a technique known as parameterization. This is one source of uncertainty in GCM-based simulations of future climate (IPCC, 2007). Nowadays, GCMs only included a representation of the atmosphere, the land surface, sometimes the ocean circulation, and a very simplified version of the sea ice. A few years ago, GCMs take more and more components into account, and many new models now also include sophisticated models of the sea ice, the carbon cycle, ice sheet dynamics and even atmospheric chemistry (IPCC, 2013).

2.2.2. Regional climate model

A regional climate model (RCM) is a climate model of higher resolution than a global climate model (GCM). It can be nested within a global model to provide more detailed simulations for a particular location. Local climate change is influenced heavily by local topographical features like mountain. Due to their coarse resolution, small-scale topographical features are not picked up by GCMs. RCMs have a higher resolution than a GCM (~ 25 km) even less and are influenced by a smaller scale of topographical features (IPCC, 2013). It is much more computationally intensive to run an RCM so they are usually run over a limited area.

Regional models have been used to conduct climate change experiments for many regions of the world. These methods of obtaining sub-grid scale estimates (commonly down to 50 km resolution or less) are able to account for important local forcing factors such as surface type and elevation, which conventional GCMs are unable to resolve (IPCC, 2013). They have the advantage of being physically based, but are also highly demanding of computer time. For this reason, until recent years there had been very few simulations for a sufficient period of simulated years to allow meaningful climate change statistics to be extracted. Furthermore, the commonest approach, nesting, is still heavily reliant on specialized GCM outputs for its boundary conditions. GCMs do not always provide good simulations of the large scale flow and there can be inconsistencies between the behavior of the physical parameterizations in the driving model and in the finer grid of the regional model (IPCC, 2007).

Any regional climate modeling approach affords an increase of resolution over a region of the globe of about one order of magnitude compared to GCMs, with regional grid-point spacing of a few tens of km in the horizontal, for operational use on climate timescales (Laprise, 2008).

2.3. Downscaling Techniques

Downscaling or regionalization is the term given to the process of deriving finer resolution data for a particular site from coarser resolution GCM or RCM data set. Although regional climate models (RCMs) are powerful tools for describing regional and even smaller scale climate

conditions, they still comprises severe systematic errors (Jakob *et al*., 2011). The projections of the estimates of GCM and RCM climate variables either for present or future period obtained directly from simulation of GCM and RCM outputs are of limited value for any study as the spatial resolution of both results are coarse in nature to resolve many sub-grid scale. This characteristics makes the outputs are always unreliable at individual grid. To solve this problem spatial downscaling methods have been proposed.

The methods used to convert GCM or RCM outputs into local meteorological variables used for hydrological modeling or any other regional climate study are referred to as downscaling techniques (Wood *et al*., 2004). Recently, there are different types of downscaling methods to provide very fine scale GCM and RCM results at point scale; for instance some of the methods are mentioned in Jakob *et al*. (2011) as linear and nonlinear empirical-statistical downscaling techniques. The other downscaling technique which is referred to as dynamical downscaling method is mainly applied to derive regional scale information from GCMs (Jakob *et al*., 2011). Particularly, small-scale patterns of daily precipitation are highly dependent on model resolution and parameterization and can often not be used directly in climate change impact assessment studies (Fowler *et al*., 2007).

Recently, the availability of regional RCM-based climate scenarios for different part of the world tremendously increased; it is possible to mention REMO. Recently this regional climate model is available for Ethiopia. However, due to the error characteristics of RCMs, it is not possible to use directly for any climate change study in the region when climate information http://uk climate projections.defra.gov.uk/24459 as visited on October 2016 at the point scale is needed. Therefore to overcome this drawback downscaling or bias correction should be employed before using the results of this RCM (Terink, 2010).

2.4. Climate Scenarios

Socio-economic and emission scenarios provide plausible descriptions of how the future may evolve with respect to a range of variables including socio-economic change, technological change, energy and land use, and emission of greenhouse gases and air pollutants (Van *et al*.,

2011). These future scenarios of forcing agents are fed in to the climate models as input, and the output of these climate models is further used in climate change analysis and hence, the assessment of impacts, adaptation and mitigation. Several sets of scenarios including the IS92 scenarios (Legegett *et al*., 1992), the scenarios from the Special Report on Emission Scenarios (SRES) (Nakicenovic and Swart, 2000) and, more recently, the Representative Concentration Pathways (RCP) (Van *et al*., 2011) are used in climate research. In the subsequent section, a brief description of the various scenarios is presented.

SA90 scenarios

According IPCC (1990) to there are four SA90 scenarios (A to D) constructed in a backward procedure based on envisaged CO_2-equivalent concentrations. Three of the scenarios assume doubling of CO_2- equivalent concentration by 2030, 2060 and 2090. The fourth scenario assumes stabilization of CO_2-equivalent concentration at a level well below a doubling of pre-industrial atmospheric CO_2 (IPCC, 1990). The economic growth and population assumptions were taken as equal for all scenarios, while the levels of technological development and environmental controls were varied (IPCC, 1990). The first assessment report (FAR) of IPCC was undertaken based on SA90 scenarios (Girod *et al*., 2009).

IS92 scenarios In contrast to the SA90 scenarios, a forward procedure is applied by calculating future emissions on the basis of the key input assumptions. There are six alternative IS92 scenarios (IS92a to f) that have been widely used prior to SRES scenarios. They embodied a wide array of assumptions affecting how future greenhouse gas emissions might evolve in the absence of climate policies. They were used in the second assessment report (SAR) of IPCC (Girod *et al*., 2009).

SRES – Emission scenarios

The greenhouse gas emissions scenarios described in the IPCC's Special Report on Emission Scenarios published in 2000, have been used to make projections of possible future change and

therefore, given the name SRES scenarios (IPCC, 2007). IPCC Third Assessment Report (TAR) and Fourth Assessment Report (AR4), published in 2001 and 2007 respectively, were based on these SRES scenarios.

The fundamental motive behind SRES scenarios was to improve upon the earlier IS92 scenarios used in earlier IPCC Second Assessment Report in 1995. SRES scenarios cover a wide range of the main driving forces of future emissions, from demographic to technological and economic developments. The scenarios encompass different future developments that might influence greenhouse gas (GHG) sources and sinks. There are total of four SRES scenarios with each one associated to a particular family. Therefore, scenario families may be thought of containing individual scenarios with common themes. Following is the brief description of each family.

A1: This scenario family describes a homogeneous future world with rapid economic growth. It assumes the global population to peak in mid-century and declines thereafter. Further major underlying themes are convergent world, capacity building, increased cultural and social interaction and a substantial reduction in regional differences in per capita income.

A2: These A2 scenarios are of a more heterogeneous world. Major underlying themes are independently operating self-reliant nations; continuously increasing population and regionally oriented economic development with per capita economic growth and technological change are more fragmented and slower.

B1: This B1 family describe a future world similar to A1, but with rapid changes in economic structures toward a service and information economy, with reduction in material intensity, and the introduction of clean and resource-efficient technologies. The emphasis is on the global solutions to economic, social and environmental stability.

B2: This scenario family describes the more divided future world, but with more ecologically friendly approach. This family is characterized by a continuously increasing population, but at a slower rate than in A2. Other major underlying themes are emphasis on local solutions to

economic, social and environmental stability; intermediate levels of economic development; less rapid and more fragmented technological change than in A1 and B1.

RCP–Emission scenarios

Among the research community, recently there has been an increasing interest in scenarios that explicitly explore the impact of different climate-policies in addition to the no climate policy scenarios such as SRES (Moss *et al.*, 2010). Therefore a set of new scenarios is constructed containing emission, concentration and land-use trajectories referred to as "Representative Concentration Pathways" (RCPs). In its name, the word "representative" signifies that each of the RCPs represents a larger set of scenarios in the literature. This implies that this set of RCPs should be compatible with the full range of emission scenarios (with and without climate policy) available in the current scientific literature.

The word "concentration pathway" emphasizes that RCPs are not the final new, fully integrated scenarios, but instead are internally consistent sets of projections of the components of radiative forcing that are used for the input to climate models. The word "concentration" also emphasizes that instead of emissions, concentrations are used as the primary product of the RCPs, designed as input to climate models. Four RCPs scenarios named according to radiative forcing target level for 2100 are used.

RCP2.6: This scenario has also been referred to as RCP3PD representing the radiative forcing trajectory which goes to a peak level of 3 W/m^2 (~490 ppm CO_2 eq) before 2100, followed by a decline (PD = Peak-Decline). The selected pathway declines to 2.6 W/m^2 by 2100 (Van *et al.*, 2011). It aims at limiting the increase of global mean temperature to 2°C above the pre industrial period.

RCP4.5: This scenario describe the stabilization without overshoot pathway to 4.5 W/m^2 (~650 ppm CO_2 eq) at stabilization after 2100 (Clarke *et al.*, 2007). RCP4.5 corresponds to that category scenarios in AR4 which contains the far majority of the scenarios assessed.

RCP6: This scenario is also similar to RCP4.5, with stabilization without overshoot pathway to 6 W/m^2 (~850 ppm CO_2 eq) at stabilization after 2100 (Fujino *et al*., 2006). The number of mitigation scenarios leading to 6 W/m^2 in the literature is relatively low however, at the same time many baseline scenarios (no climate policy) correspond to this forcing level.

RCP8.5: This scenario corresponds to the rising radiative forcing pathway leading to 8.5 W/m^2 (~1370 ppm CO_2 eq) by 2100 (Riahi *et al*., 2007). It corresponds to a scenario with no-climate policy baseline and comparatively high greenhouse gas emissions.

2.4. Bias Correction Methods

Regional Climate Models (RCMs) are an important source of climate input for climate impact studies. Nowadays, scholars are aware of the uncertainty involved in modeling, and the necessity to quantifying the model output reliability (Terink, 2010). Christensen *et al*. (2008) state that one inherent source of uncertainty comes from the RCM's inability to simulate present day climate conditions accurately. Therefore it is of major importance that RCM output is validated with historical observations. Biases in climate model simulations are commonly detected by validation with observations where the observations were considered to be "true" and unbiased (Ménard, 2010). Applying a bias correction to the RCM data often seems necessary to match the RCM data with the observations (Shabalova *et al*., 2003; Kleinn *et al*., 2005; Leander and Buishand, 2007). Sahilu and Nigussie, (2015) confirmed that bias correction satisfactorily compensate any tendency to overestimate or underestimate the mean of downscaled variables.

In various researches different bias correction methods have been applied to validate the projected climate variable to make a better comparison with the observed data. The delta change approach and the linear transformation are the two most common transfer methods and have been widely used (Middelkoop *et al*., 2001; Graham *et al*., 2007; Sahilu and Nigussie, 2015), because they are straightforward and easy to implement due to their simplicity. Often, outputs of regional climate models cannot be directly used for impact assessment as the

computed variables may differ systematically from the observed ones. Bias correction is therefore applied to compensate for any tendency to overestimate or underestimate the mean of downscaled variables.

2.5. Climate Change Projections

Due to the inherent uncertainty of the climate system and the inevitable existence of model errors, multi-model ensemble is the recommended approach for climate change projections (Nikulin *et al.,* 2012). IPCC has used several models in its coupled model inter-comparison projects (CMIP3, CMIP5) to make the various projections. There are also regional model inter-comparison projects, like the Coordinated Regional Climate Downscaling Experiment (CORDEX). CORDEX project (http://wcrp cordex.ipsl.jussieu.fr/) is an initiative of the World Climate Research Program (WCRP) performed with the intention of producing an ensemble of high resolution climate change projections by dynamically downscaling GCM simulations from Coupled Model Inter-comparison Project Phase 5 (CMIP5) data archive (Jones *et al.*, 2011).

The major aims of the CORDEX initiative are to provide a quality controlled dataset of downscaled information, coordinated model evaluation framework, and an interface to the applicants of the climate simulations for further climate change impact, adaptation, and mitigation studies (Giorgi *et al.*, 2009). Recent analyses in relation to CORDEX simulations over Africa can be found in(Nikulin *et al.,* 2012; Hernández *et al.,* 2013; Jacob *et al.*, 2012). Nikulin *et al.* (2012) evaluate the ability of ten RCMs over Africa and conclude that all RCMs simulate the seasonal mean and annual cycle quite accurately. Likewise, it is verified that the mean of multi-model outputs do better than individual simulation. Hernández *et al.* (2013) strengthen the achievement of Nikulin *et al.* (2012). They successfully reproduce the overall features of geographical and seasonal distribution over most Africa. In their report, CORDEX simulations succeed in reproducing the average distribution of precipitation and its large geographical differences.

The fifth assessment report of IPCC provided global and regional climate projections for the new RCP scenarios under CMPI5. Limited validation studies indicated good agreement with observations (Chaturvedi *et al.*, 2012).

2.6. Climate Projections for the Study Area

Several climate modeling exercises have been conducted in Ethiopia, particularly for the Awash Basin (Kim and Kaluarachchi, 2009). Most of the studies consistently predict increase in temperature. But the projections for precipitation are inconsistent in which increase or decrease in rainfall amount has been predicted by different models. This is due to inherent uncertainty of climate models and processes. This implies the need to use climate models and scenarios that capture a full spread of model predictions.

The dynamically downscaled regional climate multi-model outputs of CORDEX-Africa for RCP scenarios (RCP4.5 and RCP8.5) were used. RCP8.5 scenario gives predictions that correspond to the business-as-usual development pathways. The RCP4.5 represents the middle situation. Limited studies indicate the adequacy of CORDEX RCMs in simulating rainfall in eastern Africa (Endris *et al*., 2013).

2.7. The Predictable Impacts from Climate Change

The increasing awareness that enhanced levels of greenhouse gases of direct/natural or indirect anthropogenic origin in earth‘s atmosphere might change the climate of different regions of the world, in the long run, has recently prompted a great deal of research into the projection of regional responses to global climate change (NRC, 2010). Various general circulation model (GCM) experiments and studies indicate that a substantial rise in global temperature would be expected as a consequence of a doubling of carbon dioxide (CO_2) concentrations. As a result, climatic processes are likely to intensify, including the severity of hydrological events such as; droughts, flood waves, and heat waves (You *et al*., 2010). These projected effects of possible future climate change would significantly affect many hydrologic systems, which in turn affect the water availability and runoff and the flow in rivers.

2.7.1. Effects on Agriculture

Study on mapping poverty and vulnerability in Africa identified Ethiopia as one of the country's most vulnerable to climate change (Thornton *et al*., 2006). According to You *et al*. (2010), climate change is expected to intensify the already high hydrological variability and frequency of extreme events in Ethiopia which impair agricultural productivity and may lock subsistence farmers into poverty traps.

Some studies assessed impacts of climate change on Ethiopian economy. For example Dercon (2004) suggested that rainfall shocks would not just strongly affects food consumption in the current period, but its impact linger on for many years. Deressa and Hassan (2009) confirmed that there would be a reduction in crop net revenue per hectare by the years 2050 and 2100. Moreover, the reduction in net revenue per hectare by the year 2100 would be more than the reduction by the year 2050 indicating the damage that climate change would pose. Mideksa (2010) also point out the impact of climate change in the economic development of Ethiopia in two ways: first, by reducing agricultural production and output in the sectors linked to the agricultural sector, which is likely to reduce Ethiopia's GDP by about 10% from its benchmark level; and second, by raising the degree of income inequality in which the Gini coefficient increases by 20%, which is likely to further decrease economic growth and full poverty.

2.8. Climate Change Studies in Ethiopia

According to UNDP climate change study (date of visit 2017) which has been conducted in university of Oxford for the entire Ethiopia have pointed out that, the recent climate trend showed that mean annual temperature has increased by 1.3°C between 1960 and 2006, an average rate of 0.28°C per decade. The increase in temperature in Ethiopia has been most rapid in July, August and September (JAS) at a rate of 0.32°C per decade. Daily temperature observations show significantly increasing trends in the frequency of hot days, and much large increasing trends in the frequency of hot nights (temperature exceeded on 10% of days or nights in current climate of that region and season). The frequency of cold seven days has decreased significantly in all seasons except December, January and February (DJF). The

frequency of cold nights (temperature below which 10% of days or nights are recorded in current climate of that region or season) has decreased more rapidly and significantly in all seasons.

Regarding to the precipitation trend for current time there is not a statistically significant trend in observed mean rainfall in any season in Ethiopia between 1960 and 2006. Decreases in JAS rainfall observed in the 1980s have shown recovery in the 1990s and 2000s. In addition to current climate change trend UNDP climate change study investigated the change in climate for future case; this study investigated GCM projections of future climate in Ethiopia. According to the result, the mean annual temperature is projected to increase by 1.1 to 3.1°C by the 2060s, and 1.5 to 5.1°C by the 2090s. Under a single emissions scenario, the projected changes from different models span a range of up to 2.1°C. Moreover, a small increase in annual precipitation is expected over the country (NMA, 2012).

Research on Awash River Basin indicated that the basin would be significantly affected by the changed climate; that is, a considerable water deficit is projected for the future by employing GCM models. All the models suggested that global warming would result in a general increase in dryness, which would decrease water availability. Moreover, a 20% decrease in rainfall in the basin coupled with a 2°C increase in temperature would result in a 41% decrease in the annual runoff. Even a temperature increase of 2°C without precipitation change would result in a 9% decrease in annual runoff. On the other hand, an increase of precipitation by 10% would offset a 2 to 4°C increase in temperature and result in a surplus of runoff ranging from 4 to 12% (Belete and Semu, 2013).

In general warming in the Awash River basin simulated by various models would result in substantial decrease in annual runoff over the basin (Kinfe, 1999). With annual warming temperature in Ethiopia in 2020s will be 1.2^{O}C with a range of 0.7–2.3^{O}C and in 2050s it will be 2.2^{O}C, with a range of 1.4–2.9^{O}C. The regional differences in warming are relatively modest. Warming will be associated with greater frequency of heat wave events and is likely to lead to higher rates of evaporation. Moreover their study justified that climate models show

different projections of annual rainfall over Ethiopia, with some models projecting more rain, others less, but with a tendency for slightly wetter conditions. There are very small changes in multi model average annual rainfall for the 2020s (+0.4%) and 2050s (+1%). Climate change impact on water resource of Lake Tana sub-basin was assessed on the basis of CCCM and GFCD3 UK89 climate change prediction. The CCCM and GFCD3 GCMs predict a reduction of annual runoff by 18.2% and 12.6% respectively, while UKMo GCM predicts wetter condition and as result of an increase in 2.5% in annual runoff (Tarekegn and Tadege, 2006).

2.9. The CLUE-S Model for Land Use/cover Analaysis

The CLUE-S model was developed by Dutch scholars for the spatial simulation of LULC change on a small and medium-sized scale (Verburg *et al*., 1999). It was primarily used to explore the relationship between change and related natural and socio-economic factors using a quantitative method, which was then used LULC to simulate the LULC change process and to analyze the basic rule of the spatial-temporal evolution of land use (Hu *et al*.,2013). The model dynamically allocates land use changes to simulate the future land use change based on a combination of empirical analysis of location suitability and spatial analyses (Verburg *et al*., 1999; Zheng *et al*., 2012). Compared with other empirical models, it simulates multiple land use types simultaneously. The CLUE-S model incorporates the natural factors and social-economic factors spatial and non-spatial distribution by combining a top-down with a bottom-up method so the model is more comprehensive, open and extensive (Verburg *et al*., 2008). The CLUE-S model is preferred for addressing the spatial allocation of LULC change (Verburg *et al*., 2008).

Under certain possible future scenarios assumptions, linking the land use changes with relevant driving factors, the model decreases land use allocation uncertainty for spatial explicit and multi scale simulation of land use change (Dams *et al*., 2008; Ganasri *et al*., 2013; Han *et al*., 2015; Shimelis *et al*., 2016). It comprises two distinct modules, a non-spatial demand module, which calculates the total area of all land use types at each time step; and a spatially explicit allocation module (Verburg *et al*., 2008).

The basis of the spatially explicit allocation module is a statistical model describing the suitability of locations for each land use type under consideration, which is assumed to be a function of spatially explicit driving factors. Some land use covers are very unlikely to be converted to specific types of land use types but some land use changes are impossible. For example, forest plantation and settlement areas cannot be converted into water bodies. Most land use changes follow a certain cycle. The conversion matrix can be used to specify the possible and not possible land use conversion. The conversion matrix indicates to what other land use types the present land use type can be possibly be converted or not during the next time step. For example, forest can directly be converted to either agricultural or grass land while it is not possible to get a direct conversion of the reverse. Therefore for each land use type, a value needs to be specified that represents the relative elasticity to change, 0 for conversion is not possible and 1 for conversion is possible. A more detailed description of the model is given in (Verburg *et al*., 2002).

where P_i is the probability of the occurrence of a specific land use type, X_i is the driving factors, and β_n is the regression coefficients.

2.10. Land Use/Cover Changes in Ethiopia

For different parts of Ethiopia, land use/cover changes were studied from small scale to large scale, Abate (1994) (west Ethiopia); Zeleke and Hurni (2001) (north-western Ethiopia); Hadgu (2008); Belay (2002) (north Ethiopia); Kassa (2003) (north-eastern Ethiopia); and Mengistu (2009) (southern Ethiopia). All these studies show that agricultural land has expanded at the expense of natural vegetation, including forests, grazing land and shrub lands. In many parts of the highlands of Ethiopia, agriculture has gradually expanded from gently sloping land into the steeper slopes of the neighboring mountains (Mengistu, 2009). On the other hand Zeleke and Hurni (2001) point out an increase of woodland area in recent years due to afforestation efforts in the Blue Nile basin.

Impacts of land use/cover changes on surface hydrology, surface energy balance and surface roughness are not straightforward but rather complex to warrant any generalization as it is dependent on the scale of the watershed, seasons, climate, and soil conditions (Lambin *et al*., 2006). Subsequently, many insights into consequences of land use and land cover change on hydrology and surface energy balances have been elucidated at small spatial, observable scales (Kiersch, 2001; DeFries and Eshleman, 2004; Lambin *et al*., 2006). The impact of population growth on the environment is not one directional. Basically, the complex relationship between human development and the environment is what causes land degradation, in which the use and management of the natural resources is a central issue.

2.11. Hydrologic Modeling

Hydrological model is a simplified representation of hydrological processes a real-world system, and consists of a set of simultaneous equations or a logical set of operations contained within a computer program (Githui, 2009). Models have parameters, which are numerical measures of a property or characteristics that are constant under specified conditions. There are different types of models, with different levels of complexity, but all are a simplification of reality and aim to either make a prediction or improve our understanding of biophysical processes (Githui, 2009).

The detailed processes that link the rainfall over the catchment with the stream flow may be studied by applying physical laws. However, the complexity of the boundary conditions brings the laws of physics impracticable (Fekadu, 1999). For these reasons, instead of exact representation of the processes effort is directed to the construction of a hydrological model. It is related to the spatial processes of the hydrologic cycle and is often used to estimate basin water resources as well as for impact assessment (Githui, 2009). Many years back, different models are used to determine the performance of watersheds under inevitable land use changes, climate change, and effects of increased climate variability on hydrological process with minor modification and direct application (Legesse *et al*., 2003; Githui, 2009; Mengistu, 2009). According to the authors, this is done by establishing baseline data of climate, land cover and

stream flow, and then used to compare the effect on stream flow due to changes in precipitation, temperature and other climate variables.

Based on the hydrological process description, hydrological models can be either lumped (conceptual) or spatially distributed. In a conceptual model the internal descriptions of the various sub processes are modeled attempting to represent. It is partitioned into components that are routed through the sub processes either to the catchments outlet as stream flow or to the surface and deep storages or to the atmosphere as evapotranspiration (Price, 2001). Conceptual approaches were recognized to be able to improve the description of the hydrological response of a basin (Refsgaard, 1996). The lumped models are especially well suited for the simulation of the rainfall-runoff process when hydrological time series exist that are sufficiently long for a model calibration (Refsgaard, 1996).

Contrary to lumped models, a distributed physical-based model does not consider water flows in an area to take place between a few storage units. Instead, the flows of water and energy are directly calculated from the governing continuum equation and partial differential equations. Today, several general-purpose catchment models of this type exist, including the soil and water assessment tool (SWAT) which combines the lumped and distributed model and also called semi-distributed model (Arnold and Allan, 1998). Data driven models require extract information from data and define the relationship between system state variables without understanding the physical situations (Jembere, 2004).

2.11.1. Soil and Water Assessment Tools (SWAT)

The Soil and Water Assessment Tool (SWAT) was developed at United States Department of Agricultural Research Service in a modeling experience that span roughly 47 years (Arnold *et al*., 2012). No matter what type of problem studied with SWAT, water balance is the driving force behind everything that happens in the watershed. To accurately predict the movement of pesticide, sediments or nutrients, the hydrologic cycle as simulated by the model must conform to what is happening in the watershed. Simulation of the hydrology of a watershed can be separated into two major divisions (Neitsch *et al*., 2009). The first division is the land phase of the hydrologic cycle which controls the amount of water, sediment, nutrient and pesticides

loading to the main channel in each sub basin. The second division is the water or routing phase of the hydrologic cycle which can be defined as the movement of water, sediment etc. through the channel network of the watershed to the outlet (Neitsch *et al*., 2009).

a) The Land Phase of the Hydrologic Cycle: The hydrologic cycle simulated by SWAT is based on the water balance equation as follows.

(2)

where S_{Wt} is the final soil water content (mm), S_{Wo} is the initial soil water content in day i (mm), t is the time (days), R_{day} is the amount of precipitation in day i (mm water), Q_{surf} is the amount of surface runoff in day i (mm water), E_a is the amount of evapotranspiration in day i (mm), W_{seep} is the amount of water entering the vadose zone from the soil profile in day i (mm water), and Q_{gw} is the amount of return flow in day i (mm water)

The subdivision of the watershed enables the model to reflect differences in evapotranspiration for various crops and soils. Runoff is predicted separately for each HRU and routed to obtain the total runoff for the watershed. This increases accuracy and gives a much better physical description of the water balance (Neitsch *et al*., 2009).

Surface runoff occurs whenever the rate of precipitation exceeds the rate of infiltration. When water is initially applied to a dry soil, the infiltration rate is usually very high. However, it will decrease as the soil becomes wetter. When the application rate is higher than the infiltration rate, surface depressions begin to fill. If the application rate continues to be higher than the infiltration rate once all surface depressions have filled, surface runoff will commence.

SWAT provides two methods for estimating surface runoff: the SCS curve number procedure and the Green & Ampt infiltration method (1911). Using daily or sub daily rainfall, SWAT simulates surface runoff volumes and peak runoff rates for each HRU (Ephrem, 2011).
The SCS curve number equation is.

Q_{surf} (3)

where; Q_{surf} the accumulated runoff or rainfall excess (mm water), R_{day} = is the rainfall depth for the day (mm water), I_a is the initial abstractions which includes surface storage, interception and infiltration prior to runoff (mm water), S is the retention parameter (mm). The retention parameter varies spatially due to changes in soils, land use, management and slope and temporally due to changes in soil water content. The retention parameter is defined as:

(4)

where: C_N is the curve number for the day. The initial abstraction, I_a is commonly approximated as 0.2S and Eq. (3) become

(5)

Runoff will only occur when $R_{day} > I_a$.

The SCS curve number is a function of the soil's permeability, land use and antecedent soil water conditions. SCS defines three antecedent moisture conditions: I – dry (wilting point), II – average moisture, and III – wet (field capacity). The moisture condition I curve number is the lowest value that the daily curve number can assume in dry conditions. The curve numbers for moisture conditions II and III are calculated using equations 6 and 7.

(6)

$$CN_3 = CN_2 \exp [0.00673 (100 - CN_2)] \quad (7)$$

In which CN_1 is the moisture condition 1 curve number, CN_2 is the moisture condition 2 curve numbers, and CN_3 is the moisture condition 3 curve numbers. Typical curve numbers for moisture condition 2 are listed in various tables (Neitsch *et al*., 2005) which are appropriate to slope less than 5%. To adjust for areas with slopes greater than 5% the curve number for higher slopes an equation developed by (Williams, 1995) will be used equation 8:

$$CN_2 = (CN_3 - CN_2)/3 [1 - 2 \exp (-13.86 \cdot slp)] + CN_2 \quad (8)$$

In which CN_2 is the moisture condition 2 curve number adjusted for slope, CN_3 is the moisture condition 3 curve numbers for the default 5% slope, CN_2 is the moisture condition 2 curve

numbers for the default 5% slope, and slp is the average percent slope of the sub-basin.

Sensitivity Analyses, Calibration and Validation of SWAT Model

The ability of a watershed model to sufficiently predict water quantity and quality for a specific application is evaluated through sensitivity analysis, model calibration and validation

Sensitivity analyses

Sensitivity analysis evaluates how different parameters influence a predicted output. Parameters identified in sensitivity analysis that influence predicted outputs are often used to calibrate a model (White and Chaubey, 2005, Van Griensven *et al*., 2005). A two-step sensitivity analysis approach is described by Francos *et al*. (2003), which consists of: (1) a "Morris" screening procedure that is based on the one factor at a time (OAT) design, and (2) the use of a Fourier amplitude sensitivity test (FAST) method and recommends OAT. The most common sensitivity analysis method in the Arc SWAT interface combines the Latin Hypercube (LH), One factor-At-a-Time (OAT) sampling and global sensitivity. Global sensitivity analysis performs the sensitivity of parameter while the value of other related parameters are also changing. Its analysis's uses t-test and p-values to determine the sensitivity of each parameter. The t-test provides a measures of sensitivity (larger in absolute values are more sensitive) and the p-values determine the significance of the sensitivity. A p-value close to zero has more significance. This type of sensitivity can be performed after iteration. The main problem related to global sensitivity analysis is that it needs large number of simulations (Abbaspour *et al*., 2007).

Calibration approach

Calibration is the process whereby model parameters are adjusted to make the model output match with observed data. There are three calibration approaches widely used by the scientific community which includes manual calibration, automatic calibration and a combination of the two. Coffey *et al*. (2004) and Spruill *et al*. (2000) presented nearly 20 different statistical tests that can be used for evaluating SWAT process. They recommended Nash-Sutcliffe (E_{NS}) and

regression coefficients (r^2) for analyzing monthly output, based on comparisons of SWAT input and output. Spruill *et al*. (2000) outlined the strategy of imposing the constraints on the parameters to limit the number of interdependently calibrated values of SWAT. Automatic calibration involves the use of a search algorithm to determine best-fit parameters. It is desirable as it is less subjective and due to extensive search of parameter possibilities can give results better than if done manually.

Validation

In order to utilize any predictive watershed model for estimating the effectiveness of future potential management practices the model must be first calibrated to measured data and should then be tested (without further parameter adjustment) against an independent set of measured data. This testing of a model on an independent data set is commonly referred to as model validation. Model calibration determines the best or at least a reasonable, parameter set while validation ensures that the calibrated parameters set performs reasonably well under an independent data set. Provided the model predictive capability is demonstrated as being reasonable in the calibration and validation phase, the model can be used with some confidence for future predictions under somewhat different management scenarios (Spruill *et al*., 2000).

Weather Generator

Lack of full and realistic long period climatic data is the problem of developing countries (Danuso, 2002). Weather generators solve this problem by generating data having the same statistical properties as the observed ones. SWAT requires daily values of weather variable SWAT use WXGEN weather generator model to generate climatic data or to fill in gaps in measured records. The occurrence of rain on a given day has a major impact on relative humidity, temperature and solar radiation for the day. The weather generator first independently generates precipitation for the day. Once the total amount of rainfall for the day is generated, the distribution of rainfall within the day is computed if the Green and Ampt

method is used for infiltration. Maximum temperature, minimum temperature, solar radiation and relative humidity are then generated based on the presence or absence of rain for the day. Finally, wind speed is generated independently (Neitsch *et al*., 2005).

2.11.1.1. Application of SWAT model in hydrological study

The application of SWAT in predicting stream flow; output data performed well to measured data for a variety of watersheds (Saleh *et al*., 2000; Santhi *et al*., 2001; Van Griensven, 2005). Intention of the application was to predict various impacts of land management on water quantity and environment at both, large and small scale basins, to estimate base flow and groundwater flow. For example Matamoros *et al*. (2005) tests SWAT and AGNPS model to evaluate their potential applicability under data scarcity and the result reveals as SWAT model with less basin sub division shows to be more accurate than AGNPS model. Similarly Borah and Bera (2003) evaluated the mathematical bases of eleven leading watershed scale hydrologic and nonpoint source models and they conclude that as SWAT model was promising model for long term continuous simulation in Agricultural watershed. Another author, Shimelis (2008) evaluated the applicability of SWAT model to examine the influence of topography, land use, soil and climatic condition on stream flow, soil erosion and sediment yield and concluded that SWAT model performed to be adequately accurate. It was also proved by Easton *et al*. (2010) as SWAT model was applicable to the entire Blue Nile country.

Also it was tested to predict potential climate change impacts on water resource (Ganasri, 2013) and to evaluate effects of land use changes on the annual water balance and temporal runoff dynamics and proved as it performs well. Mahtsente *et al*. (2016) evaluate the applicability of SWAT and CROPWAT model on runoff estimation and water demand analysis for Holetta River, Awash sub basin, Ethiopia and the result reveal as the models perform well for simulation of the hydrology of the watershed.

2.12. Soil Water Availability

Soil water availability is a key state variable that controls hydrological process at various spatial scales below the surface. The spatial distribution of soil water has been studied in both ground-based and remote sensing measurements. Wendroth *et al*. (1999) studied the spatiotemporal patterns and covariance structures of soil water status, and revealed that plot spatial patterns of soil water status were persistent in time. Ridolfi *et al*. (2003) investigated the soil moisture dynamics along a hill slope and showed that the stochastic dynamics are the result of complex and nonlocal interactions between climate, soil, vegetation, and hill slope shape. Soil in the valley bottom rapidly becomes saturated during a storm (Andrew, 1995), sometimes expanding the saturated valley bottom area and rainfall on the saturated area results in saturation overland flow (Franken *et al*., 1999). Identification of patterns of soil moisture response to rainfall and especially the vertical dynamics of soil moisture at the hill slope or plot scale can be useful for the investigation of runoff generation processes in a previously ungauged or data scarce catchment (Blume *et al*., 2007).

In reverence of water holding capacity, clay soil is assumed to be at field capacity of 100 mm on the last day of rain that is greater than 0.5 PET provided that the date is not proceeded by a dry spell (less than 1mm daily rainfall) or more than five days (Stern *et al*., 2003). It is assumed that the depletion of available soil moisture below 40% of its field capacity will cause rapid reduction in water availability to crops. In the more sub humid areas, the seasonal distribution of rainfall is an important determining factor for crop growth, which in turn depends on the depth, organic matter content, structure, and texture of the soil, particularly the clay content, time of planting and crop-growth duration need to be closely fitted to the expected moisture supply for the rainy season (Andrew, 1995). Therefore inter-seasonal to seasonal rainfall prediction is an important source of information to determine soil water holding capacity and soil water management in rain-fed farming system and better crop production planning strategies.

2.13. Maize Water Needs Analysis

2.13.1. Onset date, offset date of rainy season and length of growing period

As indicated in FAO (1998) the start of the rainy season both for belg (the shorter) and kiremt (the main growing season) can be identified based on simple soil water balance model. It is recommended that utilizing Penman equation for ascertaining crop Evapotranspiration, a begin of developing period can be acquired when a decadal (ten-day) precipitation sum is equivalent or more prominent than half of the reference crop evapotranspiration (ETo) amid the start of the rainy season. Similarly, end of rainy season is obtained when a decadal rainfall amount is less than half of the corresponding reference crop (ET_O) at the end of rainy season.

Benoit (1977) used the daily data to define the onset as the date when accumulated rainfall exceeds and remain greater than 0.5 potential evapotranspiration for the remainder of the growing season provided that no spell longer than five days occurs immediately after this date (Edoga, 2007). However, determination of rainfall onset and end was made by different researchers without evaporation data input by setting different criteria that can affect the rainfall onset and end (Abiy *et al*., 2014).

The length of the growing period (LGP) may be defined by counting the number of days between the start and the end of the growing period. Evidence from the study indicated that annual crops which grow during the rainy season can utilize stored moisture in the range of 75 -125 mm by the time of maturity. (FAO, 1998 and Mersha, 2003); so that an average 100 mm of soil moistures capacity is added after end of rainy season to calculate length of the growing period. A fall in the number of rain days associated with an increase in rainfall per rainy day signifies an increased in the intensity of rainfall.

The onset of rainy season is a very important event for farmers in sub-Sahara Africa. The onset of rains marks the beginning of three main activities; planting, weeding and harvesting (Omotosho *et al.*, 2000). Omotosho *et al.* (2000) reported how variability of the onset and

cessation of the rainy season in tropical region pose a serious challenge in the process of determining when the rainy season/planting season begins. Studies in Ethiopia revealed that rainfall variability, unreliable occurrences in sufficient amount and delay in onset dates caused significant reduction in crop yield with reasonable amount almost all parts of the country (Godswill *et al*., 2007).

2.11.2. Application of CROPWAT model

CropWat is a decision support system developed by the Land and Water Development Division of Food and Agriculture Organization (FAO) for planning and management of irrigation (FAO, 1998). Additionally, CropWat is a practical tool which supported by computer programme to carry out standard calculations for reference evapotranspiration, crop water requirements from existing or new climatic and crop data. In this model, the calculation of crop water requirements is carried out per decade (Allen *et al*., 2005).

2.11.2.1. Crop water requirement

The amount of water required to compensate the evapotranspiration loss from the cropped field is defined as crop water requirement. Although the values for crop evapotranspiration and crop water requirement are identical, while crop evapotranspiration refers to the amount of water that is lost through evapotranspiration. For the calculations of the Crop Water Requirements (CWR), the crop coefficient approach is used (FAO, 1998).

2.11.2.2. Reference evapotranspiration

Various ETc estimation models have been developed in today's world. Among these models, the Penman Monteith (PTM) equation is found to be more consistent over a wide range of climatic conditions (Allen *et al*., 2005).The most challenging part in the PM equation is to calculate the canopy surface resistance. Ravazzani *et al.* (2012) compared the Hargreaves and Samani (1985) equation (HS) to FAO 56 PM equation for daily time steps in alpine river basins and found that the HS equation didn't perform well. The HS method showed overestimation of ET_O at lower elevation sites and underestimation at higher elevation sites. However, after

using a correction factor, they found that the HS equation was in very good agreement with the FAO 56 PM equation. In middle Awash river basin, Gedion (2009) appraised the concert of penman methods with reference to the measured pan evaporation in Amibara irrigation schemes to determine ET. Accordingly, the study came up with the better performance of penman than pan evaporation of ET.

2.11.2.3. Crop coefficient approach

According to FAO (2011) Crop evapotranspiration can be calculated from climatic data and by integrating directly the crop resistance, albedo and air resistance factors in the FAO Penman-Monteith approach. As there is still a considerable lack of information for different crops, the Penman-Monteith method is used for the estimation of the standard reference crop to determine its evapotranspiration rate, i.e., reference evapotranspiration (ET_O). Experimentally determined ratios of ETc/ETo, called crop coefficient (K_c), are used to relate crop evapotranspiration under standard conditions (ETc) to ET_O. This is known as the K_c approach (Allen *et al*., 2005).

$$ETc = Kc * ET_O \quad (9)$$

Radiation, air Temperature, Humidity and Wind speed are all incorporated into the ET_O estimate. Therefore, ET_O represents an index of climatic demand, while K_c varies predominately with the specific crop characteristics and only to a limited extent with climate and soil evaporation (Allen *et al*., 2005). Alternatively, FAO (1998) and Smith and Kivumbi (2006) point out that the Kc value is highly depend on relative humidity and wind speed at mid stage of crop growth. Hence, when the value of relative humidity is high (RH > 80%) and the wind speed is low (u < 2 m/sec) the K_c should be reduced by 0.05 and its values should be increased by 0.05 if the relative humidity is low (RH < 50%) and the wind speed is high (u > 2 m/sec).

2. MATERIALS AND METHODS

3.1. Description of the Study Area

3.1.1. Location of Kesem subbasin

In middle Awash River basin; Kesem subbasin is situated at about longitude of $39^{o}58'48''E$ and latitude of $8^{o}55'12''N$, in the Eastern part of Ethiopia and its area coverage is about 2,276 km^2 which is shown in the Figure 1. It is bordered by mountain and plateaus in its northern part and the outlet distant 268 km from the Ethiopian capital city Addis Ababa. In administrative terms, Kesem subbasin lies within Zone three, East Shoa and North Shoa Administrative Zone of Afar, Oromia and Amhara Regional State of Ethiopia respectively. The gauging station ($39^{o}57'40''E$, $9^{o}7'59''N$) is situated at the upper side of Kesem sugar corporation and bordered by mountain and plateaus at its northern part (MoWIE, 2013).

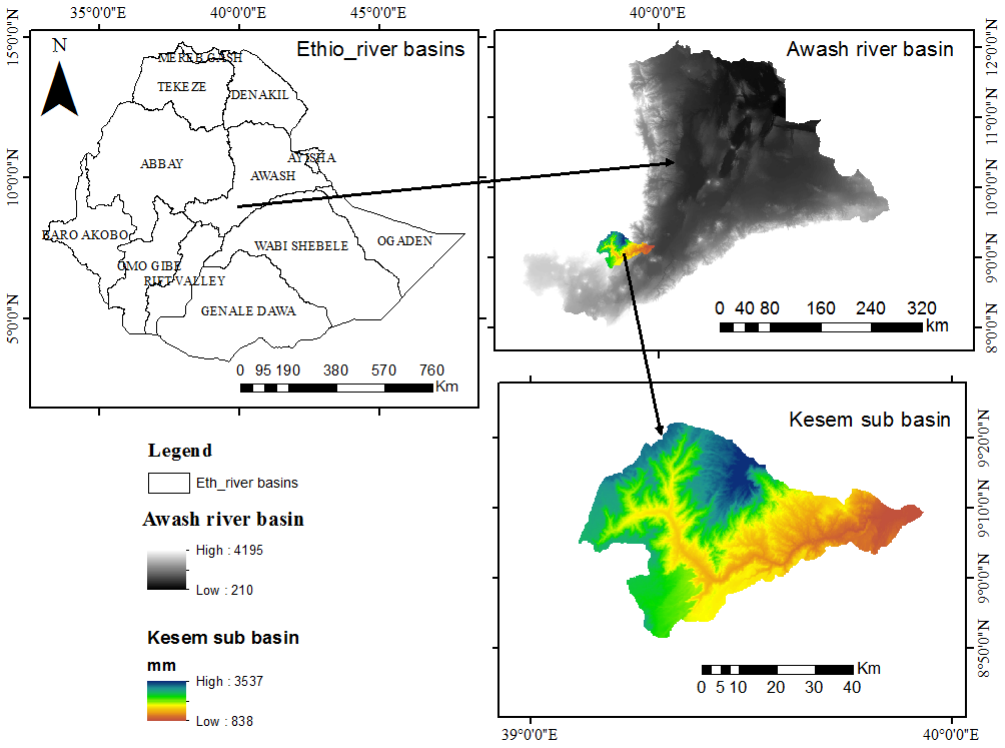

Figure 1. Location map of Kesem subbasin (2,276km^2) and DEM.

3.1.2. Topography

The middle Awash; Kesem subbasin is predominantly high land and mountain in the northern part with an altitude ranging from 838 to 3534 masl. Topographically, it is flat to pile plain with exception of some isolated volcanic cones. Small hills, points of volcanic activity and rift tectonic mark the boundaries of the area in the southeastern part. It is encircled by the northwest highlands and the central escarpments of Ethiopia rift valley. As depicted in Figure

2, the slope of the subbasin ranges from 0 to 48%. From the DEM (30 x 30m), slope of the subbasin varies from minimum 0.3 to maximum 48% and considers five classes depending on FAO slope classification standard, land slope classes as: class1: 0 to 5%, class2: 5-10, class3:10-15%, class4: 15-20%, class5: >20%.

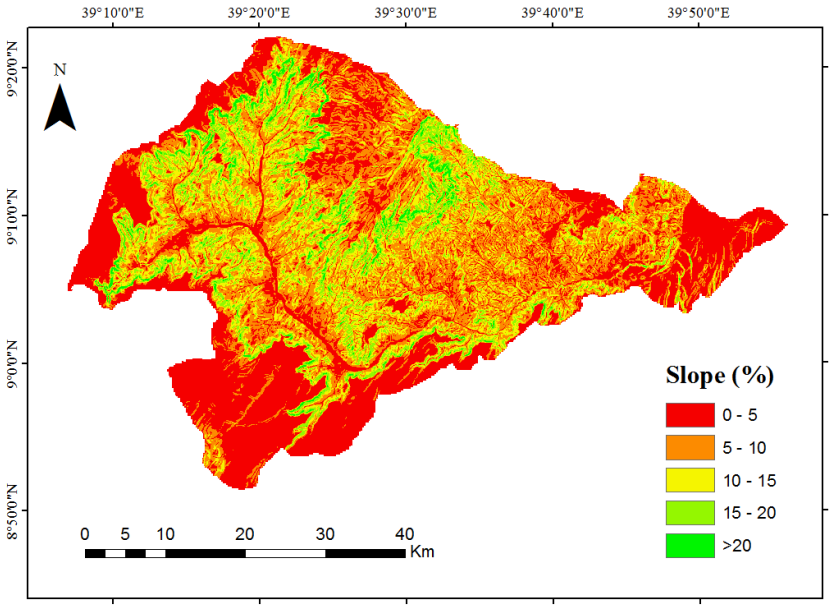

Figure 2. Slope map of Kesem subbasin

2.11.3. Climate

The Ethiopian climate system is traditionally classified based on existing altitudinal range and temperature. Hence, there are five climatic zones in the country. The arid zone is a very hot and hyper-arid region with less than 500m.a.s.l. and semiarid zone is also a hot and arid region ranged between 500-1500 m.a.s.l. altitudes. Similarly, sub humid is an optimum temperature

from 1500-2500 m.a.s.l. altitude. Humid zones are found in highland regions with 2500-3000 and greater than 3000 m.a.s.l. altitudes respectively (NMA, 2012).

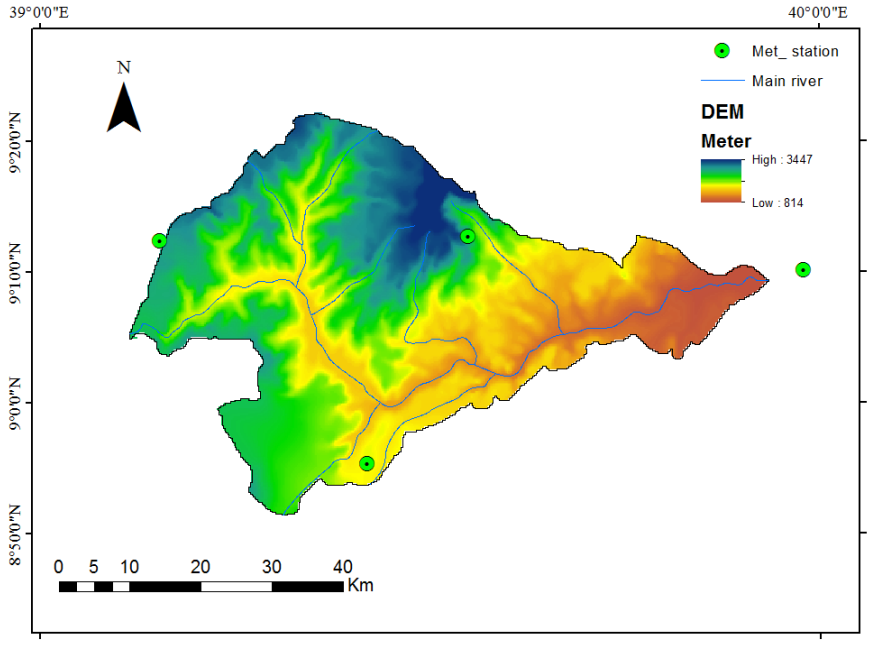

Figure 3. DEM of the Kesem sub basin, main rivers, meteorological stations and observed monthly mean rainfall, maximum and minimum temperatures for four stations.

Accordingly, Kesem sub basin is laid in between semiarid and sub humid with majority falls at sub humid zone in the northern and north west and at semiarid in the north and south east receiving a mean annual rainfall of 1009 mm and 534 mm respectively.

The mean minimum temperature is 7.2ºC and 18.5ºC in December and 6.3ºC and 23ºC in June, while the mean maximum temperature is 19.6ºC and 32.5ºC in December and 16.5ºC and 38ºC in June respectively in the north western and south eastern part of the basin. Mean relative humidity is lowest in June at 36% and highest in August at 63%. The average daily sunshine hours are 8.5 with an average solar radiation of 536 calories per square centimeter per day (cal/cm^2/day) and the mean annual potential evaporation recorded from each station is 1970 mm and 2700 mm in the north western and south eastern part.

2.11.4. Drainage networks

Kesem River which belongs to the subbasin is a main tributary to the Awash River basin to the northeast at Aware Melka (39°57′40′′E, 9°7′59′′N) outlet. Kesem subbasin is considered as one of water sources for the Awash River basin after joining Awash River in Kesem kebena. It is surrounded by Kesem beke in the south western, Blue Nile River basin in the north western and Nura Hera subbasin in the eastern part.

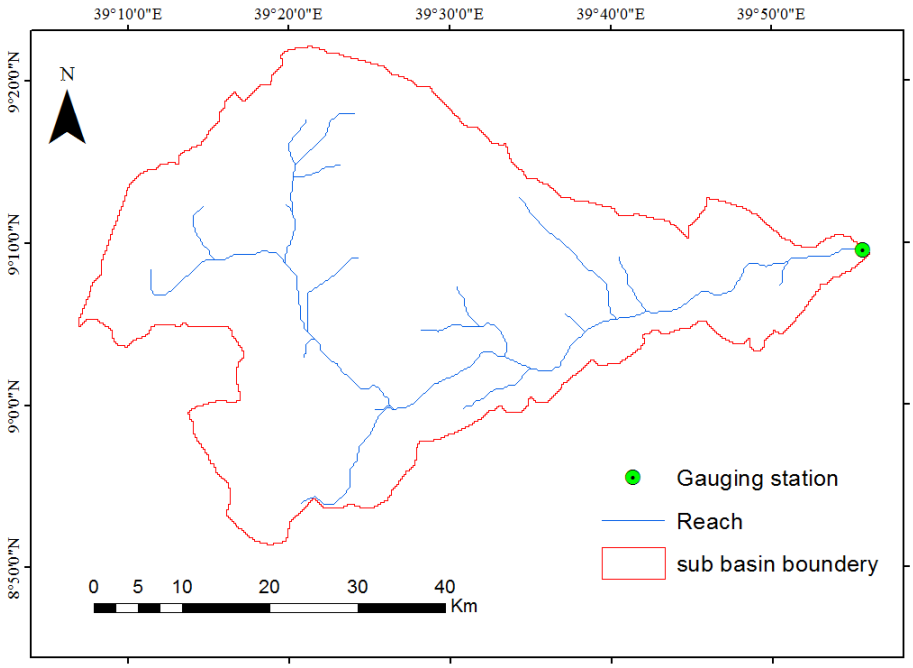

Figure 4. Map of Kesem subbasin with its drainage networks and gauging station

2.11.5. Land use/cover

The land use map of middle Awash, Kesem subbasin is dominated by Agricultural land. Away from the river, the vegetation cover varies from closed dry thicket to open shrub land, and further to grassy plains. In earlier times, there are nine land use/cover types recognized from the land use map of (2013) Kesem subbasin (Figure 5).

The crop land, at which agriculture practice takes places, is the dominant land use type in the subbasin which comprises 77.55% of the total subbasin area. Acacia, shrub and forest land use types also covers respectively 10.37%, 8.66% and 1.93% of the total land in the subbasin. Bare land, eucalyptus, settlement and water body covers 0.66%, 0.44%, 0.2% and 0.18% of subbasin areas respectively. Grassland covers insignificant area which counts less than 0.001%

share from subbasin. The agricultural system is rain-fed agriculture composed of mixed agriculture which basis on the major crops farming system and highland crops in the upstream catchment. Among the major crops maize (*Zea mays.L*) produced in the upper and downstream of the subbasin.

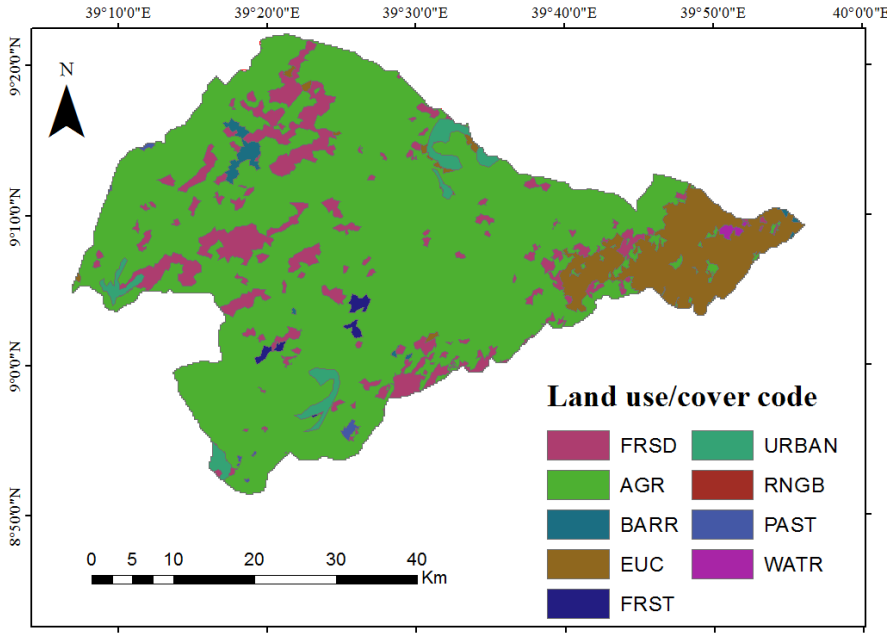

Figure 5. Land use map of (2013) Kesem subbasin

2.11.6. Soil types

According to the USDA soil classification system, six soil types are identified in the subbasin. These includes chromic luvisols, eutric cambislos, eutric leptosols; eutric vertisols, lithic leptosols and vertic cambislos. Lithic leptosols, vertic cambislos, eutric leptosols, eutric cambislos and eutric vertisols are the dominant soil types which cover 53.74%, 16.43%, 16.30%, 6.85%, and 6.37% of the subbasin area respectively. Chromic luvisols are insignificantly found in the subbasin with 0.31% from the total area of the subbasin. Most parts

of the upper stream of sub basin are dominated by lithic leptosols and lower and south eastern parts of the subbasin are covered by eutric cambislos and vertic cambislos respectively as shown in the Figure 6.

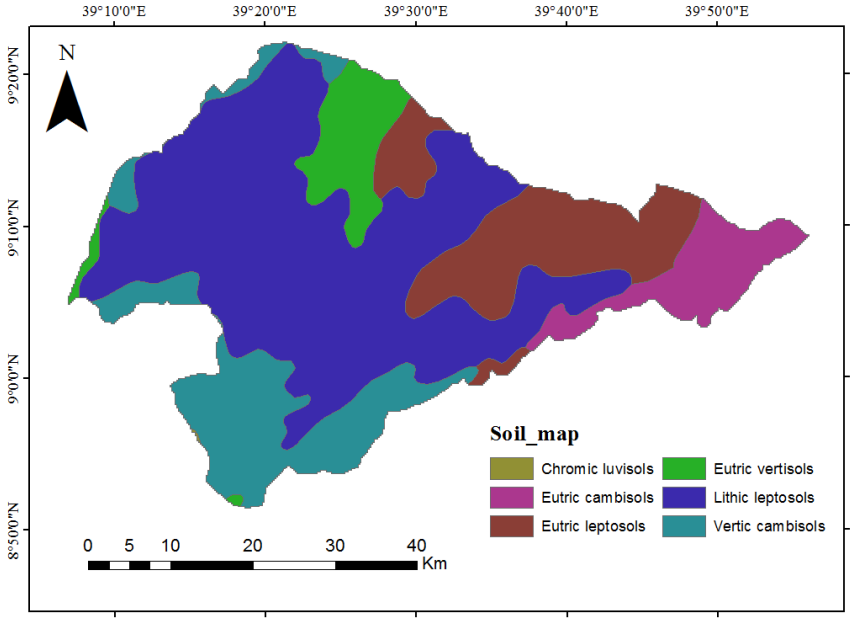

Figure 6. Soil map of the Kesem subbasin

2.11.7. Hydrology

Kesem is a perennial river exists in subbasins where gauging station was found. This river discharge is highly dependent on seasonal rainfall variability. Hence highest river discharge is measured during main rainy season of the year, which is starting from June to middle of September and peak during month of August as depict in the Figure 7.

Figure 7. Average monthly discharge of Kesem subbasin at Kesem Awara melka outlet from 1984- 2000

3.1.8. Population and farming system

The subbasin constitutes five woreda. Based on the census conducted by the Central Statistical Agency (CSA) of Ethiopia in August, 2013, those woreda has an average population density of 86.10 per square kilometers. Rain-fed agriculture mainly maize, wheat and sorghum are major crops along with livestock raring and used as the major sources of food and income for maintaining their livelihoods.

2.1. Materials and Models

2.1.1. Materials used

The materials that were used for this study are GPS for taking geographic-coordinate values (altitude, latitude and longitude), digital camera for field photographs and core sampler, auger,

plastic bag, spatula and double ring infiltro-meter for taking soil sample and infiltration rate determination from subbasin were used.

2.1.2. Models and software's used

To achieve the objective of the study, ensembles of thirty six RCM model output for impact assessment, CROPWAT model to estimate maize water needs, SWAT model for soil water Availability estimation and CLUE-S model to forecast future LULC. Software like R window to archive RCM model output from c.n file of CORDEX Africa data base, XLSTAT for homogeneity test were used.

2.2. Data Collection

2.2.1. Meteorological data

Meteorological data were collected from the meteorological stations found in and around the sub basin from the Ethiopian NMA office and downloaded from CORDEX Africa database though ensemble of thirty six RCM model output. A summary of the rainfall stations with years of record used in the thesis is given in Table 1.

Table 1. Summary of the rainfall stations

S.No.	Station name	Latitude(°)	Longitude (°)	Altitude (m)	Period of data	Missed data (%)	Remark
	Shola Gebeya	9.21	39.55	2500	1984-2013	3.38	Filled
2	Aware Melka	9.17	39.88	960	1984-2013	5.63	Filled
3	Arerti	8.92	39.42	1806	1984-2013	9.83	Filled
4	Aleltu Agriculture	9.21	39.16	1977	1984-2013	0.36	Filled

From the above table, Shola Gebeya and Aleltu Agriculture are class one metrological stations which include rainfall, max and min temperature, relative humidity, wind speed and sunshine hour whereas station Arerti and Aware Melka are class two metrological stations which contain rainfall, max and min temperature. Other parameters like relative humidity, wind speed and sunshine hour are generated by weather generator of SWAT tool for station Arerti and Aware Melka for impact assessment.

2.2.2. Hydrological data

Hydrological data, available stream flow net data of the sub basin's gauging station have been required for calibrating and validating SWAT model. Hence the gauging stations (Kesem Aware Melka) in the subbasin which have continuous record for a relatively long period and therefore average monthly stream flow discharge data (1984-2000) for these stations were collected from the Ministry of Water, Irrigation and Electricity (MoWIE).

2.2.3. Spatial data

The spatial data includes digital elevation model (DEM), digital stream network, land use and land cover map and soil map. The high resolution DEM (30 X 30 m) were obtained from the elevation databases of shutter radar topographic mission (SRTM)http://earthexplorer.usgs.gov/ Digital elevation model (DEM) used as input for SWAT model.

Land use/cover data used in this research work for change of soil water availability were seen in baseline scenario. These are land use/cover of 1998 and 2013 as baseline scenario. These land use/cover were obtained from land sat images. Land Sat images of path/row 168/053 of 30 m spatial resolution which obtained from united state geographical survey (USGS) website and was processed using ERDAS IMAGINE 2014 software.

Soil data required by SWAT model, soil textural and physiochemical properties data were obtained mainly from the following sources: Awash River basin Integrated Development Master Plan Project Semi detailed Soil Survey and Africa CD-ROM (Food and Agriculture Organization of the United Nations (FAO, 2011), Major Soils of the world CD-ROM, Digital Soil Map of the World and Derived Soil Properties CD-ROM (FAO, 2011), Properties and Management of Soils of the Tropics CD-ROM (Van Wambeke, 2011).

2.2.4. Crop and soil data for CROPWAT

To determine crop water needs, CROPWAT were used Crop and soil data in addition to climate data. Crop data which consist the crop coefficient data files, including Kc values, stage

days, root depth, depletion fraction of the crop were taken from FAO Irrigation and Drainage (FAO, 2012). Information on maize varieties used by local farmer and planting date (onset date) was obtained during survey work from local farmer by informal interview. The soil data required by the CROPWAT model were collected from the Maize focus area of Berehet woreda during survey work to determine physicochemical properties as per CROPWAT require in the subbasin.

3.4. Pre-processing of Data

Before using the weather data records of stations, it is necessary to first check the data for homogeneity, continuity and consistency. The continuity of a record may be broken with missing data due to many reasons such as damage or fault in a rain gauge during record period. A number of methods have been proposed for estimate missing data (Richard H.McCuen, 1989). Among these arithmetic average method is the simplest method. This method is accurate when the total annual rainfall at any of the 'n' region gauges differs from the annual rainfall at the point of interest by less than 10%. Therefore for this thesis work, arithmetic average method was used by using this equation:

(10)

where, P_X is the daily rainfall or temperature with missing records, P_1, P_2, P_3, n_x are recorded daily rainfall and M is the number of observations for estimation.

This study requires long term rainfall data; therefore, a test must be conducted to check homogeneity and consistency of rainfall record. This is necessary because over a period of time, it may happen that there are some construction (tree or building) may have emerged after the installation of rain gauge or its location or observational procedure might have changed. They bring the inconsistence and heterogeneity of rainfall data. Therefore for this thesis work the consistency and homogeneity of rainfall station were checked by double mass curve technique Subramanya (1998) and using XLSTATA 2017 software via SNHT test (Standard Normal Homogeneity Test).

To selected representative stations in the subbasin, knowing the average areal rainfall distribution is crucial. The computation of average areal model input data can be done by Arithmetic average method, Theissen polygon method and Isohytal method. The selected subbasin has four rainfall gauging stations within or in the vicinity of the boundary of the subbasin. For catchments having rainfall gauges more than one, Theissen polygon method was recommended to compute the areal rainfall.

2.5. Climate Model

2.5.1. Coordinated regional climate downscaling experiment model (CORDEX)

CORDEX project (http://wcrpcordex.ipsl.jussieu.fr/) is an initiative of the World Climate Research Program (WCRP) performed with the intention of producing an ensemble of high resolution climate change projections by dynamically downscaling GCM simulations from Coupled Model Inter-comparison Project Phase 5 (CMIP5) data archive (Jones *et al.*, 2011). The major aims of the CORDEX initiative are to provide a quality controlled dataset of downscaled information, coordinated model evaluation framework, and an interface to the applicants of the climate simulations for further climate change impact, adaptation, and mitigation studies (Giorgi *et al.*, 2009). This were used for limited area which applied here to download the climate parameter for the study area that are outlined by Colin Jones (Jones, 2011) and fully described in the CORDEX 'User's Manual', by Colin Jones and CORDEX group, which can downloaded from the CORDEX Africa database. CORDEX, derived variables provide daily information about small scale atmospheric condition which describes the condition at the site scale. As detailed in the document, the base resolution of each domain is assumed to be 0.44° x 0.44° for Africa (AFR-44) rotated coordinate system, resulting in a quasi-regular resolution of ~50 km

2.5.2. Regional circulation model (RCM)

RCM model output data were obtained from the Coordinated Regional Climate Downscaling Experiment model (CORDEX) Africa Coupled Model Inter-comparison Project phase 5 (CMIP5) set of integrations. Daily outputs of RCMs were used for the analysis of climate

change scenario for limited area. To achieve the data from CORDEX Africa database for limited area, thirty six RCM models in the current world are adopted for east Africa. Due to the inherent uncertainty of the climate system and the inevitable existence of model errors, multi-model ensemble is the recommended approach for climate change projections (Jones *et al*., 2011; Nikulin *et al*., 2012). They evaluate the ability of RCMs over Africa and conclude that all RCMs simulate the seasonal mean and annual cycle quite accurately. Thus, in this study, the ensemble of thirty six RCM model output were engaged by using RCP 4.5 and 8.5 scenarios to produce the future situations. The performance of the CORDEX Africa RCM model was measured by bias correction methods.

2.5.3. Climate change scenarios generation

The baseline data for the base period were from four stations in and around the Kesem subbasin within the range of 30 years period from 1984-2013 were generated. Accordingly ensemble of RCM model output was downloaded via two emission scenarios (RCP4.5 and RCP8.5) for future climate change scenarios. Each scenario assumes a distinctly different direction for future developments. Here the reasons for selecting these two scenarios are, since RCP4.5 shows middle emission scenario and RCP8.5 shows high emission scenario of GHGs concentrations and most of former researcher done via this scenarios in the rift valley of Ethiopia for instance Sahilu and Nigussie (2015).

2.5.4. Bias correction methods

In this study delta approach bias correction methods was applied. It is one of the most widely and commonly used correction methods for RCMs scenarios of future conditions for climate change impact studies (Shabalova *et al*., 2003). The average monthly precipitation /temperature were corrected to match the average monthly precipitation/temperature for 30 years. Therefore, the average monthly precipitation/temperature over the period 1984 – 2013 has been calculated for the study area. In this method mean of the downloaded data were corrected and compared by the base period based on yearly and monthly time steps and compared with respect to bias uncorrected and corrected versions. This approach was tested in the Central Rift Valley of Ethiopia and the long mean of simulated data appeared in a better

much with the long mean of the base period data (Sahilu and Nigussie, 2015). The formulas used for rainfall and temperature bias correction are indicated in Equations 11 and 12 respectively.

$$P_{bc} = P_p * P_o / P_r \quad (11)$$

$$T_{bc} = T_p + T_o - T_r \quad (12)$$

where,

P_{bc} is Bias corrected future rainfall amount in mm: P_P is predicted future rainfall amount in mm; Po is mean of observed rainfall amount in mm: Pr is mean of computed historical rainfall during the observation period in mm.

T_{bc} is Bias corrected future temperature in ^{o}C; Tp is predicted future temperature in ^{o}C; To is mean of observed temperature in ^{o}C; Tr is mean of computed historical temperature during the observed period in ^{o}C.

Furthermore, corrections factors for both precipitation and temperature were computed for each month using the Mean Absolute Error (MAE) method. A positive difference means that the downloaded value is wetter /warmer than the observed precipitation/temperature values for that specific locality. The average monthly precipitation and temperature difference between the observations and the simulated is given by equation 13 and 14:

(13)

(14)

where, MAE = Mean Absolute Error; N = the number of months; P_{simu},i = the precipitation for projection at month i and; P_{obs},i = the precipitation for the observations at month I; T_{simu},i = temperature for projection at month i and; T_{obs},i = temperature for the observations at month i.

3.6. Land Use Model

3.6.1. The CLUE-S model

The CLUE-S is an improved model for small-scale regional application (Verburg *et al*., 1999). The model dynamically allocates land use changes to simulate the future land use change based on a combination of empirical analysis of location suitability and spatial analyses (Verburg *et al*., 1999; Zheng *et al*., 2012). Compared with other empirical models, it simulates multiple land use types simultaneously. The criteria to select the CLUE-S model for this study were based on its flexibility and performance, and the possibility of linking the output to the SWAT model to estimate water balance of the subbasin. Also, input data for this model are available in the subbasin and it works on annual time step. A more detailed description of the model is given in Verburg *et al*. (2002) and also its short description was viewed in the literature part of thesis work.

3.6.2. Land use scenarios

The land use demand scenarios have been tested in this study based on past and current land use from the socioeconomic condition of the area. The near future land use change trends were derivate based on the land use changes of the recent past trends and the trends were corrected for changes in population growth to prepare the land use demand scenarios. The future scenarios focused on the following land use and land cover classes, Acacia, Agricultural land, grass land, bare land, shrub land, forest land, settlement, and water body.

The recent past land use scenario was obtained by processing land use maps of 1998 and 2013 Land sat images. These scenarios in the study are baseline scenario. In the baseline scenario, the growth in population is assumed to follow the current trend and the future land use requirement is expected to change linearly and derivate based on the trend in the time period from 1998 to 2013. The farmers in the subbasin are expected to continue doing as they have in the past. In this scenario, the historical evolution of the major land use covers such as Agricultural land are derivate till 2020s (2014-2043) using regression equations (1).

3.6.3. Regression analysis of the land use/cover change

The land use map of 2011 was used in logistic regression analysis to understand the spatial relationship between current land use/cover and driving factors were represented by beta value. For each types of land use, a separate regression model was used. SPSS software was used to extract the beta coefficients. To simulate future land use changes, it is necessary to know the factors which drive the spatial distribution of land use. Hence, in this study, the following driving factors were used, population density, soil type, soil texture, altitude, and distance to the nearest towns. The beta values calculated for each land use classes by logistic regression were used as inputs to the CLUE-S model.

3.7. SWAT Model

3.7.1. Model input

3.7.1.1. Digital Elevation Model (DEM)

Digital elevation model (DEM) used as input for SWAT model. In the SWAT model, DEM were used to delineate the subbasin. Subbasin parameters such as slope gradient, slope length of the terrain, and the stream network characteristics such as channel slope, length, and width were derived from the DEM. Also it is necessary for the stream network processing in SWAT. The calculations establishing the river system are embedded in Arc SWAT procedure facilitating the application and enables users to study long-term impacts.

3.7.1.2. Land use/cover data

LULC is one of the most important spatial input data for SWAT model that affect runoff, evapotranspiration, surface erosion and other hydrological process in a given subbasin. In this research work, land use/cover data were used in one scenario to have as input for SWAT model to assess soil water availability. These are land use/cover of 1998 and 2013 as baseline scenario. This land uses are relatively not simplistic, because it contains all categories of land uses like Agricultural Land-Genetic, Low density Rural Settlement, and others. SWAT has

predefined land uses identified by four letter codes and it uses these codes to link land use maps to SWAT land use databases in the GIS interfaces. Hence, while preparing the lookup table, the land use types were made compatible with the input needs of the model.

Table 2. Original land use/land cover types redefined according to the SWAT code and their aerial coverage for scenario one (1998, 2013); a) - LULC of 1998; b) - LULC of 2013.

a)

Original land use	Redefined land use according to SWAT data base	SWAT code	Area(km^2)	Area (%)
Acaia	Forest-Deciduous	FRSD	524.00	23.02
Agricultural land	Agricultural land	AGR	1461.00	64.19
Bare land	Barren	BARR	14.00	0.62
Eucalyptus	Eucalyptus	EUC	25.00	1.10
Forest	Forest	FRST	2.00	0.09
Settlement	Urban	URBAN	1.00	0.044
Shrub land	Range land	RNGB	248.00	0.12

b)

Original land use	Redefined land use according to SWAT data base	SWAT code	Area(km^2)	Area (%)
Acaia	Forest-Deciduous	FRSD	236.00	10.370
Agricultural land	Agricultural land	AGR	1765.00	77.550
Bare land	Barren	BARR	15.00	0.660
Eucalyptus	Eucalyptus	EUC	10.00	0.440
Forest	Forest	FRST	44.00	1.930
Settlement	Urban	URBAN	4.72.00	0.200
Shrub land	Range land	RNGB	197.00	8.660
Grass land	Pasture	PAST	0.28	0.001
Water body	Water body	WATR	4.00	0.180

3.7.1.3. Soil data

Basic physicochemical properties of major soil types in the subbasin required by SWAT model are classified on the basis of the revised FAO/UNESCO-ISWC (2012) classification system. This data were cross checked with data in SWAT database. SWAT has predefined soil data identified by letter codes and it uses these codes to link soil maps to SWAT soil databases in the GIS interfaces. Hence, while preparing the lookup table, the soil types were made compatible with the input needs of the model. Major soil types in the basin are chromic

luvisols, Eutric cambislos, Eutric leptosols, Eutric vertisols, Lithic leptosols and Vertic cambislos.

Table 3. Soil type of the study area with their aerial coverage

Soil type	Symbol	Area (km^2)	Area (%)
Chromic luvisols	CLUV	7	0.31
Eutric cambislos	ECAM	156	6.85
Eutric leptosols	ELEP	371	16.30
Eutric vertisols	EVER	145	6.37
Lithic leptosols	LLEP	1223	53.74
Vertic cambislos	VCAM	374	16.43

3.7.1.4. Weather data

SWAT requires daily meteorological data that could either be read from a measured data set or be generated by a weather generator model. In this study, the weather variables used for driving the hydrological balance are daily precipitation, minimum and maximum air temperature, relative humidity, wind speed and solar radiation for baseline period of 1984 – 2013. These data were used by dividing the baseline period into one scenarios by calling baseline scenario or scenario 1(1998, 2013) with a period of 15 year of one tri-decadal. Therefore, weather data for a period of two fifty years were used for scenario one (baseline scenario) to assess the impact in the area temporally. Finally, ensemble of RCM model output were used to generate the future climate scenarios for daily precipitation, minimum and maximum air temperature, relative humidity, wind speed and solar radiation from 2014 to 2043 of one tri- decadal of two 15 years in both scenarios.

3.7.2. Model setup

3.7.2.1. Watershed delineation

After the data was collected and prepared, the model was set up for all input data. Five steps were observed for the model setup as shown below:

The ArcGIS tool in Arc SWAT partitions watersheds into a number of hierologically connected subbasins based on flow directions and accumulations. The subbasins delineation was carried out based on an automatic delineation procedure using a Digital Elevation Model (DEM) and

digitized stream networks. The model fills all of the non-draining zones (sinks) to create a flow vector, and super imposes the digitized stream networks into the DEM to define the location of the stream network.

The Arc SWAT interface proposes the minimum, maximum, and suggested size of the subbasin area to define the minimum drainage area required to form the origin of stream. Generally, the smaller the threshold area, the more detailed are the drainage networks, and the larger are the number of sub basins and HRUs. However, this needs more processing time and space. As a result, an optimum size of a watershed that compromises both was selected. Dilnesaw (2006) did a sensitivity analysis of the threshold area on SWAT model performance and found that the optimum threshold area that can be used for the delineation procedure is ±1/3 of the suggested threshold area. Therefore, threshold area of +1/3 of that suggested by the model was used. With respect to the given area of watershed, only one outlet is defined, which is later taken as a point of calibration and validation of the simulated flows. As a result actual Kesem subbasin outlet at Aware Melka is delineated.

3.7.2.2. Hydrological response units

Hydrological Response Unit (HRU) which is the smallest unit of the model to route stream flow was established after reclassification of land use and soil maps and then overlaid one upon each other. The threshold value was assigned to sub divide the watershed area into HRU which is an area having unique land use, soil and slope combinations. In SWAT, there are two methods to determine the HRU distribution. The first method is to assign a single HRU to each sub watershed and/or the second one is to assign multiple HRUs to each sub watershed. If a single HRU per subbasin is selected, the HRU is determined by the dominant land use category, soil type, and slope class within each watershed. Whereas if multiple HRUs are selected, the major land use, soil, and slope data can be specified that will be used to determining the number and type of HRUs in each watershed. The second procedure of spatial disaggregation of subbasin was selected for this study in order to enable the model to reflect differences in evapotranspiration and other hydrologic conditions for different land covers/crops and soils.

In addition, HRU creation in Arc SWAT requires land use, soil and slope threshold inputs in order to define the level of spatial detail to be incorporated in the model (Neitsch *et al*., 2005 and Winchell *et al*., 2009). The threshold is applicable for controlling the size and number of HRUs made in each subbasin. For a more detailed description of the Arc SWAT land use and soils threshold application refers to the Arc SWAT manual. For defining of the number of HRU formulated in the subbasin, there is no general approach, and rather depends on the objective of the project in which it is studied. According to Winchell *et al*., 2009; Teshome and Koch, 2013, the default threshold values of land use and soils used in the model are sufficient for most water resources assessment projects. For this study, threshold value of 20%, 10% and 20% which are the default values of the model were applied for land use, soil and slope respectively in order to keep the number of HRUs to a reasonable number for modeling the water assessment of the basin. Stream flow is predicted separately for each HRU and routed to obtain the total runoff for the watershed. This improves the accuracy of runoff predictions of the model and provides a much better physical description of the water balance.

3.7.3. Sensitivity analysis

The current version of SWAT model, SWAT2012, provides the algorithmic technique for sensitivity analysis. Two types of sensitivity analysis are allowed when using SUFI2 (sequential uncertainty fitting version 2) those are global sensitivity and One-factor-At-a-Time sensitivity analysis (Van Griensven, 2005; Abbaspour *et al.*, 2007). The two aforementioned sensitivity analysis methods may yield different results since the sensitivity of one parameter depends on the value of other related parameters. In case of global sensitivity analysis, the parameter sensitivities are determined by calculating the multiple regression system, which regresses the Latin hypercube generated parameters against the objective function values. It uses t-test to rank the most sensitive parameter that corresponds to greater change in output response. A t-test result provides a table of output having columns of t-test and p-values. A t-test provides a measure of sensitivity (larger in absolute values are more sensitive) and p-values determined the significance of the sensitivity. A value close to zero has more significance.

Whereas in case of the one-at-a-time sensitivity presents the sensitivity of a single parameter to the changes in a model outputs keeping all the other parameters are to be maintained constant. The problem with this method is that it never knows what the exact values of other constant parameters should be at the commencement of simulation. Therefore, in this study global sensitivity analyses were performed. To improve simulation result and thus understand the behavior of hydrological system in Kesem subbasin, sensitivity analyses were conducted using the 28 flow parameters.

3.7.4. Model calibration and validation

Model calibration involves modification of input parameters and comparison of predicted output with observed value until a defined objective function is achieved (Coffey *et al*., 2004). Parameters identified in sensitivity analysis that influence significantly the simulation result were used to calibrate the model. Model sensitivity and calibration was performed using the output of SWAT-CN method for flow simulation.

Calibration describes the effort to support the model with fitted parameters for a given set of local conditions in order to reduce the prediction uncertainty (Spruill *et al*., 2000). In this study, calibration was carried out with the SWAT calibration and uncertainty program (SWAT-CUP) 2012, version 5.1.6.2 using SUFI2 (sequential uncertainty fitting version 2) , which facilitates the calibration process (Arnold *et al*., 2012). It is an open source model developed by the Swiss Federal Institute of Aquatic Science and Technology (SFIAST) and is distributed by Neprash Technology (Canada). It was carried out for a period of eleven years from January 1, 1984 to December 31, 1995. These were done according to existence of LULC data. However, the first three years of the recording period (1984 to 1986) of fifteen years were used for the stabilization of model runs (warm up period). The calibration was therefore performed for a period of nine years (January 1, 19987 to December 31, 1995) on monthly bases. The second fifteen years (1999-2013) of baseline period were simulated by parameterizing the parameters of the first fifteen years (1984-1998).

The graphical and statistical approaches E_{NS} and R^2 were used to evaluate the SWAT model performance number of times until the acceptable values were obtained for surface runoff and base flow independently. The flow calibration procedure made by SWAT developers in Santhi *et al* (2001) and Neitsch *et al* (2005) were carefully followed. For each calibration run and parameter change, the corresponding model performance statistics R^2 and E_{NS} were calculated. This procedure was continued until the acceptable calibration statics recommended by SWAT developer for hydrology was achieved. SWAT developers assumed an acceptable calibration for hydrology at $R^2 > 0.6$ and $E_{NS} > 0.5$ (Santhi *et al*., 2001; Moriasi *et al*., 2007).

After doing the model calibration and checking its performance, the model validation was done with independent data to use the model for scenario analysis. Stream flow data of three years (1996-1998) from scenario one of fifteen years were used for validation. The two statistical model performance measures used in calibration procedure were also used in validating monthly stream flow.

3.7. 5. Model performance evaluation

In order to evaluate the performance of SWAT model to determine the quality and reliability of prediction compared to the observed values, the following methods for goodness-of-fit measures of model predictions were used during the calibration and validation periods. The coefficient of determination (R^2) describes the proportion of the total variance in the observed data that can be explained by the model. The closer the value of R^2 to 1, the higher is the agreement between the simulated and the measured flow and is calculated as follow:

$$R^2 = \qquad (15)$$

where: X_i - measured value, X_{av} average measured value, Yi - simulated value, Yav - average simulated value.

Nash and Sutcliffe simulation efficiency (E_{NS}) indicates the degree of fitness of observed and simulated data and given by the following formula.

$$E_{NS} = 1- \quad (16)$$

where: X_i is measured value, X_{av} is average measured value, Y_i is simulated value, Yav is average simulated value.

The value of E_{NS} ranges from 1 (best) to negative infinity. The E_{NS} indicates how well the plot of observed versus simulated value fits the 1:1 line. If the measured value is the same as all predictions, E_{NS} is 1. If the E_{NS} is between 0 and 1, it indicates deviations between measured and predicted values. If E_{NS} is negative, predictions are very poor, and the average value of output is a better estimate than the model prediction (Moriasi *et al*., 2007).

Table 4. General performance ratings for recommended statistics of flow on monthly time step.

Performance Rating	E_{NS}
Very Good	$0.75 < E_{NS} < 1.00$
Good	$0.65 < E_{NS} < 0.75$
Satisfactory	$0.50 < E_{NS} < 0.65$
Unsatisfactory	$E_{NS} < 0.50$

Source: Moriasi *et al*. (2007).

3.7.6. Simulation of soil water availability

In baseline period, since there is no observed data of soil water availability in the study area, the determination of soil water availability were assessed after an intensive model calibration and validation for stream flow. SWAT model provides two methods for estimating surface runoff. Those includes SCS curve number method (SCS 1972) and Green and Ampt infiltration method (1911). Even though the Green and Ampt infiltration method is better in estimating runoff volume accurately, unavailability of sub-daily time step data makes it difficult to use for this study (Ephrem, 2011). Hence, the SCS curve number method which depict in equation (3) was used for this study to estimate surface runoff.

3.8. CROPWAT Model

For this study the meteorological modeling, CROPWAT 8.0 for window was selected to determine Maize water needs on a decadal (10-day) basis. CROPWAT 8.0 is an update of

earlier versions, which was based on the modified penman method, and is the sole recommended FAO Penman-Monteith method of estimating ET_O. The program uses monthly climatic data for the calculation of reference evapotranspiration. Crop water needs depend on climatic conditions, crop type, soil type; growing seasons and crop production frequency were used.

3.8.1. Determination of onset and offset date of the rainy season

Daily rainfall data of thirty years for baseline (1984-2013) and future (2014-2043, 2044-2073) period of Shola Gebeya station were taken and the mean onset and offset dates, and length of grown period were analyzed. For the purposes of this study, the onset of rainy season is defined as the first occasion from the first of June that records 20mm of rainfall amount or more over a 3-day period, and will not be followed by a period of more than 9 consecutive dry days in the following 30 days (Stern *et al*., 2003). The condition of having no dry spells of more than 10 days after start of rainy season eliminates the possibility of a false start of the season. A period of 30 days is the average length for the initial growth stage of most crops (Allen *et al*., 2005).

The end of season is computed using first-order Markov chain modeling by considering maximum daily evapotranspiration of 5mm and soil available water holding capacity of 100mm. Given with the above definitions, Instat statistical tool (Version 3.36) was used to analyze the daily rainfall data for start and end of rainy. The acquired information was compared with local farmer experience and the true onset and offset dates, and length of grown period were recommending for farmer and other concerned body in the area.

3.8.2. Reference evapotranspiration

The FAO Penman-Monteith method is the sole recommended method for determining reference crop evapotranspiration (Allen *et al*., 2005). This method overcomes the values that are more consistent with actual crop water use data in all regions and climates. First monthly maximum and minimum temperature, relative humidity, sunshine hour, and wind speed data of

thirty years for baseline and future period of two scenarios (RCP4.5 and RCP8.5) were arranged and fitted in CropWat model. Then, the model calculates daily value of reference evapotranspiration based on the FAO Penman-Monteith equation. For this study, in terms of the availability of data and accuracy, FAO-Penman-Monteith ET_O estimation methods were selected.

ETo = (17)

where,

ETo = Reference evapotranspiration(mm/day)

Δ = Slope of the saturated vapour pressure curve (kPa $°C^{-1}$);

R_n = Net radiation (MJ m^{-2} day^{-1});

G = Soil heat flux density (MJ m^{-2} day^{-1});

T_m = Mean air temperature (°C) at 2.0 m;

U_2 = Average wind speed at 2.0 m height (m s^{-1});

e_s = Saturation vapour pressure (kPa) at temperature Tm;

e_a = Actual vapour pressure (kPa); ($e_s - e_a$) is the vapour pressure deficit (kPa); and

γ = Psychrometric constant (kPa $°C^{-1}$).

2.5.3. Soil data

3.8.3.1. Soil sampling procedure

At office, predefined sampling points within the selected area of Kesem subbasin were randomly assigned using geographical information system (GIS) software with Arc GIS 10.1. The combined subbasin shape file and predefined sampling points were converted to KML file to import the data to google earth. After importing to google earth, just by zooming out, agriculturally important land uses were targeted and recorded. Hence, predefined sampling points falling on potential agricultural lands were used for data and soil sample collection.

These were done by emphasizing on the Berehet woreda of Maize production area in the subbasin.

Therefore, depending on this a total of 15 sampling point covering all selected area of Maize production land types were generated for sample collection. During survey work, the pre-defined sample locations were navigated in the field and the location were geo-referenced using the GPS (geographical positioning system) receiver with Arc GIS 10.1. Once the sampling points are navigated and reached, physicochemical description of the selected study basin were performed through soil sample. These were done by classifying the selected area in three classes (higher, middle and lower) depending on its topography, slope and soil heterogeneity. The map of soil sampling point and its class were shown in the Appendix Figure 1.

3.8.3.2. Soil sampling and analysis

For each sampling point, 5 to 10 composite subsamples were taken based on the complexity of topography and heterogeneity of the soil type from three classes by making zigzag shape. Disturbed soil samples were collected using soil auger and then composited. Soil samples were taken at three depths (0-30, 30-60, and 60-90 cm). From the composited sample, one kilogram (kg) of soil was taken with labeled soil sample bag. To reduce the probable of cross-sample contamination among samples, the soil auger and other sampling tools were cleaned before taking the next sample at different locations. After processing (drying, grinding and sieving), the soil were analyzed for soil physicochemical properties following the standard procedure compiled by Sahlemedin and Taye (2000). The analyses were conducted at werer agricultural research centre soil laboratory.

Determination of soil physical properties

Soil physical parameters like soil texture, bulk density (P_d), field capacity (FC), permanent wilting point (PWP), available water holding capacity (AWHC), water infiltration rate were determined using appropriate procedures and methods.

Soil texture of the field was determined in the laboratory using pipette method (Martin, 1993). This is based on direct sampling of the density of the solution. Using a pipette, samples of the suspension (usually 20 cm^3) are withdrawn at a given depth after various periods have elapsed after initiation of sedimentation. As per Stoke's law at a depth 'L' below the surface of the suspension and at time t, all particles whose terminal velocity v is greater than passed below this level e.g silt passes through but clay remains.

Soil bulk density was determined from undisturbed soil sample taken using a metal cylinder (core sampler) of known volume (100 cm^3) that was driven into the soil of desired depth and calculated as the ratio of oven dry weight of soil to a known cylinder core sampler volume. Since bulk density varies considerably spatially, the measurements were taken at three different soil depths of the soil profile and fifteen samples from selected area of the subbasin during wet (maize production period) season. The gravimetric method was used to determine the soil moisture content and calculated as a dry weighed fraction (Michael, 2008).

Soil water content at field capacity and wilting point in percentage (%) value were determined in undisturbed samples, saturated and equilibrated at 1/3 and -15.0 bars on a tension table and pressure-plate apparatus, respectively. When water is no longer leaving the soil sample, the soil moisture was taken as field capacity and when water is longer leaving the soil sample, the soil moisture was taken as permanent wilting point. Available water holding capacity was calculated by finding the differences between moisture percent at field capacity and wilting point (Klute and Dirksen, 1986).

Soil infiltration rate were determined at 3 sample locations (1 subclass x 1 replication /sample) one sample from each class. The measurement on each sample site was done in one replications using double ring infiltrometer as show in the Appendix Table 15.

3.8.4. Crop data

In indication of reference evapotranspiration and soil data, crop (maize) data were used as input for CROPWAT to determine crop (maize) water needs. According to werer agricultural

research centre (WARC, 2016) and inference of local farmers, dominated and recommended maize varieties in middle awash basin is Melkassa hybrid two (MB2). The crop coefficient at different growth stage, root depth and depletion fraction of the crop were used and taken from FAO Irrigation and Drainage (FAO56) and convert to local area. Depletion fraction was affect by ET_O as shown below (Smith and Kivumbi, 2006).

$$P = P_{tab} + 0.04\ (5 - ET_O),\ \text{for } ET_O \approx 5,\ P = 0.55 \quad (18)$$

where: P- depletion fraction, P_{tab} – tabulated depletion fraction

According to Smith and Kivumbi (2006), the K_c value is highly depending on relative humidity and wind speed at mid stage of crop growth. Hence, when the value of relative humidity is high (RH > 80%) and the wind speed is low (u < 2 m/sec) the k_c should be reduced by 0.05 and its values should be increased by 0.05 if the relative humidity is low (RH < 50%) and the wind speed is high (u > 5 m/sec). The intervals out of the above situation were adjusted as:

$$K_{c\ adj} = K_{c\ (tab)} + (0.04(U_2 - 2) - 0.004\ (RH_{min}-45))\ (h/3)^{0.3},\ h = 2m \quad (19)$$

where: $K_{c\ adj}$ - adjusted crop coefficient, $Kc_{(tab)}$ - tabulated crop coefficient, U_2 - wind speed, h- height of crop, RH_{min} - minimum relative humidity

3.8.5. Computation of effective rainfall

Effective rainfall was calculated for the total growing period and their respective growing stages of maize using the USDA, S.C (1985) method. Effective rainfall can be calculated as monthly steps:

$$P_{eff} = P_{month} * (125 - 0.2 * P_{month}) / 125,\ \text{for } P_{month} <= 250\ mm \quad (20)$$

$$P_{eff} = 125 + 0.1 * P_{month},\ \text{for } P_{month} > 250\ mm \quad (21)$$

where, P_{eff} = Effective precipitation; P_{month} = monthly precipitation

3.8.6. Baseline and future period crop evapotranspiration (ET_C)

Crop water needs for maize grown in the study area were estimated for baseline period (1984-2013) and future (2014-2043; 2044-2073) period via RCP4.5 and RCP8.5 scenarios. Monthly reference crop evapotranspiration (ET_O) obtained at 80% probability of exceedance through probability analysis as described by FAO (1998) and the adjusted crop coefficients at different growth stages in CROPWAT 8.0 software were used. The water needs of maize were then derived through a crop coefficient that integrated the combined effects of crop transpiration and soil evaporation into a single crop coefficient (K_c) based on the following relationship;

$$ETcrop = K_c * ET_O \quad (22)$$

where; ET_O is reference crop evapotranspiration, K_c is crop coefficient, ETc is defined as the evapotranspiration from a disease-free, well fertilized crop, grown in large fields, under optimum soil water conditions, and achieving full production under the given ecological environment (Kassam and Smith, 2011).

3. RESULTS AND DISCUSSION

4.1. Data Quality Control and Adjustment for Model Input

4.1.1. Missing data value estimation

Using arithmetic mean method the missing data has been filled to check the data for continuity and consistency. In these work, the method was used for temperature and precipitation data gap filling for station Arerti and Aware Melka and for all parameters of station Shola Gebeya and Aleltu Agriculture. For other parameters of Arerti and Aware Melka station, SWAT model built weather generators by considering data of Shola Gebeya and Aleltu Agriculture stations.

For missing data, SWAT weather generator was filled with no data values by -99 for mentioned parameters. This value enlightens SWAT to generate data for weather variable of that day and the model would then revert to estimate data based on its weather generate program.

4.1.2. Homogeneity test

To select representative meteorological stations, checking homogeneity of group stations is essential. The homogeneity of annual rainfall data for each station was tested using XLSTATA 2017 software by means of SNHT test (Standard Normal Homogeneity Test). As shown in the Table 6 the greater p-value from significance level alpha and the red horizontal broken line shown in the Figure 8 implies homogeneity of rainfall station.

Table 5. Summary statistics of homogeneity test

S.No.	Station name	Variable	Obs	Mean	SD	*To*	P-value	Alpha
1	Aleltu Agriculture	Prec	30	1112.27	211.79	6.93	0.13	0.05
2	Arerti	Prec	30	741.56	194.79	3.39	0.46	0.05
3	Shola Gebeya	Prec	30	937.18	97.48	6.19	0.11	0.05
4	Aware Melka	Prec	30	616.83	145.77	5.92	0.12	0.05

To = statistic derives, SD= standard deviation, prec= precipitation, Obs= observation

Figure 8. Homogeneity test for areal rainfall stations

4.1.3. Consistency analysis

To check consistency of recording data, double mass curve method was used as explained in Subramanya (1998). The accumulated totals of the gauge in question are compared with the corresponding totals for a representative group of nearby gauge station. If a decided change in

the regime of the curve is observed, it should be corrected. Unfortunately, all the selected stations in this study were consistent; there is no need of further correction.

Figure 9. Consistency test graph for all stations

4.1.4. Estimation of model input areal data

To compute spatial areal rainfall, Theissen polygon method was used in ArcGIS environments. By taking each subbasin, the Theissen gauge weights developed for sub-catchments with more than one rainfall gauging stations are presented in Table 6.

Table 6.Theissen gauge weights for Kesem subbasin

S.No.	Rainfall stations	Area weight (km^2)	Gauge weight (%)
1	Shola Gebeya	985	43.28
2	Arerti	548	24.08
3	Aleltu Agriculture	569	25.00
4	Aware Melka	174	7.64

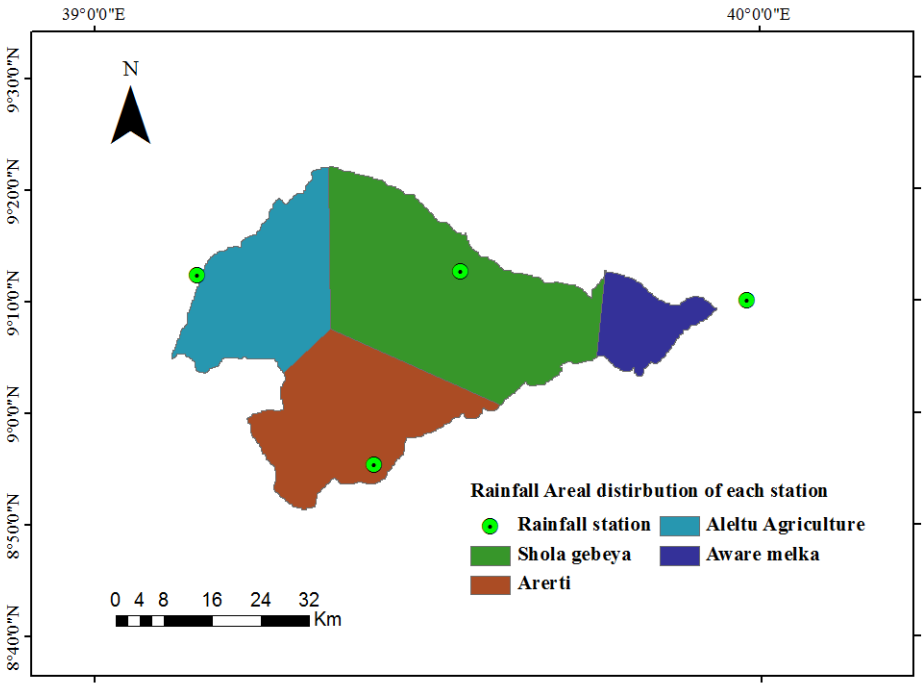

Figure 10. Theissen polygon developed for Kesem subbasin

4.2. Climate Change

4.2.1. Baseline change

The baseline scenarios downloaded for the four stations; 30-year period from 1984 to 2013 was selected for Aware Melka, Shola Gebeya, Aleltu Agriculture and Arerti as representatative of this study area. Thus, the ensembles of RCM model output was downloaded for the baseline period and were checked with observed data. In some stations the downloaded base line temperatures shows over and under estimation with observed data. In the case of precipitation, also even though there were little variations in individual months of all stations, the downloaded values have well captured with observed data. In general, in all stations the

downloaded climate variables (precipitations, maximum and minimum temperatures) have not shown good fit with observed data. That is why it needs bias correction for impact studies with base period data (Shabalova *et al*., 2003; Kleinn *et al*., 2005).

4.2.1. 1. Rainfall

Rainfall is the most variable and fundamental element in the climate system and its characteristics as bimodal pattern in the study area. Similarly, various authors have reported the bimodality of rainfall pattern in Central Rift Valley of Ethiopia in general (Kassie *et al.,* 2013) and at middle Awash in particular. The mean annual rainfall was calculated as 616.8mm and 610.8mm, 1114.12mm and 631.91mm, 983.58mm and 899.28mm, 436.74mm and 663.23mm for station Aware Melka, Shola Gebeya, Aleltu Agriculture and Arerti for both observed and model output of baseline period respectively based on the long term rainfall data.

Figure 11 shows the comparison between observed and downloaded data for base line period at Shola Gebeya, Arerti, Aleltu Agriculture and Aware Melka station. The graph shows maximum changes at Shola Gebeya and Arerti stations, and minimum changes at Aware Melka stations

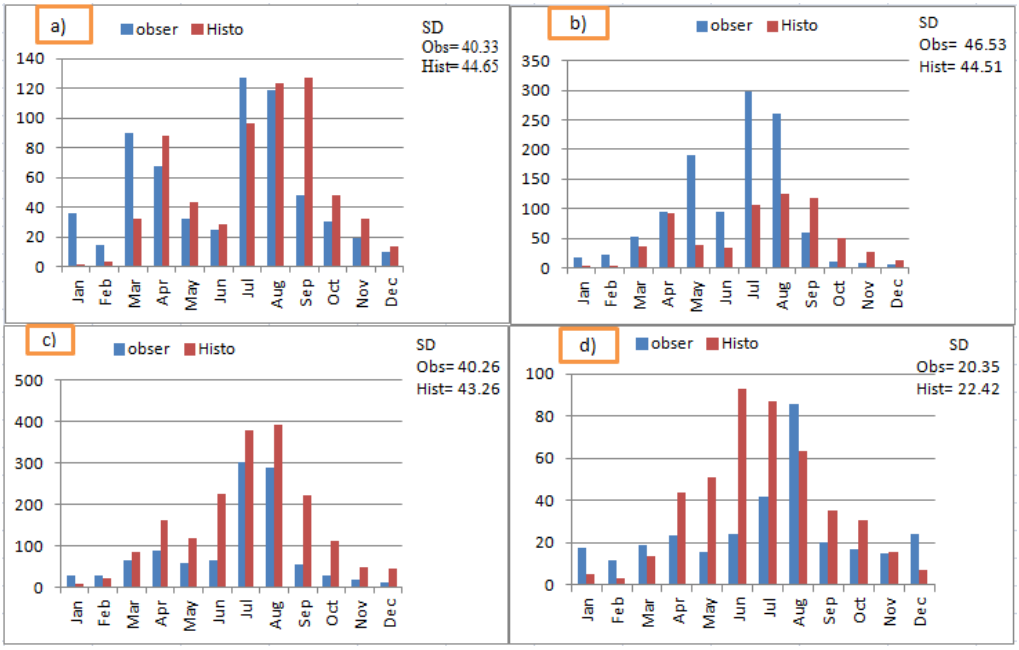

Figure 11. Baseline period of each meteorological stations observed and historical model rainfall data. STD= Standard deviation, a) Aware Melka; b) Shola Gebeya; c) Aleltu Agriculture; d) Arerti

On the seasonal basis, maximum rainfall was shown during kirmet season for all stations with the range of 173 to 713.95 mm for observed and 279 to 1215 for downloaded data of base period. Therefore in the subbasin historical model output shows over estimation than observed data of each station during kirmet season. Hence bias correction is needed for future impact studies.

4.2.1.2. Maximum temperature

During base line period as it depict in the Figure 12, the observed mean monthly maximum temperature shows over estimation at station Aware Melka and Aleltu Agriculture compared

with model output and under estimation for station Shola Gebeya and Arerti on monthly basis. It ranges from 23.6 to 36.3^{o}C for observed and 21.2 to 29.43^{o}C for downloaded data of base period. In the sub basin maximum temperature of observed data were shown at station Aware Melka and minimum temperature at Shola Gebeya and Aleltu Agriculture as shown in the Figure 12. On seasonal basis, maximum temperature were shown at belg season for station Shola Gebeya and Aleltu Agriculture and on kiremt season at Arerti station for both observed and model data.

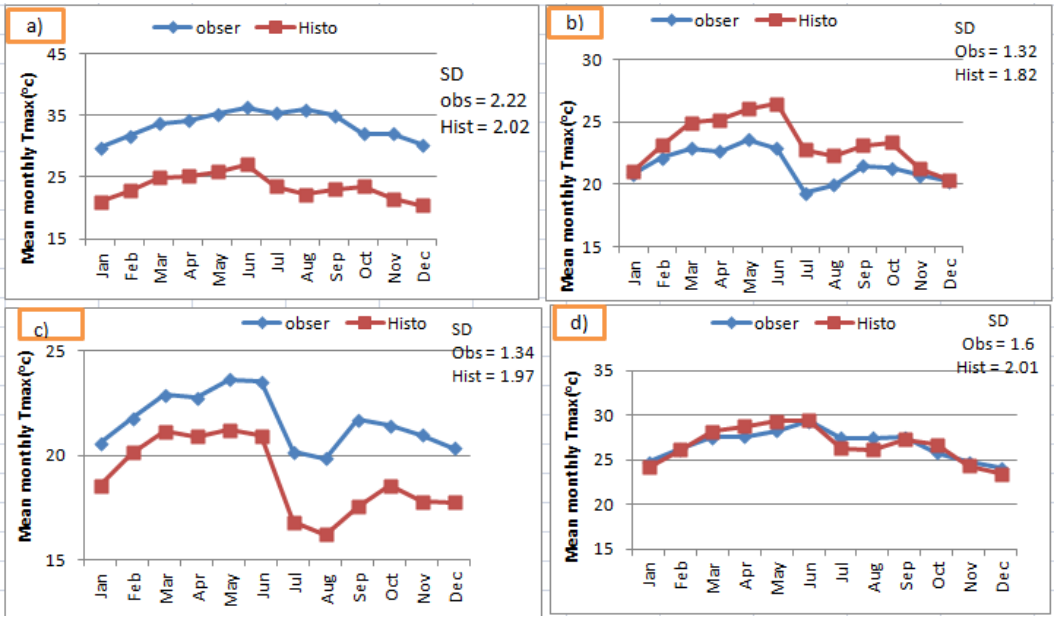

Figure 12. Baseline period of each meteorological stations observed and historical model maximum temperature data. STD= Standard deviation, a) Aware Melka; b) Shola Gebeya; c) Aleltu Agriculture; d) Arerti

4.2.1.3. Minimum temperature

During base line period as it shown in the Figure 13, the mean monthly model output minimum temperature shows over estimation at three stations except station Aware Melka as compared with observed data on monthly basis. It ranges from 2.71 to 7.73^{o}C for observed and 5.1 to 7.70^{o}C for downloaded data of base period. In the sub basin min maximum temperature were shown at station Aware Melka and min minimum temperature at Shola Gebeya and Aleltu

Agriculture as shown in the Figure 13. On seasonal basis, minimum temperature was shown at bega season for all stations and maximum temperature at kirmet season of both observed and model output data. Generally, observed and historical model outputs are mismatch; therefore bias correction was needed for impact studies.

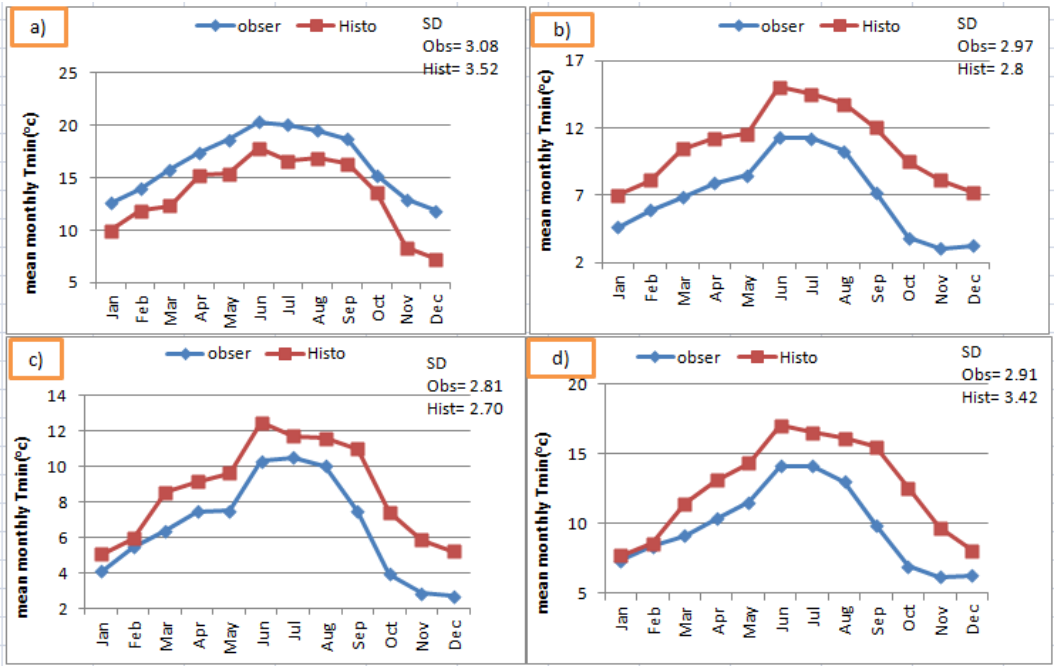

Figure 13. Baseline period of each meteorological station observed (obs) and historical model (Hist) minimum temperature data. STD= Standard deviation, a) Aware Melka; b) Shola Gebeya; c) Aleltu Agriculture; d) Arerti

4.2.2. Future change

Future climate scenarios downloaded for three climate variables (precipitation, maximum and minimum temperature) with the aid of CORDEX Africa RCM model, the ensembles of RCM model output are used for development of future climate scenarios on daily time series basis for the period of 30 years (2020s and 2050s) for both RCP4.5 and RCP8.5 scenarios. The following sections presents the future changes in climate for each meteorological station with corresponding changes for the climate variables.

4.2.2.1. Projected annual rainfall change

The diversity of rainfall patterns is inherent and naturally explained as erratic in this region. Here the downloaded values of precipitation for the future were averaged into a yearly time step and the bias was corrected with the base period for each year based on the technique described in chapter three.

As shown in Figure 14, generally, its trend is likely to have a change of -68% to +18.24% for bias uncorrected and +0.001% to +27.92% for bias corrected from the base period of both scenarios for ensemble of RCM model output. Yet, each station perceives a different trend. From the RCM model output two and one stations show increasing annual rainfall for RCP4.5 and RCP8.5 scenario within the range of +1.8% to +27.92% and +16% to +24.73% respectively for bias corrected. However, stations like Arerti and Aleltu Agriculture show an increasing trend for near century (2020s) and decreasing trend for mid-century (2050s) period of RCP4.5 scenario and decreasing trend for RCP8.5 scenario of RCM model output.

Regarding to unbiased correction, three station shows the increasing trend in range of +0.06 to + 20.03% and +0.06 to +18.24% for RCP 4.5 and RCP 8.5 scenario respectively and station shola gebeya shows decreasing trend for near century (2020s) and mid-century (2050s) period for both RCP4.5 and RCP8.5 scenario within the range of -61.5 to 37.6 and -68.8 to -44.6 respectively. Generally, the mean annual rainfall in the sub basin shows increasing trend within the range of +5.7 to +9.51% and +3.45 to +6.43% for both RCP4.5 and RCP 8.5 scenario for bias corrected respectively and inverse for bias uncorrected. This result clearly implies that Wet condition will be the prevailing weather of the future in the sub basin. The result of this analysis is quite similar with the result obtained by Sahilu and Nigussie (2015).

According to their study the uncorrected version of inter-annual rainfall variability, in the Central Rift Valley of Ethiopia, shows the decreasing trend. This similarity possibly arises due to the analogous in spatial coverage of the two studies. IPCC (2011) also point out that there would be a likely increase of rainfall over areas of central and eastern Africa for high emission scenario. Similarly, Cook and Vizy (2013) projected as there would be heavy precipitation over

the eastern Africa region. The bias corrected version shows that the total annual rainfall decreased from greater than 1000 mm to less than 200 mm due to bias correction.

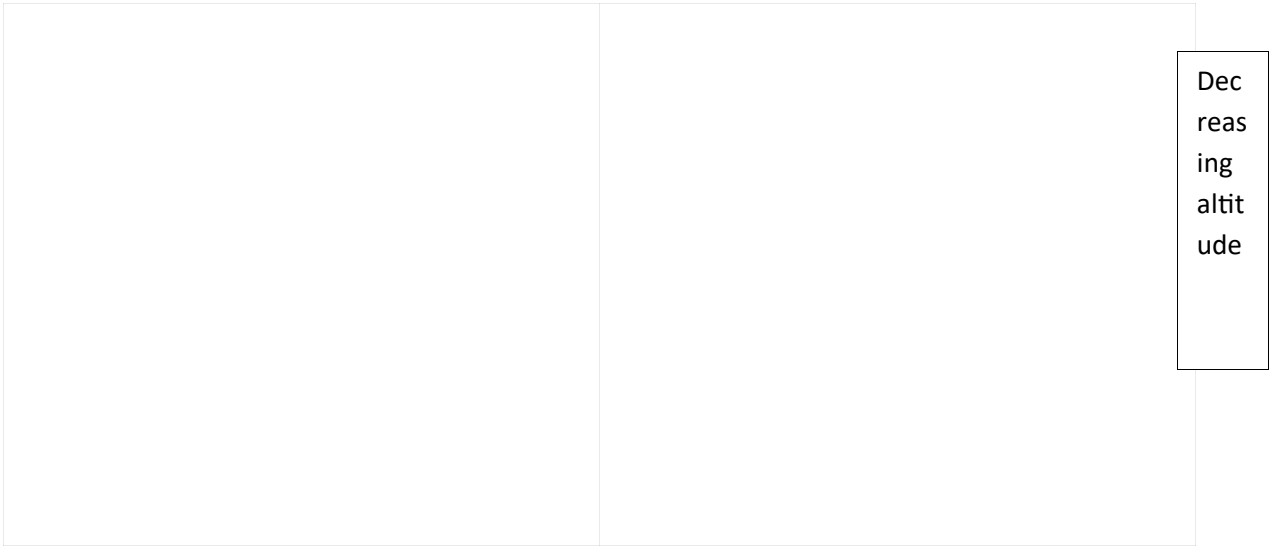

Figure 14. Projected percentage change in annual rainfall from base period for RCP 4.5 and RCP8.5 scenario, Ensemble of RCM model output, stations are ordered by decreasing altitude

4.2.2.2. Projected seasonal and monthly rainfall

The sub basin has two rainy season (bi-modal) "*Kiremt*" begins beginning of June and ends mid of September (JJAS) and "*Belg*" starts at beginning of February and ends last part of May (FMAM).

For bias corrected, *Kiremt's* precipitation change did not obvious a systematic increase or decrease for both RCP4.5 and RCP8.5 scenarios. About 0.41 to 20.1% *kiremt* precipitation changes will be expected for stations Shola Gebeya and Aware Melka; stations Aleltu Agriculture and Arerti shows decreasing trend by about 0.22% to 2.4% and by more than 20% for both RCP4.5 and RCP8.5 scenario of bias corrected respectively. The *belg* precipitation changes by about -26% to +19.1% for stations shola gebeya, Aware Melka and Aleltu

Agriculture and decreasing trend by more than 25% in Arerti station for both scenarios in all time horizons (Figure 15).

For bias uncorrected, the precipitation change for *kirem*t will be expected by about -69% to -21% for station Arerti and Shola Gebeya and +20% to 149.4% for station Aware Melka and Aleltu Agriculture and for *belg* about -69.35% to -0.64% for stations Arerti, Aware melka and Shola Gebeya and +10% to 80% for station Aleltu Agriculture will be expected under both RCP4.5 and RCP8.5 scenarios. In the case of the main rainy months (*Kiremt*) the analysis of the uncorrected projection shows that there will be decrease of rain by 2020s and 2050s for both scenarios. This result is in conformity with Sahilu and Nigussie (2015).

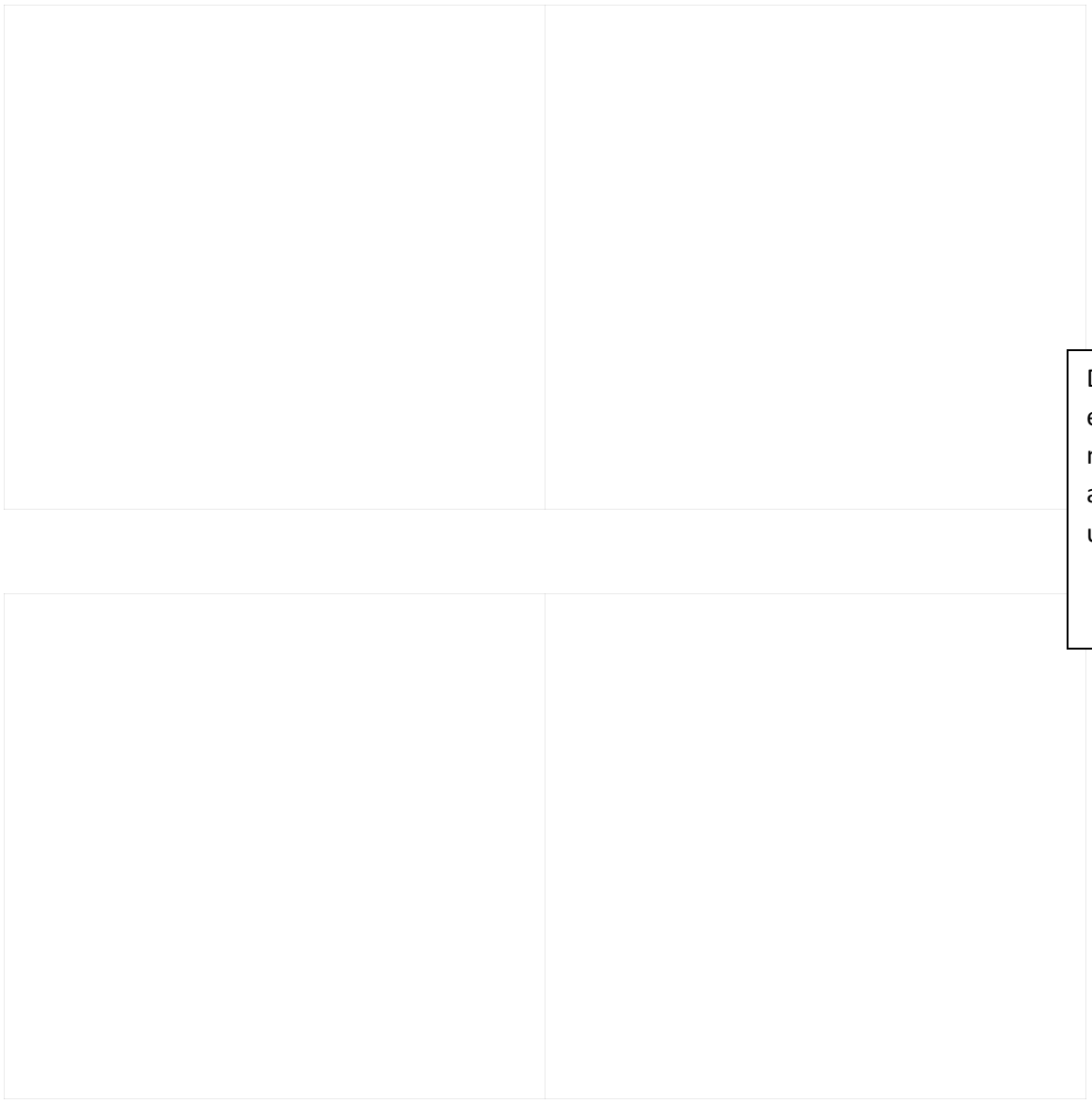

Figure 15. Projected percentage change in seasonal rainfall from base period for RCP 4.5 and RCP8.5 scenario, Ensemble of RCM model output, stations are ordered by decreasing altitude.

Generally ensemble RCM model output shows *Kiremt* precipitation change in the range -0.22% to +18.8% and -2.44% to +20.1% and for *belg* by about -2.6 to 19.1 and -30% to -13.5 for both RCP4.5 and RCP 8.5 scenario respectively in near and mid-century, except stations Arerti which show decreasing trend by more than 25% change for bias corrected. As indicated in Figure 15, RCM model output for both scenario projected *Kiremt* rainfall likely to change by -0.22% to +21.1% for the Kesem subbasin. Normally Ensemble RCM model output shows a

similar direction of change for rainy seasons in the time period (2014-2073), nevertheless higher differences are found for stations Arerti under both scenarios for bias corrected (Figure15)

In the case of monthly bases of bias corrected, particularly on the month of July and August, the increasing rainfall would be expected for station Aware Melka, Aleltu Agriculture and shola gebeya for RCP8.5 and decreasing in Aleltu Agriculture, constant in Aware Melka and increasing for Shola Gebeya for RCP4.5 scenarios. But station Arerti in all rain month shows erratic change in sub basin. In February to May; +0.2 to +1% would be anticipated. This result contrast that of (Kassie *et al.,* 2013) which suggested that under intermediate warming scenarios, parts of equatorial East Africa will likely increase rainfall from December to February and decrease rainfall from June to August by 2050. Rowell (2012) and Asfaw *et al*. (2013) also confirmed that precipitation projections are more uncertain than temperature projections and precipitation projections are exhibit higher spatial and seasonal dependence than temperature projections. Generally the monthly analysis revealed that the main rain season of the study area would be highly affected by the future climate change condition with respect to amount and distribution.

4.2.2.3. Projected annual maximum temperature

The downloaded values of maximum temperature for the future period were averaged into a yearly time step and the bias was corrected with the base period for each year based on the technique prescribed in chapter 3 as that of precipitation. As depicted in Figure 16, it can be seen that generally increasing annual trend is likely for maximum temperature in all stations for bias corrected under both scenarios for near and mid-century. In case of bias uncorrected, the annual maximum temperature of the sub basin shows increasing trend in station of Shola Gebeya and Arerti for near century and station Shola Gebeya, Arerti and Aleltu Agriculture for mid-century of both scenarios. And decreasing trend would be expected at station of Aleltu Agriculture and Aware Melka for near century and only Aware Melka for mid-century.

Ensemble of RCM model output result shows that there might be a general incremental trend of maximum temperature for RCP4.5 and RCP8.5 scenarios for the period of near and mid-century in the range of +0.95°C to +1.98°C and +1.38°C to +2.83°C respectively. It is also noted that the projected change appears to show generally increasing trend with decreasing altitude in the basin (Figure 16) for bias corrected and this result is consistent with (Tekleab *et al*., 2013).

In case of bias uncorrected for both scenarios, generally increasing annual trend will be expected for the period of near and mid-century in the range of +0.93°C to +3.76°C and +1.3°C to +4.61°C respectively. However, the decreasing annual trend for Aleltu Agriculture and Aware Melka stations for near and mid-century in the range of -9.16°C to -0.9°C and -8.73°C to 2.83°C respectively. It doesn't feel the results are correct, however, the sub basin wide temperature increase is evident even with this mode for bias correction.

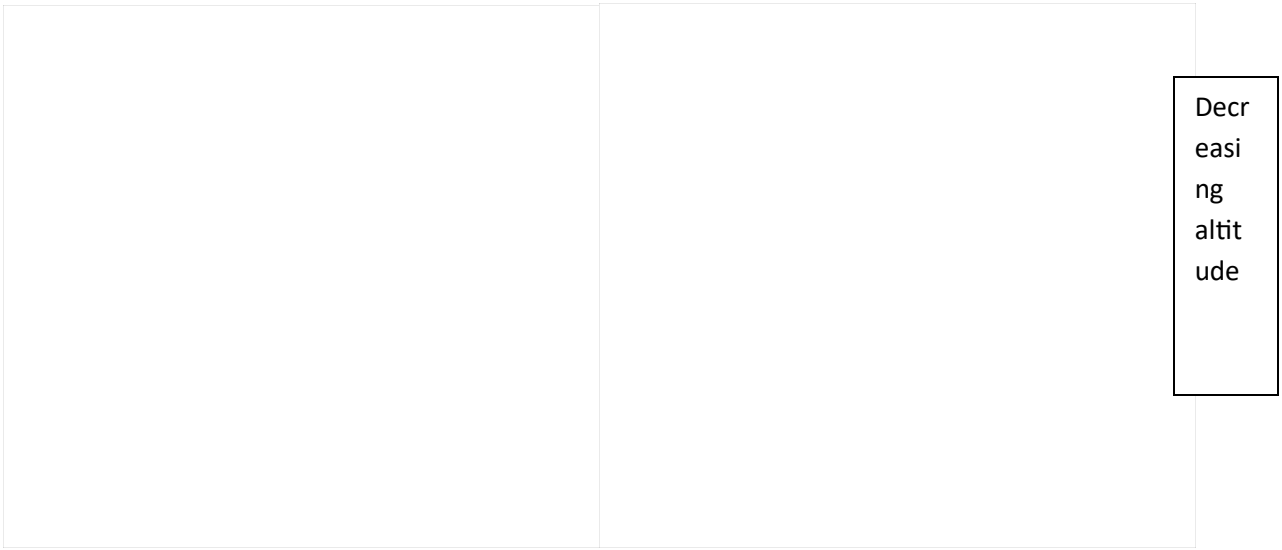

Figure 16. Projected change in annual Tmax from base period for RCP4.5 and RCP8.5 scenario, Ensemble of RCM model output, stations are ordered by decreasing altitude.

Other studies in Ethiopia and the central part in particular shows similar pattern to this work. Kassie *et al.* (2013) found mean temperatures increasing to 0.8°C in 2020s and 1.2°C in 2050s in Ethiopia. Conway (2011) also indicates that, with respect to the future climate in the Nile basin, there is high confidence that the temperature will increase. Also projected that, the change in average temperature would be in the range of 1.0°C to 1.1°C by 2020s, in the range of 1.8–2.0°C by 2050s over the central part of Ethiopia relative to the 1961–1999 normal.

4.2.2.4. Projected seasonal and monthly maximum temperature

In seasonal and monthly basis, looking for the maximum temperature change scenario has great practical importance, because in the sub basin activities like Agriculture specially crop water requirement on rain-fed was stand. As compared with observed maximum temperature, the bias uncorrected downloaded data comparatively shows a tendency of underestimation (colder) for stations Aware Melka and Aleltu Agriculture and overestimation (warmer) for stations Shola Gebeya and Arerti for both scenarios. And the bias corrected shows overestimation (warmer) for all stations under both scenarios of two century.

The Mean Absolute Error (MAE) was calculated and a positive and negative result was obtained for both scenarios. Thus, the MAE of bias uncorrected ranges from -9.16ºC to -7.33ºC, -1.73ºC to +0.12ºC, +0.93ºC to +4.61ºC and +0.93ºC to +2.71ºC for both RCP4.5 and RCP8.5 scenario for station Aware Melka, Aleltu Agriculture, Shola Gebeya and Arerti respectively. And for bias corrected it ranges from 0.9ºC to +2.73ºC, +0.95ºC to +2.80ºC, +1.38ºC to 4.30ºC and +0.93ºC to +2.75ºC for both RCP4.5 and RCP8.5 scenario for station Aware Melka, Aleltu Agriculture, Shola Gebeya and Arerti respectively (Figure 17 and 18). This implies that the RCMs output exhibited a tendency of overestimate in the sub basin for bias corrected.

Based on monthly analysis, the observed value shows that maximum temperature begins to rise from the month of May to Sept for Aware Melka, March to June for Aleltu Agriculture, April to Sept and Feb to June for Shola Gebeya and March to September for Arerti station respectively for bias corrected under both scenarios.

In the case of bias uncorrected projections, all the monthly patterns for the two scenarios show a tendency for underestimation of the downloaded variables. This result shows that the observed ones appear with warmer temperature relative to the projected ones for all stations under both scenarios. Often, the uncorrected downloaded temperature value appears warmer than the observed one (Terink *et al*., 2010).

Obs-observed, SD-standard deviation, MAE- means absolute error, uncor-bias uncorrected, cor-bias corrected

Figure 17. Projected change in monthly Tmax from base period for RCP 4.5(left panel and RCP8.5 (right panel) scenario, Ensemble of RCM model output, station Aware Melka (top panel) and Aleltu Agriculture (bottom panel).

Obs-observed, SD-standard deviation, MAE- means absolute error, uncor-bias uncorrected, cor-bias corrected

Figure 18. Projected change in monthly Tmax from base period for RCP 4.5(left panel) and RCP8.5 (right panel) scenario, Ensemble of RCM model output, station Shola Gebeya (top panel) and Arerti (bottom panel).

The change in maximum temperature for the bias corrected version reveals that there is an increasing in maximum temperature during *Kiremt* for station Aware Melka and Arerti and begins to decline for the rest station. This temperature fall is possible due to the likely increase of cloud cover in the area. For *Bega* seasons, increasing maximum temperature would be shown for shola Gebeya and Aleltu Agriculture in both RCP4.5 and RCP8.5 scenarios. Sahilu and Nigussie (2015) confirmed that there would be an increase of rain in the *Bega* season in the central rift valley. With further insight in Figure 17 and 18, it is observed that the basic seasonal pattern of maximum temperature does not change in either of the two scenarios, except on April, March May and June. Nonetheless, the peak maximum temperature value shifts to the end month of May and beginning June during *kiremt* from its historical position, in both scenarios.

4.2.2.5. Projected annual minimum temperature

As regards to minimum temperature, the future scenario shows increasing trend for all stations with the range of +1.04°C to +3.02°C and +0.03°C to 5.13°C under both scenario for near and mid-century. Here the projection shows that minimum temperatures have increased slightly faster than maximum temperatures for these all stations for bias corrected under RCP4.5 and RCP8.5 scenarios. In case of bias uncorrected for both scenarios, generally increasing annual trend will be expected for the period of near and mid-century in the range of +3.38°C to +5.75°C and +1.85°C to +6.80°C respectively for station Shola Gebeya, Arerti and Aleltu Agriculture. However, the decreasing annual trend shown in Aware Melka station for near and mid-century in the range of -4.6°C to -3.69°C and -4.35°C to -2.64°C respectively for both scenarios.

This result shows that the highest temperature difference considering minimum temperature in both bias uncorrected and corrected was 6.8^{o}C. On the other hand, the lowest difference was 0.03^{o}C in either case. Generally, in the sub basin the minimum temperature increasing annual trend will be expected in the range of +0.03°C to +5.30°C for all stations of bias corrected and consistency with the result of (IPCC, 2013; Tekleab *et al*., 2013) and +1.85°C to 6.80°C for all

stations of bias uncorrected respectively for RCP4.5 and RCP8.5 scenario except decrease trend for Aware Melka station of bias uncorrected as shown in Figure 19.

Figure 19. Projected change in annual Tmin from base period for RCP 4.5 and RCP8.5 scenario, Ensemble of RCM model output, stations are ordered by decreasing altitude.

4.2.2.6. Projected seasonal and monthly minimum temperature

As that of maximum temperature, looking for seasonal and monthly basis minimum temperature change scenario has great practical importance. As compared with observed minimum temperature, the bias uncorrected downloaded data comparatively shows a tendency of underestimation (colder) for stations Aware Melka and overestimation (warmer) for stations Aleltu Agriculture, Shola Gebeya and Arerti for both RCP 4.5 and RCP8.5 scenarios. And the bias corrected shows overestimation (warmer) for all stations under both RCP4.5 and RCP8.5 scenarios.

The Mean absolute error (MAE) was calculated and a positive and negative result was obtained for both scenarios. Thus, the MAE of bias uncorrected ranges from -4.61ºC to -2.64ºC for Aware Melka, 3.11ºC to +6.80ºC for station Aleltu Agriculture, Shola Gebeya and Arerti respectively for both RCP4.5 and RCP8.5 scenarios. And for bias corrected it ranges from 1.05ºC to +3.24ºC, for all station of both RCP4.5 and RCP8.5 scenario (Figure 20 and

21). This implies that the RCMs output exhibited a tendency of overestimate in the sub basin for bias corrected.

Obs-observed, SD-standard deviation, MAE- means absolute error, uncor-bias uncorrected, cor-bias corrected

Figure 20. Projected change in monthly Tmin from base period for RCP 4.5(left panel) and RCP8.5 (right panel) scenario, Ensemble of RCM model output, station Aware Melka (top panel) and Aleltu Agriculture (bottom panel).

Obs-observed, SD-standard deviation, MAE- means absolute error, uncor-bias uncorrected, cor-bias corrected

Figure 21. Projected change in monthly Tmin from base period for RCP 4.5(left panel) and RCP8.5 (right panel) scenario, Ensemble of RCM model output, station Shola Gebeya (top panel) and Arerti (bottom panel).

Based on monthly analysis, the observed value shows that maximum temperature begins to rise from the month of April to Sept for Aware Melka, June to August for Aleltu Agriculture, May to August and June to August for Shola Gebeya and June to August and May to August for Arerti station respectively for bias corrected under both scenarios. Subsequently, it begins to decline from the month of September for station Aleltu Agriculture and August for Shola Gebeya and Aware Melka.

In the case of bias uncorrected projections, the monthly patterns for the two scenarios show a tendency for underestimation of the downloaded variable for Aware Melka. However, the result shows that the observed one appear with warmer temperature relative to the projected which shows overestimation (warmer) for stations Aleltu Agriculture, Shola Gebeya and Arerti in both RCP4.5 and RCP8.5 scenarios. Often, the uncorrected downloaded temperature value appears warmer than the observed one (Terink *et al*., 2010).

The change in minimum temperature for the bias corrected version reveals that there is increasing in minimum temperature during *Kiremt* and *Belg* for all station in RCP4.5 and RCP8.5 scenarios. With further insight in Figure 20 and 21, it is observed that the basic seasonal pattern of minimum temperature does not change in either of the two scenarios, except on April, May and June.

4.3. SWAT Model

4.3.1. Watershed delineation and HRU definition

Based on DEM, the study area was divided into 27 subbasins based on threshold area of 113.8 km^2 and 347 HRUs. The total drainage area derived from SRTM was calculated to be 2276km^2, with an average slope and elevation of 19.85% and 2015m above sea level respectively. The subbasin area ranged from 0.99 km^2 to 217 km^2 with an average area of 216.63km^2. The delineated subbasin is shown in the Figure 22.

SWAT divides all subbasins into one or more representative HRUs by defining and overlaying the land use, soil and slope of the area. Sub dividing the subbasin into areas (HRU) having unique land use, soil and slope combinations enables the model to reflect deference in water

balance, soil moisture and other hydrologic process for different land use and soils. In order to balance the number of HRU, threshold values (minimum percentage of the feature in the basin) were determined respectively for land use/cover (20%), for soil (10%) and slope (20%) in this study. SWAT simulates water balance, PET and soil moisture availability for each HRU and path to the outlet to obtain the water balance (steam flow) yield. Figure 22 shows delineated watershed and subbasins of the study area.

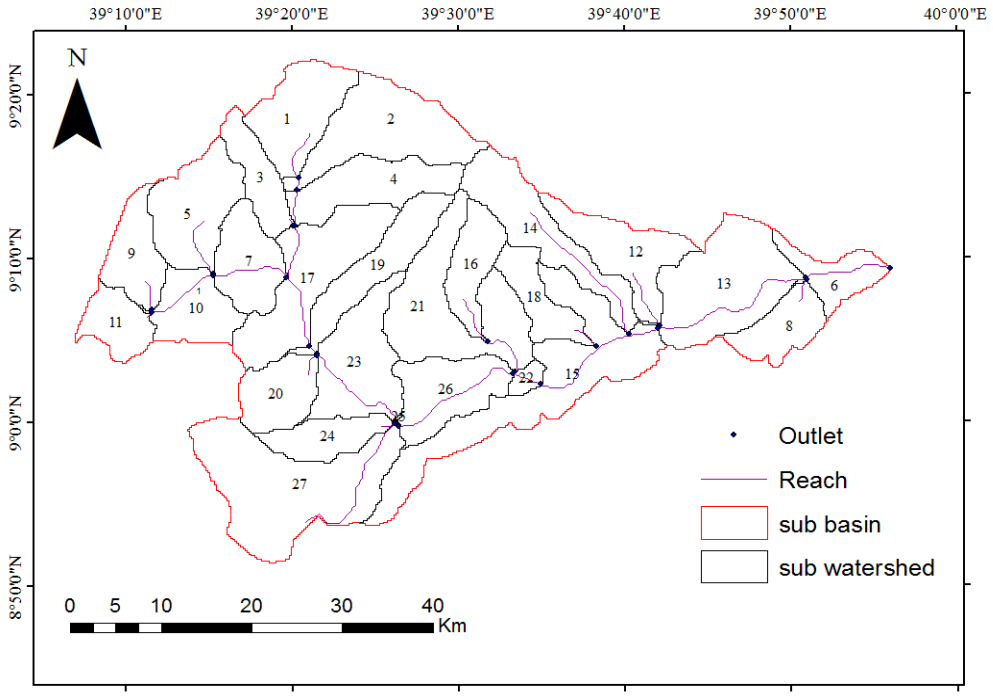

Figure 22. Delineated watershed of Kesem subbasin.

4.3.2. Catchment characteristics

4.3.2.1. Land use/cover characterization

As described in chapter three, the land use/cover used for this analysis was used for baseline scenario of two periods (1998 and 2013). The land use/cover of first period consists of seven land use types and of second period consist nine land use/cover types which were described in Table 7; with the dominance of Agricultural land use. A reclassification of the land uses was implemented by using a land use lookup table to group similar crops into one category and to define SWAT land use/covers type during model setup.

Table 8. Land use/cover type and their change in period for Kesem subbasin

Land use/cover type	S W A T code	LULC(1998)		LULC (2013)		Change (%)
		Area km2	Area (%)	Area km2	Area (%)	
Acacia	FRSD	524	23.02	236.00	10.37	-12.65
Agricultural land	AGR	1461	64.19	1765.00	77.55	+13.36
Bare land	BARR	14	0.62	15.00	0.66	+0.04
Eucalyptus	EUC	25	1.10	10.00	0.44	-0.66
Forest	FRST	3	0.13	44.00	1.93	+1.80
Settlement	URBAN	1	0.044	4.72	0.20	+0.16
Shrub land	RNGB	248	10.90	197.00	8.66	-2.24
Grass land	PAST	*	*	0.28	0.001	0.001
Water body	WATR	*	*	4.00	0.18	0.18
Total Area (%)		2276.00	100.00	2276.00	100.00	

* - shows there are no land use, LULC- land use/cover

As shown in the above table, LULC change of the Kesem subbasin in different period of baseline shows increasing and decreasing trends. The percentage change of LULC shows negative and positive sign which implies decreasing and increasing trend in the subbasin. As a result of this, in the year of 2013, the new land use/cover types were created when compared to the year 1998. This was due to decline of shrub and acacia for creation of grass land and the construction of reservoir for Kesem irrigation project for sugar plantation at downstream and other man made pond formation for water body in the subbasin.

(a)

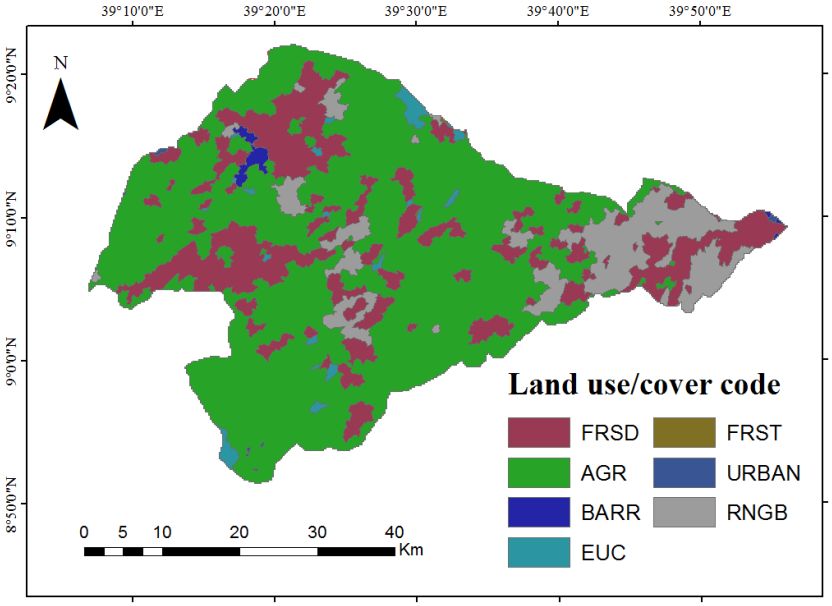

(b)

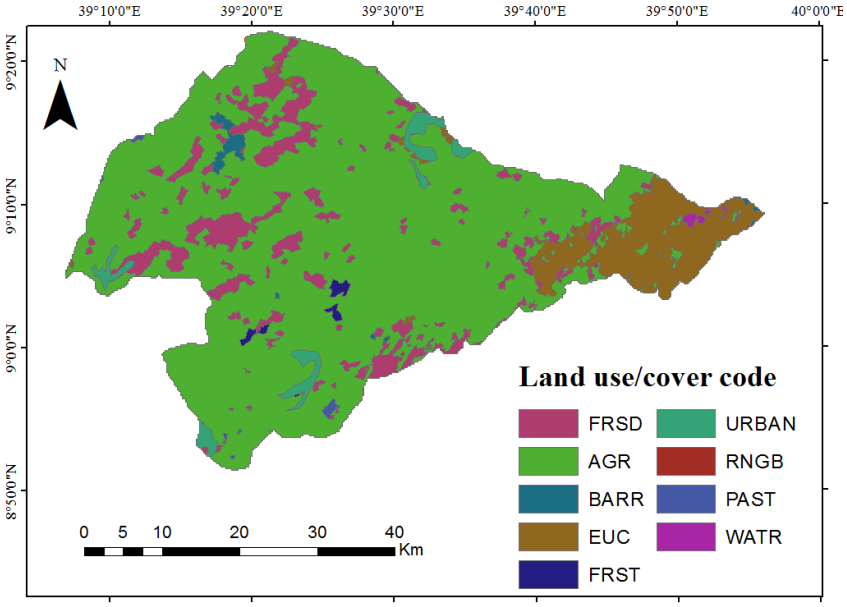

Figure 23. Land use/cover map of Kesem subbasin for baseline period. (a) LULC of 1998; (b) LULC of 2013

4.3.2.2. Soil characterization

The subbasin is covered with six different soil types such as chromic luvisols, eutric cambislos, eutric leptosols, eutric vertisols, lithic leptosols and vertic cambislos with their total aerial coverage of 0.31%, 6.85%, 16.30%, 6.37%, 53.74%, and 6.43% respectively.

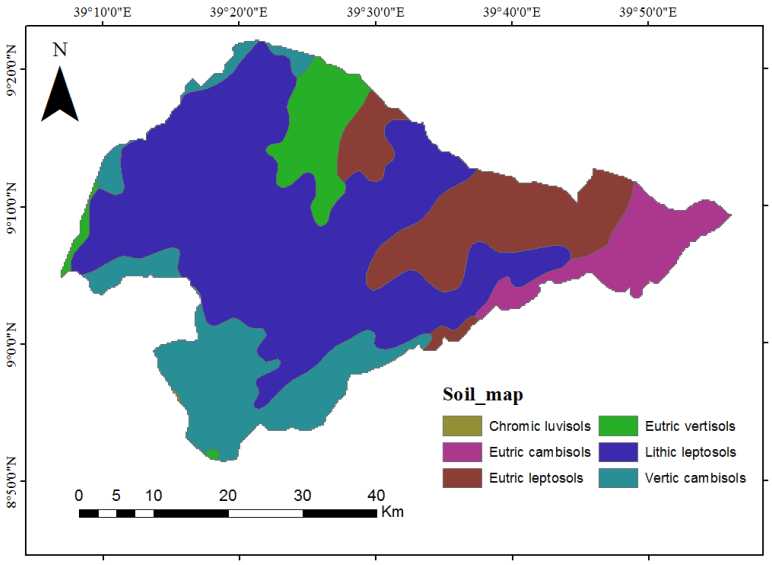

Figure 24. SWAT delineated subbasins with soil types in the Kesem subbasin

4.3.2.3. Slope characterization

As shown in the Table 8, 30.15% of the subbasin lies within slope less than 5% and while 13.34% of the area lies within slope of greater than 20% slope class. Most of the agricultural area lies within the slope of 5-10% and most of the riparian areas were located in the slope of less than 20% as it shown in the Figure 2.

Table 8. Kesem subbasin slope class based up on FAO classification system.

No	Slope class	Description	Area (km^2)	Area (%)

1	0-5	Flat to almost flat	686.30	30.15
2	5-10	Gently flat to undulating terrain	620.33	27.26
3	10-15	Rolling terrain	404.65	17.78
4	15-20	Hilly terrain	261.10	11.47
5	>20	Slope desiccated to mountainous terrain	303.62	13.34
Total			2276.00	100.00

4.3.3. **Model sensitivity analysis**

Even though 28 parameters were well thought-out for the sensitivity analysis, only 14 of them are effective for monthly flow simulation analysis of baseline period of fifteen years with the category of sensitivity ranging from very high to small. The parameters identification was done by using monthly flow data from 1984-1998. Global sensitivity analysis was done for parameter as shown in the Table 9. According to the result from global sensitivity analysis, the most sensitivity parameters for Kesem subbasin simulation are those representing surface runoff, ground water recharge, soil water and slopes. Generally, the selected are within the range of parameter used by Mutenyo *et al*. (2013) for the evaluation of SWAT performance on mountains of tropical Africans.

In this study, the response of the model towards parameter involves ground water parameters and BALI was found to be the low sensitive parameters in water balance simulation. On the other hand parameters involving CN2 and HRU-SLP found to be the most effective hydrologic parameters for the simulation of water balance. Process occurring at soil level followed at the second position parameter as pointed out by sensitivity of ESCO, Sol_Awc, Sol_Z, and EPCO. As they shown in Table 9, the larger absolute values of t-statistics and their p-values are significant at 5% level of significance. Sensitive parameters, t-test, p_value, parameter ranking and their category are presented in the Table 9. A brief description of each hydrologic parameter are listed in the SWAT model user's manual (Neitsch *et al*., 2005).

Table 9. Results of sensitivity analysis of parameters

Flow Parameters	t_test	P_vluae	Rank	Category of Sensitivity
Initial curve number (II) value; CN2	-51.02	0.00	1	High
Manning's "n" value for overland flow; OV_N	11.432	0.00	2	High
Average slope steepness [m/m];	8.851	0.00	3	High

HRU_SLP				
Soil evaporation compensation factor; ESCO	-6.08	0.00	4	High
Available water capacity [mm water /mm soil];Sol_Awc	2.898	0.000376	5	Medium
Soil depth [mm]; Sol_Z	2.612	0.00659	6	Medium
Saturated hydraulic conductivity [mm/h]; Sol_K	2.136	0.00836	7	Medium
Maximum potential leaf area index; Blai	1.948	0.06980	8	Medium
Groundwater Delay [days]; Gw_Delay	1.8134	0.0984	9	Medium
Threshold water depth in the shallow aquifer for flow [mm]; Gwqmn	-1.519	0.12891	10	Medium
Threshold water depth in the shallow aquifer for "revap" [mm]; Revapmin	-0.649	0.5161	11	Small
Groundwater "revap" coefficient; Gw_Revap	-0.126	0.8996	12	Small
Surface runoff lag time; Surlag	-0.074	0.9476	13	Small
Base flow alpha factor [days]; Alpha_Bf	-0.063	0.96072	14	Small

4.3.4. Model performance evaluation

4.3.4.1. Model calibration

Model calibration followed sensitivity analysis. To improve the efficiency of the model during calibration the top fourteen ranking parameters were considered to account for the over and under prediction processes of the model as suggested by Neitsch *et al*. (2005). The final fitted value of the most sensitive parameters for the stream flow of the subbasin is given in the Table 10. The over prediction nature of the model is controlled by decreasing CN2 from the initial value 0.174 to 0.155. On the other hand under prediction of the model were adjusted by increasing REVAPMN from 12.130 to 17.709. Moreover, the simulated flow patterns with observed flow pattern were adjusted with HRU_SLP and Ov_N value.

Calibration for water balance was done at monthly time scale. The simulated and observed monthly average discharge at the outlet of the subbasin was plotted for visual comparison in the Figure 25. The model was calibrated by using the values of parameters that were identified as high to small sensitive to stream flow as it was described under sensitive analysis section. At the initial run of the model i.e model run using the default values of parameters. There were three major problems in the water balance of the shallow aquifer (SWAT considers only

shallow aquifer water balance): a) low surface runoff b) high lateral flow and c) low base flow (inter flow or return flow). Fixing these problems was quite challenging task. Low surface runoff was adjusted by increasing curve number (CN2) and decreasing the soil evaporation compensation factor (ESCO). In addition, the saturated hydraulic conductivity (SOL_K) of the soil layers was also adjusted. Higher lateral flow is related to SOL_K of the soil layer.

After all these adjustments in SWAT, simulation were done and parameters were first calibrated manually which was very time consuming process, followed by automatic calibration using Para Sol (Parameter Solutions), an auto calibration tools (SUFI2 in SWAT_CUP) and the calibrated parameters were updated in the model and final simulation was run.

Table 10. Finally calibrated parameter and fitted values of stream flow (1987-1995)

Flow Parameters	Model process	Bounds/Ranges	Initial value	Fitted value
CN2	Surface runoff	-0.20 – 0.20	0.174	0.155
OV_N	Channel flow	0.01 – 300	25.124	23.153
HRU_SLP	Geomorphology	10.00 – 50.00	27.000	29.000
ESCO	Evaporation	0.01 – 1.00	0.985	0.958
Sol_Awc	Soil water	-0.20 - 0.200	0.125	0.140
Sol_Z	Soil water	-25.00 – 25.00	12.263	14.210
Sol_K	Surface runoff	-25.00 – 25.00	15.381	18.100
BLAI	Evaporation	0.00 – 1.00	0.135	0.160
GW_Delay	Ground water	0.00 – 10.00	3.651	4.938
Gwqmn	Ground water	0.00 – 4000.00	249.261	259.300
Revapmin	Ground water	0.00 – 500.00	12.130	17.709
GW_Revap	Ground water	0.02 - 0.20	0.116	0.190
Surlag	Surface runoff	0.05 – 23.00	21.245	20.219
Alpha_Bf	Ground water	-0.036 – 0.036	0.0245	0.031

Table 11. Summary of model performance for calibration results

Period	Mean annual water yield (mm)		Monthly model efficiency measures	
	Observed	Simulated	R^2	E_{NS}
1987-1995	168.48	145.72	0.84	0.78

The thorough hydrologic calibration resulted good SWAT predictive efficiency at monthly time scale of the subbasin when compared to measured flow data (Figure 25 and 26). The hydrograph of observed and simulated flow indicated that the SWAT model is capable of simulating the hydrology of Kesem subbasin. However, the model was unable to capture the extreme values mainly, observed discharge on the month of August, 1993 and 1995. The under prediction of flow during peak events by the SWAT model has been reported in many studies for instance Sathian *et al*.(2001).

Figure 25. Calibration results of average monthly simulated and gauged flows at the outlet of Kesem subbasin; (1987-1995)

Figure 26. Scatter plot of observed and simulated monthly flow for the calibration period; (1987-1995)

4.3.4.2. Model validation

It was found that the model has good predictive capability with R^2 and E_{NS} values of 0.78 and 0.73 for validation period. Statistical model efficiency criteria fulfilled the requirement of $R^2 > 0.6$ and $E_{NS} > 0.5$ which is recommended by SWAT developer (Santhi *et al*., 2001). This showed the model parameters represent the processes occurring in the Kesem subbasin to the best of their ability given available data and may be used to predict basin response for various outputs. The model validation results for monthly flow (Figure 27 and 28) indicated generally a good fit between measured and simulated output results. Since the model performed well in the validation period as for the calibration period, the set of optimized parameters listed in Table 11 during calibration process for Kesem subbasin can be taken as the representative set of parameters for the subbasin.

Figure 27. Validation results of average monthly simulated and gauged flows at the outlet of Kesem subbasin; a) 1996-1998

Figure 28. Scatter plot of observed and simulated monthly flow for the validation period (1996-1998)

Table 12. Summary of model performance for validation results

Period	Mean annual water yield (mm)		Monthly model efficiency measures	
	Observed	Simulated	R^2	E_{NS}
1996-1998	184.78	143.92	0.78	0.73

4.3.5. Implication of climate change on soil water availability simulation of baseline period

After the model performance evaluation was checked for first fifteen (1984-1998) years of baseline period; the sensitive parameters were used for second fifteen (1999-2013) years of the same period by parameterizing in SWAT model for stream flow simulation. Thereafter, the simulation of soil water availability was determined for the same years of baseline period.

4.3.5.1. Monthly and seasonal soil water availability simulation

The model demonstrates satisfactory performance in capturing the patterns and trend of the observed flow with simulated flow series, which confirmed the appropriateness of the model for soil water availability simulation of baseline period in the subbasin. Soil water availability (SWA) is largely dependent on the amount of precipitation falling on its watershed area and the actual evapotranspiration amount released into the atmosphere. Hence, there is no doubt that changes in precipitation and temperature can significantly influence seasonal soil moisture patterns. It was simulated for the year 1984 to 2013 on monthly time step for two different periods from 1984 - 1998 and 1999 - 2013.

Temporally, the result was summarized in monthly and seasonal bases as comparatively *Belg* (Feb-May), *Kiremt* (Jun-Sep), *Bega* (Oct-Jan) and annual bases, after an intensive model calibration and validation for sensitive flow parameters. Comparison of monthly simulated soil water availability (SWA) in baseline periods shows increasing trend by about 3.6mm and decreasing by -0.95mm for 1984-1998 and 1999-2013 years respectively. On seasonal basis, it shows decreasing trend for belg, kiremt and bega season by about 31.61%, 14.33% and 18.02% respectively from first to second fifteen years of baseline period. Basically these were due to the increment of Agricultural land and exceedance of precipitation over actual evapotranspiration. As Agricultural land increase, base flow decrease and runoff increase this expose increment of stream flow (water yield) at gauge station and decrease soil water availability. In addition to monthly and seasonal basis, annual soil water availability between

two base line period (1984-1998; 1999-2013) shows decreasing trend from 1179.39 to 937.56 mm.

Figure 28. Mean monthly, seasonal and annual SWAT simulation of soil water availability in the subbasin for base period (1984-1998; 1999-2013)

Spatially, the variability of each sub watershed (SW) soil water availability rate is shown in the Figure 29 and average annual subbasin was estimated 1179.39 to 937.56 mm for first and second fifteen years. As it can be seen from the Figure 29 the highest rate of SWA was occurred at the South-Western and central part of the subbasin (at SW5, SW7, SW12, SW14, SW16, SW17 and SW21) for first fifteen year and (at SW1, SW3, SW5, SW7, SW12, SW14, SW16, SW17, SW18 and SW21) for second fifteen year, whereas the lowest SWA had mainly occurring at the Eastern and North-Eastern part of the subbasin (at SW6, SW8, SW13, SW20, SW24, SW25 and SW27), and (at W6, SW8, SW13, SW20, SW24, SW26 and SW27) for corresponding period. Lithic leptosols was the major dominant soil type existing in the area

where the highest SWA were occurred; while in the case of Eutric and Vertic cambislos it was lowest. According to FAO (2012) lithic leptosols is characterized as shallow in soil depth, low water holding capacity, excessive drainage and have ground water at shallow depth. Regarding LULC, the highest SWA have been occurred at Acacia and forest land use/cover and while lowest were occurred at Agricultural land use/cover for both periods.

a)

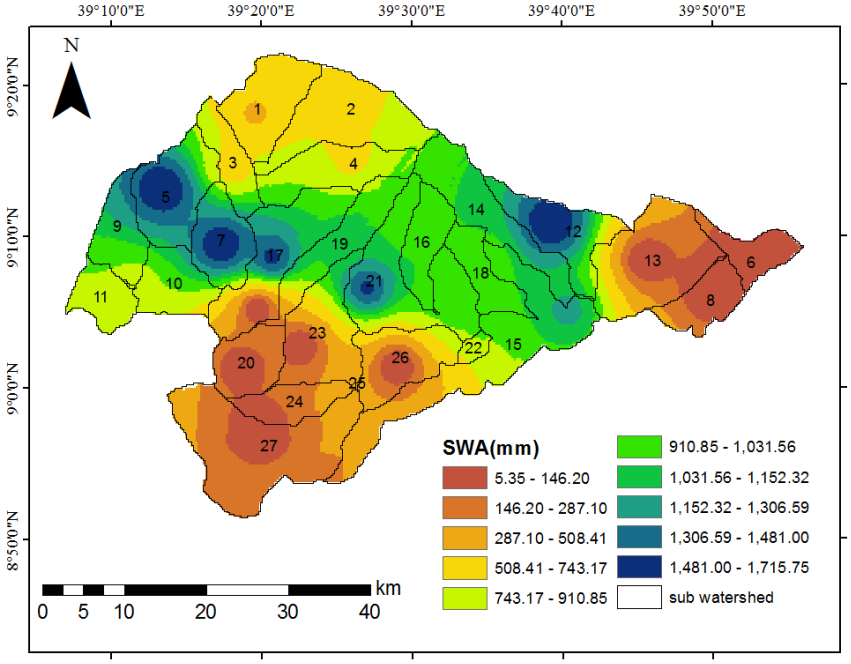

b)

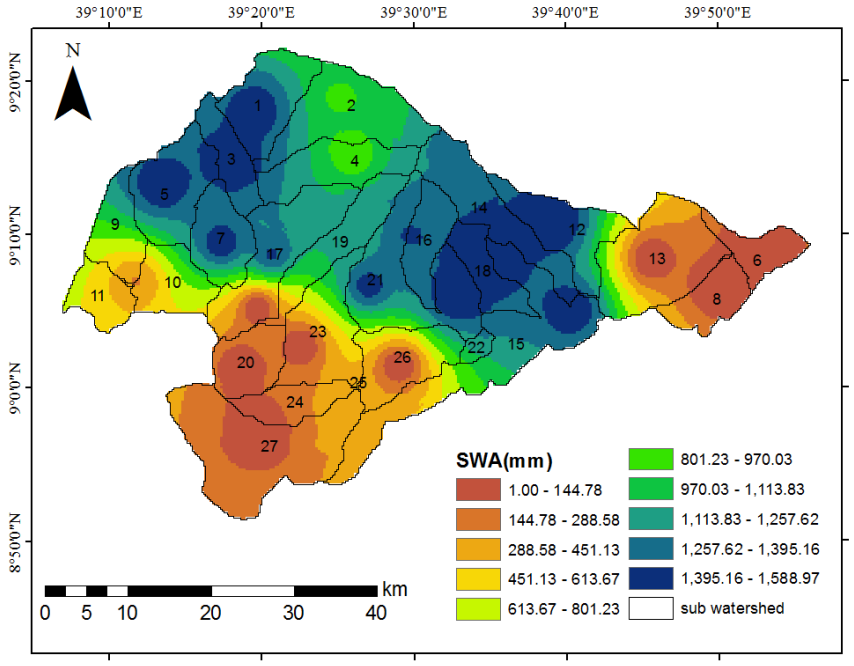

Figure 29. Spatial distribution of soil water availability in the subbasin; a) 1984-1998; b) 1999-2013

4.3.6. Implication of climate change on soil water availability simulation of future period

4.3.6.1. Predicted land use and land cover changes

The relationship between land use change and its driving factors of the study area was established through logistic regression for each land cover type given a set of defined driving factors (Verburg *et al*., 2002). The statistics of the driving factors were tested using the ROC (receiver operation characteristics) curve proposed by (Pontius *et al*., 2005) which evaluates the predicted probabilities by comparing them with the observed value. Pontius *et al*. (2005) found that any ROC above 50% was better than random. The obtained value was greater than 50%, indicating a probability distribution consistent with the actual distribution of land use

types. Generally, a ROC above 70% shows that the driving factors had a greater explanatory power for a certain land use type.

Table 13. Regression analysis results between land uses and driving factors in the subbasin

Driving factors	Acaia	Agricultural land	Bare land	Eucalyptus	Forest	Settlement	Shrub land	Grass land	Water body
Elevation	-0.0003	-0.009							
Population density	-0.0022	-0.04803						-0.0015	-0.0014
Slope	-0.04	-0.1121	-0.0334	-0.1275		0.4011			
Distance to urban centre	0.0003	-0.0089		0.0508				0.0533	
Soil type		-0.4065							
Soil texture					1.0419				
Constant	-0.8373	-0.0341	-4.8566	6.2650	3.256	-3.742	-3.130	-3.132	4.256
ROC	0.7312	0.7009	0.7560	0.6981	0.8325	0.7103	0.6501	0.8127	0.7320

Analysis of simulation results

Unremitting Acaia and shrub land decline, and expansion of Agricultural land along with rapid population growth rate in the watershed have led to a significant change on soil moisture availability. One future land use scenarios were assumed which is baseline. Using these scenarios, on future land use land cover maps were predicted for 2020s (2014-2043) using the CLUE-S model as shown in Figure 30. Under certain possible future scenarios assumptions, linking the land use changes with relevant driving factors, the model decreases land use allocation uncertainty for spatial explicit and multi scale simulation of land use change (Dams *et al*., 2008; Ganasri *et al*., 2013; Shimelis *et al*., 2016).

Under baseline scenario, the land use and land cover changes are expected to occur at the same rate as the land use change trend between 1998 and 2013. However, one land use/covers were created in 2013 which is not more than 0.01% of total area. Therefore, in this analysis, its change is neglected and kept same for future analysis. Derivation was made for four main land uses and land cover types, Acacia, eucalyptus, agricultural land and shrubs land.

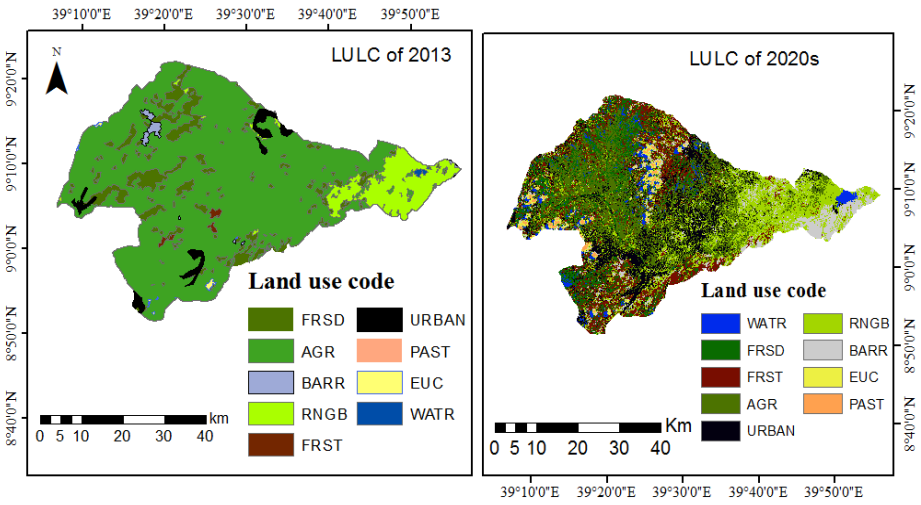

Figure 30. Predicted land use maps using CLUE-S model

All land use types cover more than 98% of the total area of the subbasin (Table 14). Agricultural land was the largest land cover type, about 77.55% of the total area in 2013 and steadily increased throughout the entire simulation period while acacia land and eucalyptus declined. This may due to fire wood, house construction, and selling. Expansion of agricultural land in the subbasin by the local farmers was used for food and financial benefit since more than 80% of the population in the area was depend of agricultural product and productivity (CSA, 2011). The increment of water body has been observed in 2020s by 0.09% from 2013. This is due to construction of Kesem reservoir and other manmade pond in the subbasin. In essence, the expansion of manmade pond in the subbasin is due to center prominence on water harvesting technology in the entire country by government of Ethiopia in the form of pond. Little increment of forest plantation was also noticed, from 1.93% cover in 2013 to 2.19% in 2020s. This is due to focus emphasis of Ministry of forest, environment and climate change on environmental protection to reduce climate change implication on agriculture and others in country side.

Table 14. Simulated land use and land cover changes between 2011 and 2020s

LULC classes	2011		2020s (2014-2043)	
	Km^2	%	Km^2	%
Acacia	236.00	10.37	181.00	7.95
Agricultural land	1765.00	77.55	1822.00	80.05
Bare land	15.00	0.66	16.00	0.70
Eucalyptus	10.00	0.44	5.00	0.22
Forest	44.00	1.93	50.00	2.197
Settlement	4.72	0.20	15.00	0.66
Shrub land	197.00	8.66	180.00	7.92
Grass land	0.28	0.001	0.28	0.001
Water body	4.00	0.18	6.00	0.27
Total	2276.00	100.00	2276.00	100.00

4.3.6.2. Change in monthly soil water availability

The soil water availability in a given time period, calculated from land phase of SWAT water balance equation is used for estimation of future soil water availability variation with respect to the baseline period. As shown in Figure 31, the average monthly soil moisture of the two fifteen years of RCP4.5 and RCP8.5 scenarios for 2020s climate periods has portrayed decreasing trends in the months of main rainy season. Although there might be a general decreasing pattern of the average monthly soil moisture, the overall decrease in the months of main rainy season (Jun, Jul, Aug and Sept) seems to be considerable. These months are the main Kiremt season for the study area, in which the soil water availability attains its maximum field capacity. And also soil moisture has shown decreasing trends during the months of bega and belg seasons.

Figure 31. Mean monthly soil moisture change for the future relative to base period.

4.3.6.3. Change in seasonal and annual soil water availability

By considering the soil water balance, the variation in soil water availability is aggregated on seasonal and annual basis. Some of the hydrological variables considered for assessing impacts of climate change on soil water availability are the basic variables that are highly influencing the spatial and temporal variability of soil water. Precipitation is the main source of soil water availability. Hence, changes in this parameter highly influence the soil water in any time horizon.

Figure 32. The percentage change of mean seasonal soil water for the future periods relative to base period.

Therefore, understanding the impact of climate change on the rainfall for the given time period would offer good reasonable implication for estimation of climate change impacts on the soil water availability.

Figure 32 illustrates the estimation of percentage change in mean seasonal and annual soil water in the future. In both scenarios of (near future) 2020s periods, the mean JJAS soil moisture per month might decrease by 6.02% and 5.22% for RCP4.5 and 2.21% and 2.36% for RCP8.5 respectively for first and second fifteen years. Similarly, 3.22% and 2.37% increase in mean seasonal soil moisture for ONDJ season for RCP4.5 and RCP8.5 respectively. Also a decline in mean seasonal soil moisture by 3.51% and 2.10% in FMAM for RCP4.5 and 1.66% and 1.38% for RCP8.5 might happen in 2020s of both periods. This is mainly because of the dominant impact of seasonal precipitation and LULC change.

In near future, Agricultural land and rainfall during kiremt season of both scenarios shows increasing trend. However due to its unpredictability and erratic variability, rainfall in Awash basin was characterized by high intensity and low duration (Belete and Semu, 2013). These characteristics leads to increase surface runoff; decrease lateral flow and infiltration rate which pilots to decreases soil moisture availability in main rainy seasons from base period. On the other hand, as surface runoff increase, soil bulk density (soil compaction) increases and leads to decrease again soil moisture availability. The increment of runoff was consistence with (Rizwan *et al.,* 2010; Mekonnnen and Tadele, 2012). Rizwan *et al.* (2010) carried out research on the upper Blue Nile using different GCM outputs including HadCM3 and canESM2 and the results reveal as runoff increases in the future in the major rainy seasons (June-September) which causes the possibility of flood occurrences in the future due to the extreme runoff. In general, the mean seasonal and annual change of soil moisture availability varies with LULC change, precipitation and evapotranspiration due to increased temperature within that prospective climate periods.

4.4. Implication of Climate Change on Maize Water Needs; Application of CROPWAT Model

4.4.1. **Onset, offset and length of the growing period**

The result from Instat statistical tool in the Table 15 revealed that the main rainy season (Kiremt) starts during the 1st meteorological decade of June for baseline period and 2nd decade to 3rd decade of June for both RCP4.5 and RCP8.5 of near (2020s) and mid (2050s) future period.

The onset date for Shola Gebeya station, the respective lower and upper quartile falls between 152 to 167 DOY (day of the year) for base period, and 156 to 184 DOY for 2020s and 2050s for both scenarios as shown in Table15. This implies that the chance of getting onset date on 167 and 184 DOY is 75 % in the study area and can expect the situation at 152, 156, 151 and 161 DOY for both period. The earliest date of onset date of the rainy season was 131, 136,149 and 150 DOY while the latest date was 181 (base period), RCP4.5 (186, 196) and RCP8.5

(209, 192) and the optimal planting date was 156 (base period), RCP4.5 (161, 171), RCP8.5 (168, 173) as shown in Table 15 for base period, 2020s and 2050s.

In any case, late onset is the least preferred situation, obviously because it shortens the available length of the crop growing period and the potential to satisfy the crop water requirement (Green, 1966). However, the historical and future variability of onset date showed less variability as compared to LGP but highly variable than cessation date. As shown in the Table 15 onset date has less standard deviation as compared to LGP but higher than cessation, the higher standard deviation of the onset date of the seasons indicates that patterns could not be easily understood and consequently decisions relating to crop planting and related activities will be made with high risk. The result is similar with the study undertaken by Abiy *et al.* (2014).

Regarding offset date, the result shown in Table 15 offered that, on an average, the main rainy season ceased in the range of 270 (base period), RCP4.5 (278, 284) and RCP8.5 (281, 274) DOY for baseline, near and mid future period. Similar result was reported by Hoefsloot (2009). The cessation date for Shola Gebeya station, the upper quartile, lower quartile, minimum and maximum for base period was shown in Table 16. This indicates that the chance of getting 75% of the time, the end date will occur at 270 to 284 DOY.

As indicated in Table 15, the length of growing period for localized maize production in the main rainy season in the study area ranged from 93 to 165 rainfall days for baseline and future period respectively. The mean LGP of the station was ranges between 113 to 118 rainfall days. However, according to the result of key informant discussion about the planting period of maize, the insight of farmers toward planting date were 2nd to 3rd decade of May months which is 140 to 150 (DOY) and dominate Maize varieties in the area were Melkassa hybrid two (MB2). In this regard there is no exaggerated gap between farmer and model output for base period. Also, according to WARC (2016) in middle Awash MB2 Maize varieties was used and recommended with LGP of 110 to 115. In line with this Instat statistical tool on Markov chain model probabilities gives LGP in terms of soil moisture content during growing period (Table 15) which is great than the mentioned LGP of maize. These reveal that the Maize was

harvested before moisture denied out but its accessibility was determined by CropWat in proceeding section.

According to NMA (2012) small rainy period (*Belg*) rainfall season in rift valley of Ethiopia was recommended for land preparation, sowing short cycle crop like Haricot bean while *kiremt* season used for rest crop production planning activity. Hence, in relation to problems of small rainfall amount, high risk of dry spells, too small length of minor season and small gap with major season leads to none of harvesting time makes the small rainy season very difficult in the planning of all rain-fed crop production activity that is why this work omit *belg* season and prefer *kiremt* season for further analysis.

Table 15. Descriptive statistics of onset, offset and length of growing period for Shola Gebeya station; onset date (a), offset date (b), LGP(c)

a)

Descriptiv	Base period	RCP4.5		RCP8.5	
e statistics	1984-2013	2014-2043	2044-2073	2014-2043	2044-2073
N	30	30	30	30	30
Min	131	150	136	136	149
Q1 (25%)	152	156	151	156	161
Q2 (50%)	156	161	171	168	173
Q3 (75%)	167	169	184	178	181
Max	181	186	196	209	192
Mean	157	162	168	168	170
SD	14	10.1	17.8	17.3	13.2
CV (%)	8.9	6.2	10.6	10.3	7.7

b)

Descriptiv	Base period	RCP4.5		RCP8.5	
e statistics	1984-2013	2014-2028	2028-2043	2014-2043	2043-2073
N	30	30	30	30	30
Min	267	274	274	274	274
Q1 (25%)	267	274	274	274	274
Q2 (50%)	270	278	284	281	274
Q3 (75%)	278	291	299	287	288
Max	289	300	316	303	297
Mean	275	281	286	282	279
SD	3.86	8.9	12.8	8.2	8.1
CV (%)	1.4	3.2	4.5	2.9	2.9

c)

Descriptive	Base period	RCP4.5		RCP8.5	
statistics	1999-2013	2014-2043	2044-2073	2014-2043	2044-2073

N	30	30	30	30	30
Min	88	89	78	78	82
Q1 (25%)	115	113	99	100	95
Q2 (50%)	114	117	118	117	112
Q3 (75%)	111	130	134	120	124
Max	139	138	165	145	131
Mean	113	118	117	113	108
SD	13	13	22.9	16.5	14.7
CV (%)	12.4	11	19.4	14.5	13.6

N, number of data set; min; minimum value, Q1 (25%), first quartile; Q2 (50%), second quartile; Q3 (75%), third quartile; max, maximum value; SD (±); standard deviation; CV, coefficient of variation

4.4.2. Implication of climate change on Maize water needs under baseline period

4.4.2.1. Reference crop evapotranspiration (ET_O) under current climate

Using the decadal averaged daily ET_O, reference evapotranspiration of Shola Gebeya station are calculated by using Penman-Monteith method as shown in the Table 16. It is observed that the annual reference crop evapotranspiration was estimated at 1587.75 mm per year which is equal to 43.5 mm per ten days. The mean annual rainfall (1114.12 mm per year) was lower than the reference crop evapotranspiration by 473.63 mm per year.

Table 16. The monthly decadal (mm/dec) and daily (mm/day) average reference ET_O at the selected area of study under current climate (1984-2013)

Month	1st decade		2nd decade		3rd decade	
	Per day	Decade	Per day	Decade	Per day	Decade
Jan	3.77	37.70	3.16	31.60	3.92	39.20
Feb	4.19	41.90	3.65	36.50	4.88	48.80
Mar	4.87	48.70	4.12	41.20	4.94	49.40
Apr	4.80	48.00	4.12	41.20	4.72	47.20
May	4.86	48.60	4.06	40.60	5.21	52.10
Jun	4.37	43.70	3.86	38.60	4.60	46.00
Jul	3.34	33.40	3.47	34.70	3.43	34.30
Aug	3.70	37.00	3.81	38.10	3.88	38.80
Sep	4.30	43.00	3.98	39.80	4.41	44.10
Oct	4.55	45.50	3.72	37.20	4.54	45.40
Nov	4.14	41.40	3.25	32.50	4.04	40.40
Dec	3.73	37.30	2.92	29.20	3.87	38.70

Kirem t	3.93	39.28	3.78	37.80	4.08	40.80
Belg	4.68	46.80	4.24	42.40	4.94	49.38
Bega	4.05	40.48	3.99	39.90	4.09	40.93

According to the result in Table above, the maximum reference crop evapotranspiration was occurred in month of March which is 49.4 mm/dec and minimum was occurred in month of Dec with a mean of 29.20 mm/dec. In the case of decadal, the maximum mean reference crop evapotranspiration is 52.10 mm i.e. equivalent to 5.21 mm per day and happened in the 3rd decade of May and the minimum value was occurred during the 2nd decade of July with a mean value of 29.20 mm per decade. From this Table, it clearly implies that ET_O will be high during the *belg* seasons for baseline period. This is due to high extreme temperature, wind and solar radiation and low relative humidity. However, the progressive enhancement of rainfall distribution have already discussed in the previous section to be increased in *belg* seasons. These results clearly imply that the enhancement of rainfall couldn't be a guarantee to reduce the rate of evapotranspiration. This is possibly due to the change in temperatures. In this regard, it was confirmed that climate change would have a severe consequence even in better rainfall distributions. Therefore using this season for Maize production would affect the yield in terms of water stress in selected area of the subbasin.

4.4.2.2. Crop data

The suggested values of k_c for Maize growth by FAO-56 guidelines are 0.15 for initial, 1.5 for mid-seasons and 0.5 for late-season. However, as prescribed in Appendix Table 16 the relative humidity is in between 50 and 80% and wind speed is greater than 2m/s in month of June, July, Aug and Sep. Hence the k_c value was adjusted as per the equations 19 for mid season as shown in the Table 17.

Table 17. The suggested and adjusted k_c and growth stage value for each growth stage of maize growing period

Crop stage	Suggested K_c	Computed K_c	Suggested growth stage	Computed growth stage
Initial	0.15	0.15	20	18
Mid-season	1.50	1.51	35	31

Late season	0.50	0.50	30	26

Evapotranspiration during the initial stage for annual crops is predominately in the form of evaporation. Therefore, accurate estimates for $K_{c\ ini}$ were considered the frequency with which the soil surface is wetted during the initial period. Where the soil is frequently wet from rain, the evaporation from the soil surface can be considerable and $K_{c\ ini}$ were large. On the other hand, when the soil surface is dry, evaporation is restricted and the $K_{c\ ini}$ were small (Table 17). $K_{c\ mid}$ is less affected by wetting frequency than is $K_{c\ ini}$, as vegetation during this stage is generally near full ground cover so that the effects of surface evaporation on K_c are smaller. For frequent rain of crops, the $K_{c\ mid}$ of less than 1.0, the value can be replaced by approximately 1.1 - 1.3 to account for the combined effects of continuously wet soil (FAO, 2011). Consequently, both the soil surface and vegetation are dry and the value for $K_{c\ end}$ was relatively small.

Regarding depletion fraction, the suggested depletion fraction by FAO was 0.55% for $ET_O \approx 5$. But the average ET_O during Maize growing period in Kesem subbasin was 4.06 mm/day which is less than the suggested one. Hence the depletion fraction during maize production period needs adjustment using equation 18. As per the equation, the adjusted value of depletion fraction in percentage was adjusted to 0.59%.

4.4.2.3. Characterization of soil in the selected study area

The result of the textural analysis of the soil from the study site of three class showed that the composition of clay, silt and sand percentage were shown in the Table 18. Thus as per the USDA soil textural classification, the soil was classified as silt loam (higher class), clay loam (middle class) and clay loam (lower class) soil.

Table 18. Average particle size distribution of 5 sampling point for each class of selected area

Class		Particle size distribution (%)			Textural class
	Soil depth (cm)	Clay	Silt	Sand	
Higher	0-30	10.6	77.6	11.8	

	30-60	20.4	69.2	10.4	Silt loam
	60-90	22.4	67.8	9.8	
Average		17.8	71.5	10.7	
	0-30	47.8	33.0	19.2	Clay loam
Middle	30-60	33.2	42.6	24.2	
	60-90	31.2	44.6	24.2	
Average		37.4	40.1	22.5	
	0-30	41.4	35.8	22.8	Clay loam
Lower	30-60	38.4	37.0	24.6	
	60-90	39.6	35.0	25.4	
Average		39.8	35.9	24.3	

Table 19. Results of laboratory analysis from samples of Berehet district, Kesem subbasin

Soil texture	Soil depth (cm)	P_d	Mc	FC (%)	PWP (%)	TAW (cm/cm)
	0-30	1.43	18.10	31.70	7.93	23.77
Silt loam	30-60	1.47	20.60	30.92	9.44	21.48
	60-90	1.52	21.23	29.87	10.14	19.89
	Average	1.47	19.98	30.83	9.17	21.71
	0-30	1.40	18.54	38.88	25.44	13.44
Clay loam	30-60	1.43	21.17	37.28	22.31	14.97
	60-90	1.45	22.36	36.56	21.98	15.01
	Average	1.43	20.69	37.57	23.24	14.47
	0-30	1.39	23.81	41.56	28.38	13.44
Clay loam	30-60	1.40	22.62	41.20	25.10	16.10
	60-90	1.43	19.85	40.65	25.02	16.56
	Average	1.41	22.09	41.14	26.17	15.37

$P_{d,}$ bulk density in $gmcm^{-3}$, Mc, Available soil moisture dry weight basis, %, FC- field capacity-%, PWP-permanent wilting point-%, TAW, total available water- cm/cm

Soil bulk density of the area showed variation with land class (Table 19) for all soil textures. It varied between 1.41 to 1.47 gm cm^{-3} and generally the lower class soil has slightly lower bulk density than the middle and higher class with average bulk density of 1.42 gm cm^{-3} for clay loam texture. From higher to lower class, the soil bulk density was decrease. As bulk density increase, pore space of the soil is small this intend to increase soil compactions. The smaller soil compactions, the greater moisture content at field capacity and permanent wilting point in the selected area and the reverse was true for higher soil compaction.

The average water content at field capacity and permanent wilting point of the soil were determined to be 30.83 and 9.17%, respectively for silt loam and 41.8 to 24.74 for clay loam. The moisture content at field capacity varied with depth between 31.7 to 30.9% and 37.28 to 41.56% on mass basis for silt loam and clay loam respectively. The top (0-30cm) has larger average water content of field capacity while the subsurface 30-90 cm has a lower value of field capacity in all texture. The moisture content at permanent wilting point also showed variation with depth as shown in Table 19. Total available water (TAW) which is the depth of water that a crop can extract from its root zone is directly related to variation in field capacity and permanent wilting point. The total average available soil moisture for silt loam texture was 21.71 cm/cm and 14.47 to 15.37 cm/cm for clay loam. As show in the Appendix Table 15, the measurement of infiltration rate on each sample site ranges between 10-15 mm hr^{-1} for silt loam and 5-7 mm/hr for clay loam soil using double ring infiltrometer. Hence, the average value of soil infiltration rate in the selected area of Kesem subbasin was 12.0 and 6.0 mm hr^{-1} for silt clay and clay loam which analogous with (WARC, 2016). For further detail, the list of fifteen soil sample with their sample code name was prescribed in Appendix Table 14.

4.4.2.4. Computation of effective rainfall

As per the USDA, S.C (1985) method, the effective rainfall were calculated for each growing period and stage of maize as shown below on monthly basis for baseline period.

Table 20. The monthly basis recorded and effective rainfall (mm/month) for baseline period 1984 - 2013).

Months	Rec. Rain (mm)	Eff. rain (mm)
Jan	19.10	18.50
Feb	14.80	14.40
March	61.60	55.60
Apr	109.70	90.40
May	216.80	141.60
Jun	83.30	72.20
Jul	327.40	157.70
Aug	318.60	156.90
Sep	85.80	74.00
Oct	15.0	14.60
Nov	12.80	12.50

Dec	8.70	8.60

Rec. rain – recorded rainfall; Eff. Rain - effective rainfall

4.4.2.5. Maize crop evapotranspiration (ETc) of baseline period

The amount of rainfall is important but often not adequate to cover the water requirement of the crops (Smith and Kivumbi, 2006). Crop production in the dry season is only possible with irrigation, while crop production in the rainy season may be possible but unreliable because of prolong dry spell and drought; yields will be less than optimal production. If there is some rainfall, but not enough to cover the water needs of the crops, irrigation water has to supplement the rain water in such a way that the rain and irrigation water together cover the water needs of the crop.

It is essential to know water requirement of a crop which is the total quantity of water required from its sowing time up to harvest. Obviously different crops may have different water requirements at different places of the same country, depending upon the climate, type of soil, method of cultivation and effective rain. At the same time water supplies available for irrigation will become more variable and will decline because of climate variability and change. Climate change will significantly impact agriculture by increasing water demand, limiting crop productivity and by reducing water availability in areas where irrigation is most needed or has comparative advantage.

Thus, once climate change impacts are appraised, it is important to analyze what measures should be taken to adapt the potential consequences of climate variability related to irrigation. One possibility is to expand irrigation with locally available water sources. Where rain-fed cropping systems are displaced to the margins, the provision of irrigation is likely to play a strategic role in either stabilizing the production of grains or in supporting a low risk, high value production system with a strong commercial focus.

Therefore the water needs by Maize crop during baseline (1984 - 2013) were done for clay loam soil textures since it covers more than 70% of the selected area. Table 21 shows summaries of crop water and irrigation needs of maize in the study area. A Maize variety with a growing period of 110 days to maturity would require 403.2 mm depth of water, while 67 mm would be required as supplementary irrigation depth.

Table 21. Summary for total water and irrigation requirements for maize under the base line period (1984 - 2013)

Month	Decade	Stage	Kc	ETc (mm/day)	ETc (mm/dec)	Eff rain (mm/dec)	Irr. Req. (mm/dec)
Jun	1	Init	0.15	0.72	7.20	2.70	0.70
Jun	2	Init	0.15	0.68	6.80	16.70	0.00
Jun	3	Deve	0.17	0.72	7.20	28.70	0.00
Jul	1	Deve	0.48	1.73	17.30	45.80	0.00
Jul	2	Deve	0.86	2.73	27.30	56.70	0.00
Jul	3	Deve	1.26	4.28	47.00	55.20	0.00
Aug	1	Mid	1.49	5.47	54.70	55.00	0.00
Aug	2	Mid	1.49	5.69	56.90	56.10	0.80
Aug	3	Mid	1.49	6.01	66.10	45.60	20.40
Sep	1	Late	1.32	5.62	56.20	33.10	23.00
Sep	2	Late	0.96	4.26	42.60	23.60	19.10
Sep	3	Late	0.65	2.90	20.30	12.10	2.90
Total					403.20	431.40	67.00

4.4.3. Implication of climate change on maize water needs under future period

As per the baseline period, Maize water needs for future period under RCP4.5 and RCP8.5 scenarios needs input data like ET_O, soil data, crop data and effective rainfall for computation of Maize water needs. Even though it is recommended to estimate future soil data, its value varies between pointed intervals (FAO, 2011). Therefore, soil data of base period were used for future one and ET_O, crop data and effective rainfall were determined here in below.

4.4.3.1. Future reference crop evapotranspiration (ET_O)

According to the bias corrected future climate scenarios, the reference evapotranspiration (ET_O) was estimated. Based on these result, there is an expectation of high values of ET_O in the future scenarios in accordance to the higher temperature. The ET_O in the baseline period, 2020s and 2050s by scenarios are presented in Figure 33. The figure shows that ET_O in the base period varies in the range of 33.4 to 52.1 mm/dec. It increases roughly from 33.4 mm/dec in the 1st decade of July to the peak value of about 52.1 mm/dec in the 3rd dec of May. The highest ET_O in March can be explained by the hot (before the afternoon time) and windy weather condition in this month.

In the RCP8.5 scenarios, minimum and maximum ET_O was predicted to be in the range of 44.3 to 75.3 mm/dec. In the 2nd decade of August ET_O was minimal (44.3 mm/dec) while in the 1st decade of April ET_O was maximum (75.3 mm/dec). It increases roughly from about 44.3mm/dec in the 2nd decade of August to the peak value of about 75.3 mm/dec in the 1st decade of April. In the case of RCP4.5 scenario, ET_O varies in the range of 33 to 48 mm/dec. The ET_O increases roughly from approximately 33 mm/dec in the 1st decade of Dec to the peak value of about 48 mm/dec in the 3rd decade of May. The projected ET_O change between RCP4.5 and RCP8.5 is significant (Figure 33).

Figure 33. Change in evapotranspiration (ET_O) by period and scenarios at the study area

Comparison between the base period and the scenarios show that the peak value ET_O increases from 33 to 48 mm/dec for RCP4.5 and from 44.3 to 75.3 mm/dec for RCP8.5. The yearly ten day average ET_O was 40.88 mm/dec in the base period, which was predicted to be 41.57 mm/dec for RCP4.5 and 58.44 mm/dec for RCP8.5 scenarios. The percentile change in ET_O was found as -0.04, 1.02% for RCP4.5 of 2020s and 2050s and 21.24, 24.29% change in ETo for RCP8.5 of 2020s and 2050s respectively. The result is similar with the study undertaken by (Rao *et al*., 2011).

The mean decadal change in ET_O for the two scenarios is presented by period in Figure 34 and 35. These figures clearly reveal that ET_O will be high during the *Belg* and *kiremt* seasons of the year. The progressive enrichment of rainfall distribution have already discussed in the previous section to be increased in *Bega* and *kiremt* seasons. These two results clearly imply that the enhancement of rainfall couldn't be a guarantee to reduce the rate of evapotranspiration at least at the study locality. This is possibly due to the change in extreme temperatures. In this regard, it was confirmed that climate change would have a severe consequence even in better rainfall distributions (Tarekegn, 2016). The main rain season (Kiremt) will be characterized by the

lower rate of reference evapotranspiration in both 2020s and 2050s for the two scenarios in respect of *belg* season.

Figure 34. The ten day change pattern of ET_O at the study area by period for RCP4.5 scenario

Figure 35. The ten day change pattern of ET_O at the study area by period for RCP8.5 scenario

4.4.3.2. Crop data

The suggested values of K_c for Maize growth by FAO-56 guidelines are 0.15 for initial, 1.5 mid-seasons and 0.5 for late-season. However, as prescribed in Appendix Table 17 the relative humidity is in between 50 and 80% and wind speed is greater than 2m/s in month of June, July, August and Sep. Hence the K_c value was adjusted by the equations 19 for mid season as shown in the Table 22.

Table 22. The suggested and adjusted K_c and growth stage of maize

Crop stage	Suggested K_c	Computed K_c			
		a	b	C	D
Initial	0.15	0.15	0.15	0.15	0.15
Mid-season	1.50	1.51	1.50	1.48	1.48
Late season	0.50	0.50	0.50	0.50	0.50

RCP 4.5: a) 2020s; b) 2050s, RCP8.5: c) 2020s; d) 2050s

Regarding depletion fraction, the suggested depletion fraction by FAO was 0.55% for $ET_O \approx 5$. But the average ET_O during Maize growing period in Kesem subbasin (Shola Gebeya station) was 4.25 and 5.15 mm/day for RCP4.5 and RCP8.5 respectively which is greater than the suggested one. Hence the depletion fraction during Maize production period needs adjustment using equation 18. As per the equation, the adjusted value of depletion fraction in percentage was adjusted to 0.58 and 0.544% for RCP4.5 and RCP8.5 of both periods.

4.4.3.3. Computation of effective rainfall

As that of baseline period the effective rainfall of the future period were calculated via the USDA, S.C (1985) method, for each growing period and stage of Maize as shown below on monthly basis.

Table 23. The monthly basis recorded and effective rainfall (mm/month) for future period under two scenarios for near century of bias corrected.

Month	RCP4.5 (a)		RCP4.5 (b)		RCP8.5 (c)		RCP8.5 (d)	
	Est. Rain	Eff. rain	Est. rain	Eff. Rain	Est. rain	Eff. rain	Est. rain	Eff. Rain
Jan	54.3	49.6	54.3	49.6	24.6	23.6	51.8	47.5

Feb	47.2	43.6	29.5	28.1	26.8	25.7	20.3	19.7
March	43.2	40.2	16.8	16.4	46.3	42.9	33.6	31.8
Apr	106.5	88.4	37.0	34.8	59.6	53.9	63.6	57.2
May	209.5	139.3	84.8	73.3	169.2	123.4	164.0	121
Jun	126.3	100.8	184.0	129.8	97.5	82.3	123.9	99.4
Jul	274.7	152.5	126.7	101.0	294.5	154.5	325.0	157.5
Aug	278.9	152.9	316.5	156.6	263.8	151.4	315.4	156.5
Sep	67.8	60.5	309.2	155.9	61.1	55.1	65.4	58.6
Oct	11.1	10.9	68.2	60.7	12.5	12.3	13.8	13.5
Nov	6.8	6.7	14.1	13.8	12.8	12.5	16.1	15.7
Dec	4.1	4.1	10.4	10.2	1.4	1.4	3.8	3.7

Est., estimated rainfall, mm Eff., effective rainfall, mm; RCP 4.5: a) 2020s; b) 2050s, RCP8.5: c) 2020s; d) 2050s

4.4.3.4. Maize crop evapotranspiration (ETc) of future period

Based on the bias corrected future scenarios, the crop water and irrigation requirement of Maize was estimated as shown in the Table 24. Accordingly, the crop water and irrigation requirements of maize variety with a growing period of 110 days to maturity was predicted to be 436.1 and 445.1 mm depth of water during 2020s and 2050s of future period for RCP4.5, while 101.8 to 63.7 mm depth of water would be required as supplementary irrigation respectively. Whereas, 441.3 and 447.3 mm depth of water during 2020s and 2050s of future period for RCP8.5, while 142.9 to 134.0 mm would be required as supplementary irrigation for both period of RCP8.5 scenarios.

These results clearly reveal that the average rate of CWN is increased approximately by 8.16 and 10.39% for RCP4.5 and by 9.45 and 10.94% for RCP8.5 scenarios of 2020s and 2050s respectively. The result is similar with the study undertaken by (Rao *et al*., 2011). According to Rao *et al*.(2011) the crop water requirement of maize for future period of 2025 and 2050 ranges between 404 to 447mm in Semi humid to semi arid Agro-ecology from base period of 1990s. Also, it is significant to note that projections of water demands of semi humid to arid for the future period which is worked out by IWMI (International Water Management Institute) said that even with lower estimates projected by IWMI, there shall be substantial future increase in irrigation water requirements (Sharma, 2006)

a)

Table 24. Summary for total water and irrigation requirements for Maize under future climate.2014-2043(a); 2044-2073(b)

Month	Decade	Kc coeff		ETc(mm/day)		ETc(mm/dec)		Eff rain(mm/dec)		Irr. Req.(mm/dec)	
		4.5(a)	4.5(b)	4.5(a)	4.5(b)	4.5(a)	4.5(b)	4.5(a)	4.5(b)	4.5(a)	4.5(b)
Jun	2	0.13	0.13	0.82	0.82	8.20	8.20	29.30	47.30	0.00	0.00
Jun	3	0.14	0.14	0.80	0.80	8.00	8.00	36.50	42.80	0.00	0.00
Jul	1	0.40	0.40	1.97	1.97	19.70	19.70	46.70	34.20	0.00	0.00
Jul	2	0.76	0.76	3.26	3.26	32.60	32.60	53.20	29.70	0.00	2.90
Jul	3	1.14	1.14	4.95	4.95	54.40	54.40	52.50	37.20	1.90	17.20
Aug	1	1.39	1.41	6.20	6.20	62.00	65.00	53.80	47.80	8.20	14.20
Aug	2	1.39	1.41	6.21	6.21	62.10	64.10	55.40	54.90	6.70	9.20
Aug	3	1.39	1.42	6.26	6.26	68.90	70.90	43.60	53.90	25.20	15.00
Sep	1	1.26	1.26	5.71	5.71	57.10	58.10	29.10	55.00	28.10	2.10
Sep	2	0.90	0.89	4.11	4.11	41.10	41.10	18.10	56.40	22.90	3.00
Sep	3	0.57	0.60	2.76	2.76	22.00	23.00	10.60	35.50	8.70	0.00
Total						436.10	445.10	428.90	494.70	101.80	63.70

b)

Month	Decade	Kc coeff		ETc(mm/day)		ETc(mm/dec)		Eff rain mm/dec)		Irr. Req.(mm/dec)	
		8.5(a)	8.5(b)	8.5(a)	8.5(b)	8.5(a)	8.5(b)	8.5(a)	8.5(b)	8.5(a)	8.5(b)
Jun	2	0.14	0.14	0.89	0.89	2.70	2.70	6.60	8.80	2.70	2.70
Jun	3	0.14	0.14	0.81	0.81	8.10	8.10	31.90	37.10	0.00	0.00
Jul	1	0.18	0.18	1.01	1.01	10.10	10.10	45.80	47.90	0.00	0.00
Jul	2	0.51	0.51	2.46	2.46	24.60	24.60	55.00	55.30	0.00	0.00
Jul	3	0.88	0.89	4.13	4.13	45.40	45.40	53.50	54.30	0.00	0.00
Aug	1	1.29	1.28	5.59	5.59	55.90	55.90	53.70	55.40	2.20	0.60
Aug	2	1.45	1.48	5.81	5.81	58.10	60.10	54.90	56.80	3.30	1.40
Aug	3	1.47	1.48	6.03	6.03	66.30	67.30	42.70	44.40	23.60	22.00
Sep	1	1.47	1.47	6.27	6.27	62.70	62.70	27.40	28.70	35.30	34.00
Sep	2	1.15	1.15	5.35	5.35	53.50	53.50	15.90	17.00	37.70	36.50
Sep	3	0.81	0.79	3.95	3.95	39.50	39.50	11.90	12.80	27.60	26.70
Oct	1	0.54	0.55	2.87	2.87	14.30	17.30	3.80	4.00	10.60	10.30

Total	441.30	447.30	403.20	422.50	142.90	134.00

4. SUMMARY, CONCLUSSION AND RECOMMENDATIONS

5.1. Summary and Conclusions

This study strives to quantify the climatic change impact of the study area, the likely change of rainfall and temperatures from the base period by near and mid future century using ensemble of CORDEX Africa RCM model output under two alternative scenarios, and the corresponding possible implications of those changes on soil water availability and crop water needs of Maize in Kesem subbasin, middle Awash, Ethiopia. According to the study, in the base line climate (1984 - 2013) the average monthly distribution of rainfall for all stations was found in the range of 5.81 to 297.8 mm. The corresponding highest and lowest rainfall in a year was found in July and December. This can be explained by the influential synoptic meteorological weather systems which prevail during the months. The average monthly maximum temperature oscillated in the range of 23.6 to 36.3^{O}C. The highest mean value record was in the month of June and the corresponding lowest mean value was in the month of December. The year to year trend showed an increasing pattern by about 0.21^{O}C per decade year. Historically, the monthly average minimum temperature was in the range of 2.71 to 20.33^{O}C. The highest and lowest value of average minimum temperature was in the month of June and December respectively. The annual trend showed an increasing pattern by about 0.31^{O}C per decade year.

For the future period, two emission scenarios were applied: (i) medium emission scenario (RCP4.5), and (ii) high emission scenario (RCP8.5). Based on the result obtained from the bias corrected future scenarios, the rainfall was projected to be increased by 2020s and 2050s for both scenarios. Concerning the seasonal change in rainfall, it was projected that Kiremt rain would likely to be increased by about 1.8% by 2020s and 20% by 2050s for RCP4.5 scenario and 6% by 2020s and 21.73 by 2050s for RCP8.5 scenario.

The study additionally identified that the mean maximum temperature was predicted to be from +0.95 to 1.98^{O}C from the base period by 2020s and 2050s for RCP4.5 and +1.38 to 2.83^{O}C by

2020s and 2050s for RCP8.5 scenario respectively. Minimum temperature also predicted for the future period. Accordingly, it will be increased from 1.04 to 3.02^{O}C by 2020s and 2050s for RCP4.5 scenario. In case of RCP8.5 scenario the corresponding increase of minimum temperature would be from 0.03 to 5.13^{O}C by 2020s and 2050s. Beside climate change, Land use/land cover data were used in one scenario (1998, 2013) to see the impact of LULC with climate change on soil water availability and it shows increasing trend in Agricultural land, settlement and decreasing in shrub land and Acacia land in the sub basin during baseline period. In near future, the LULC was simulated using CLUE-S model to project the variation of land use changes under current baseline scenarios. The result from the simulation revealed an increase in Agricultural land and decline in Acacia and shrub land.

The result of hydrological model calibration and validation indicated that the SWAT model simulates the stream flow appreciably well for the study area. The model performance criterion which is used to evaluate the model result, the regression coefficient and the Nash Sutcliffe simulation efficiency values obtained proved this fact.

According to the hydrological analysis carried out, ground water parameters (Alpha base flow (Alpha_Bf), soil available water capacity (SOL_AWC), the threshold water depth in the shallow aquifer for flow (GWQMN), the groundwater Revap coefficient (GW_REVAP), the saturated hydraulic conductivity (Sol_K),curve number (CN2), Evapotranspiration (soil evapotranspiration factor (ESCO) and sub basin slope are the most sensitive parameters affecting the soil water of the subbasin.

In baseline period, SWA was simulated for the year 1984 to 2013 on monthly time step in Kesem subbasin of two different periods from 1984 - 1998 and 1999 - 2013. After an intensive model calibration and validation for sensitive flow parameters, comparison of monthly simulated soil water in baseline period shows increasing trend by about 3.6 mm and decreasing by -0.95 for 1984-1998 and 1999 - 2013 years respectively. On seasonal basis, it shows decreasing trend for belg, kiremt and bega season by about 31.61%, 14.33% and 18.02% respectively from first to second fifteen years of baseline period. These were due to exceedance of precipitation over actual evapotranspiration and LULC changes in base periods.

Hydrological impact of future climate change scenarios indicated that there will be high seasonal variation of soil water than in the monthly or annual basis. Relative to base period, the soil water in the main rainy season (JJAS) will reduce 6.02 and 5.22% for RCP4.5 and 2.21 and 2.36% for RCP8.5 respectively for first and second fifteen years of 2020s. Similarly, the soil water in the small rainy season (FMAM) will decrease by 3.51% and 2.10% for RCP4.5 and 1.66% and 1.38% in FMAM for RCP8.5 might happen in 2020s of both periods. This is mainly because of the dominant impact of seasonal precipitation and LULC change. In near future, Agricultural land and rainfall during kiremt of both scenarios shows increasing trend. However due to its unpredictability and erratic variability, rainfall in Awash basin was characterized by high intensity and low duration. These characteristics leads to increase runoff; decrease lateral flow and infiltration rate which pilots to decreases soil moisture availability in main rainy seasons from base period.

To estimate reliable maize production in terms of water demand, determination of onset, offset and LGP is crucial. The result from Shola gebeya station revealed that the main rainy season (Kiremt) starts at 156 DOY for baseline period and 161 to 171 DOY for RCP4.5 of 2020s and 2050s and 168 and 173 DOY for RCP8.5 of 2020s and 2050s of future period. Regarding offset date, the result offered that, on an average, the main rainy season ceased in the range of 274 to 286 DOY for baseline and future period and the mean LGP of the station was ranges between 113 to 118 rainfall days.

Based on the bias corrected future climate scenarios, ETo and CWN were estimated. This study indicated that ETo was in the range of 33.4 to 52.1mm per dekade in the first and second fifteen years of base period, which have been predicted to be in the range of 44.1 to 75.3 and 33 to 77.3 mm per dekade for RCP4.5 and RCP8.5 scenarios respectively for first and second fifteen years of near century. Overall, 0.04, 1.02% for RCP4.5 of 2020s an 2050s and 21.24, 24.29% change in ETo for RCP8.5 of 2020s and 2050s were predicted from base period. CWN were predicted to be in the range of 436.10, 445.1mm for RCP4.5 scenario and 441.30, 447.3 mm for RCP8.5 scenario for the full production season and IR ranges between 63.7 to 101.8mm for RCP4.5 and 142.9 to 134.0mm for RCP8.5 of 2020s and 2050s.

In the study area due to the likely impact of climate change CWN might be increased by 8.16 and 10.39% for RCP4.5 and by 9.45 and 10.94% for RCP8.5 scenarios of 2020s and 2050s from the base period for the same level of production. Increase in CWN for the same level of maize production can cause an increase stress on the water resource. This study tries to explain the effects of climate change on soil water availability and CWN in the study area. Despite some limitations, this study sheds a light on the possible implication of climate change on soil water availability and maize water demand. Future study must understand the overall implication of climate change in the Kesem subbasin and investigate the possibility of scheduling and/or shifting maize planting date.

5.2. Recommendations

For sustainability of future soil moisture availability and Maize production in the sub basin, the following recommendations should be considered as better alternatives and complementary actions.

- In near future period of both scenarios, soil moisture availability decrease during *kirem*t season from base period. But rainfall, runoff and surface flow increase and lateral flow decrease in the season. Therefore to enhance future soil moisture in the subbasin, appropriate soil moisture conservation practice is recommended.
- Accurate definition of planting time is very important element in Agriculture, because it enables the optimum utilization of water from rainfall. Therefore it is recommended for farmers to plant maize in 1^{st} to 2^{nd} decade of June in near future period of Shola Gebeya station under RCP4.5 since it is intermediate scenario.
- The calibrated parameters value can be considered for further hydrologic simulation of the sub basin. The model can also be taken as a potential tool for simulation of hydrology of unguaged subbasin in mountainous areas, which have hydro-metrologically similar with Kesem subbasin.
- Further studies on climate modeling that integrates soil-water-atmosphere, socio-economic and institutional aspects of a climate system under different emission scenarios by using multiple hydrological and crop simulation models should be

conducted in order to assess the potential impact of future climate change on crop production and design adaptation strategies for development policy for the future.

- Future studies on Kesem subbasin modeling should address the issue related to water quality, soil moisture conservation practice and evaluate best management practices to solve different sub basin management issues.

6. REFERNCES

Abate Shiferaw. 1994. Land use dynamics, soil degradation and potential for sustainable use in Metu area, Illubabor Region, Ethiopia. PhD Thesis, Universität Bern, Switzerland.

Abbaspour, K.C., Yang, J., Maximov, I., Siber, R., Bogner, K., Mieleitner, J., Zobrist, and J., Srinivasan, R. 2007. Modeling hydrology and water quality in the pre-alpine/alpine Thur watershed using SWAT. J. Hydrol. 333, 413–430, http://dx.doi.org/10.1016/ j.jhydrol. 2006.09.014

Abiy Gebremichael, Shoeb Quraishi and Girma Mamo. 2014. Analysis of Seasonal Rainfall Variability for Agricultural Water Resource Management in Southern Region, Ethiopia Journal of Natural Sciences Research, Vol.4, No.11, 2014.

Allen Richard G., Dirk, R and Martin, S. 2005. Crop Evapotranspiration (guidelines for computing crop water requirements) FAO Irrigation and Drainage Paper No. 56. FAO, Water Resources, Development and Management Service Rome, Italy http://www.fao.org/docrep/X0490E/ X 0490E00.htm.

Andrew, K. 1995. Farming systems of the African Savanna continent crisis. IDRC ISBN Out of print e-ISBN 1-55250-280-5 176 pp.

Arnold, J.G. and Allen, P.M. 1998. Automated methods for estimating base flow and ground water recharge from stream flow records. J. Am. Water Resour. Assoc. 35, 411–424, http ://dx.doi.org/ 10.1111/j.1752-1688.1999.tb03599.x.

Arnold, J. G, Srinivasan R, Muttiah R. R and Williams J. R. 2012. Large area hydrologic modeling and assessment part I: Model development, J. Am. Water Resources. Assoc.

Asfaw Kebede, Diekkrüger B and Semu Ayalew. 2013. An Assessment of Temperature and Precipitation Change Projections using a Regional and a Global Climate Model for the Baro Akobo Basin, Nile Basin, Ethiopia. J Earth Sci Climate Change 4: 133. doi:10.4172/2157-7617.1000133.

Bates B. C, Kundzewicz Z. W and Palutik J. P. 2008. *Climate change and water*. Technical Paper of the Intergovernmental Panel on Climate Change. Intergovernmental Panel on Climate Change, IPCC Secretariat, Geneva, Switzerland.

Belay Takele. 2002. Land cover/land-use changes in the Derekolli catchment of the South Welo Zone of Amhara Region, Ethiopia. Eastern Africa Social Science Research Review 18(1): pp. 1–20.

Belete Berhanu and Semu Ayalew. 2013. Background report: Hydro-meteorological trends Analysis, Coping with water scarcity the role of Agriculture Developing a National Water Audit for Awash Basin, Ethiopia. Springer Science and Business media.

Benoit. P. 1977. The start of the growing season in Northern Nigeria. AgricMeteorol, 18:91-9.

Blume T, Zehe E, and Bronstert. A. 2007. Use of soil moisture dynamics and patterns for the investigation of runoff generation processes with emphasis on preferential flow. Hydrol Earth Syst Sci Discuss 4:2587–2624.

Boko M., Niang, A. Nyong, C. Vogel, C. A. Cutheko, B. Osman-Elasha and Tobo,P. 2007. Impacts, Adaptation and Vulnerability. Working Group II Contribution to the Fourth Assessment Report of the IPCC, Cambridge University Press, Cambridge, pp. 433-467.

Borah, D.K. and Bera, M. 2003. Watershed scale hydrological and nonpoint source pollution models: Reviews of mathematical bases, transactions of the ASAE, vol.46.No.6, and pp.1553-1566.

Brekke L.D., Maurer E.P., Anderson J, D., Dettinger M.D., Townsley E.S., Harrison A. and Pruitt T. 2009. Assessing reservoir operations risk under climate change. Water Resources 45:W04411. Doi: 10.1029/ 2008WR006941.

Chaturvedi, R.K., Joshi, J., Jayaraman, M. Bala, G. and Ravindranath, N.H. 2012. Multi model climate change projections for India under representative concentration pathways. Current science 103 (7).

Chipindu, B. 2009. Training, Climate Change and the Environment. *Engaging the Public through Medial workshop held at Kadoma Hotel and Conference Centre,* 15-18 June 2009. A paper presented by Barnabas Chipindu, Department of Physics, University of Zimbabwe during the British Council-UNESCO Initiative Media, Zimbabwe.

Christensen, J., Boberg, F., Christensen, O., and Lucas-Picher, P. 2008. On the need for bias correction of regional climate change projections of temperature and precipitation.

Clarke L., Edmonds J., Jacoby H., Pitcher H., Reilly J. and Richels R. 2007. Scenarios of Green house Gas Emissions and Atmospheric Concentrations. Sub-report 2.1A of Synthesis and Assessment Product 2.1 by the U.S. Climate Change Science Program and the Subcommittee on Global Change Research. Department of Energy, Office of Biological & Environmental Research, Washington, 7 DC., USA, 154 pp.

Coffey, M.E., S.R. Workman, and A. W. Fogle. 2004. Statistical procedures for evaluating daily and monthly hydrologic model predictions. *Transactions of the ASAE* 47(1): 59-68.

Collier, P., Conway, G. and Venables, T. 2008. Climate change and Africa. *Oxford review of* economic policy, 24(2): 337-353.

Conway, D. and Schipper, E.F. 2011. Adaptation to climate change in Africa: Challenges and opportunities identified from Ethiopia. *Global Environmental Change*, 21(1): 227-237.

Corner, A., Whitmarsh, L.and Xenias, D. 2012. Uncertainty, scepticism and attitudes towards climate change: biased assimilation and attitude polarization. *Climatic Change,* 114(3/4): 463-478

Cook, K. H., and Vizy E. K. 2013. Projected changes in East African rainy seasons.J. Climate, 26, 5931–5948, doi:10.1175/JCLI-D-12-00455.1

CSA (Central Statistical Agency). 2011. Agricultural Sample Survey 2010/2011: Volume I Report on Area and Production of Major Crops. Statistical Bulletin 532, Addis Ababa, Ethiopia.

Dai A. 2011. Drought under global warming WIREs Clim Change2 45–65 DOI: 10.1002/wcc.81.

Dams J, Woldeamlak S.T, and Batelaan. O. 2008. Predicting land-use change and its impact on the groundwater system, Kleine Nete catchment, Belgium. Hydrol Earth Syst Sci 12:1369–1385.

Danuso, F. 2002. Stochastic model for weather data generation. *Italian Journal of Agronomy* 6(1):57-71.

DeFries, R. and Eshleman, K. N. 2004. Land-use change and hydrologic processes: a major focus for the future. Hydrological processes 18: pp. 2183–2186.

Dercon, S. 2004. Growth and shocks: evidence from rural Ethiopia. *Journal of Development Economics 74, 309-329.*

Deressa, T. and Hassan, R. 2009. "Economic Impact of Climate Change on Crop Production in Ethiopia: Evidence from Cross-section Measures," Journal of African Economies 18, no. 4: 529–554.

Dessler, E. and Parson, E. 2006. *The science and politics of climate change*; A guide to the debate. Cambridge University press, New York.

Dilnesaw Alamirew. 2006. Modeling of Hydrology and Soil Erosion of Upper Awash River Basin. PhD Thesis, University of Bonn: 233pp.

Easton, Z.M., Fuka, D.R., White, E.D., Collick, A.S.Biruk Ashagre, McCartney, M. and Steenhuis, T.S. 2010. A multi basin SWAT model of runoff and sediment in the Blue Nile, Ethiopia. Hydrology and Earth sciences, 14(10), 1827-1841.

Edoga N. R. 2007. Determination of Length of Growing Season in Samaru Using Different Potential Evapotranspiration Models: Soil Science Department, Ahmadu Bello University, Zaria Nigeria.

Eid H. M., Samia, M. El-Marsafawy and Samiha A. Ouda. 2006. Assessing the impact of climate change on crop water needs in Egypt: The CROPWAT analysis of three districts in Egypt. CEEPA Discussion Paper No. 29. Special Series on Climate Change and Agriculture in Africa, July 2006.

Ephrem Alemu. 2011. Effects of Watershed characteristics on River Flow for the Case of Rib and Catchments, Upper Blue Nile Basin. MSc thesis.

Eshetu, Z., Simane, B., Tebeje, G., Negatu, W., Amsalu, A., Berhanu, A., Bird, N., Welham, B. and Trujillo, N.C. 2014. *Climate finance in Ethiopia: Overseas Development Institute.* Climate Science Centre, Addis Ababa, Ethiopia.

FAO (Food and Agriculture Organization). 1998. The Soil and Terrain Database for northeastern Africa (CDROM) FAO, Rome.

FAO (Food and Agricultural Organization). 2011. Facts, perspectives, impacts and actions required in the 21st century: Ensuring food security in a changing world. Background paper prepared for the High Level Conference on World Food Security: The challenges of climate change and bio energy, Italy, Rome.

FAO (Food and Agricultural Organization). 2012. Digital Soil Map of the World and Derived Soil Properties (CDROM) Food and Agriculture Organization of the United Nations, FAO

Fekadu Mulugeta. 1999. Runoff models for different time steps with special consideration for semi-arid and arid catchments. PhD thesis, Vrije Universiteit Brussel, Belgium.

Fowler H.J and Kilsby C.G. 2007. Using regional climate model data to simulate historical and future river flows in northwest England. Climatic Change 80: 337–367.

Francos, A., F. J. Elorza, F. Bouraoui, G. Bidoglio and L. Galbiati. 2003. Sensitivity analysis of distributed environmental simulation models: Understanding the model behavior in hydrological studies at the catchment scale. *Real. Eng. Syst. Safe*. 79(2): 205-218.

Frankenberg J.R, Brooks E.S, Walter M.T, Walter M.F, and Steen Hui T.S. 1999. A GIS-based variable source area hydrology model. Hydrol Process 13:805–822.

Fujino J., Nair R., Kainuma M., Masui T. and Matsuoka Y. 2006. Multi-gas mitigation analysis on stabilization scenarios using AIM global model. Multigas Mitigation and Climate Policy. In: The Energy Journal, 3 (Special Issue).

Ganasri B.P, Raju A and Dwarakish G.S. 2013. Different approaches for land use land cover change detection: a review. J Eng Technol 2(3):44–48.

Gedion Tsegaye. 2009. Surface Water - Groundwater Interactions and Effects of Irrigation on Water and Soil Resources in the Awash Valley. M.Sc thesis, Addis Ababa University, Ethiopia.

Girod, B. Wiek, A., Mieg, H. Hulme, M. 2009. The evolution of the IPCC's emission scenarios. Environmental Science & Policy 12, 103-118.

Giorgi, F., Jones, C., and Asrar, G. R. 2009. Addressing climate information needs at the regional level: the CORDEX framework.

Githui, F. W. 2009. Assessing the impacts of environmental change on the hydrology of the Nzoia catchment, in the Lake Victoria. PhD thesis, Vrije Universiteit Brussel, Brussels, Belgium.

Godswill, M, Dawit. K. and Dejene A. 2007. A comparative analysis of rain fed and irrigated agricultural production in Ethiopia .Journal of Irrigation and Drainage, Vol 21 No1, Springer Netherlands.

Graham L., Andréasson, J., and Carlsson, B. 2007. Assessing climate change impacts on hydrology from an ensemble of regional climate models, model scales and linking methods – a case study on the Lule River basin, Clim. Change, 81, 293–307, doi: 10.1007/s10584-006-9215-2, 2007a.

Green, G.C. 1966. The Evaluation of Methods of Rainfall Analyses and the Application to the Rainfall Series of Nelspruit. MSc thesis (Agro-meteorology) University of the Orange Free State, Bloemfontein. pp147.

Gwimbi K and Mundoga B. 2010. Impact of climate change on cotton production under rainfed conditions: case of Gokwe. Journal of Sustainable Development in Africa (Volume 12, No.8, 2010) ISSN: 1520-5509.

Hadgu, K. M. 2008. Temporal and spatial changes in land use patterns and biodiversity in relation to farm productivity at multiple scales in Tigray, Ethiopia. PhD thesis, Wageningen Universities, The Netherlands.

Hailemariam Kinfe. 1999. Impact of Climate Change on the Water Resources of Awash River Basin, Ethiopia, Climate Research. International and Multidisciplinary Journal, 12:91-96.

Han, H., Yang, C., & Song, J. 2015. Scenario Simulation and the Prediction of Land Use and Land Cover Change in Beijing, China, 4260–4279. https://doi.org/10.3390/su7044260.

Hargreaves, G.L., Hargreaves, G.H., and Riley, J.P. 1985. Agricultural benefits for Senegal River basin. J. irrigation and Drainage Engineering; 111(2): 113-124.

Hernández-Díaz L, Laprise R, Sushama L, Martynov A, Winger K, and Dugas B. 2013. Climate simulation over CORDEX Africa domain using the fifth-generation Canadian Regional Climate Model (CRCM5). Clim. Dyn. 40: 1415–1433, DOI: 10.1007/s00382-012-1387.

Hoefsloot, P. 2009. LEAP (Livelihood Early Assessment Protection) version 2.1 for Ethiopia. By collaborative action of FAO, World Bank and World food programme. The Netherlands.

http://www.brc.tamus.edu/swat/soft_links.html,SWAT (Arc SWAT) website accessed June, 10, 2012.

http://www.euro-cordex.net CORDEX data files are downloaded from the Canadian Institute for Climate Studies (CICS) website accessed July, 20, 2009.

http://mesonet.agron.iastate.edu/mailman/listinfo/cordex website accessed Jan, 2015.

Hunt A, and Watkiss P. 2011. Climate change impacts and adaptation in cities: a review of the literature. Clim Chang 104:13–49. doi: 10.1007/s10584-010-9975-6.

IPCC (Intergovernmental Panel on Climate Change). 1990. Climate Change- The IPCC Scientific Assessment, Houghton, J.T., Jenkins, G.J., Ephraums, J.J. (eds.) Cambridge University Press, Cambridge, UK

IPCC (Intergovernmental Panel on Climate Change). 2007. The Physical Science Basis. Contribution of Working Group I to the Fourth Assessment Report of the IPCC [Solomon, S., D. Qin, M. Manning, Z. Chen, M. Marquis, K.B. Averyt, M.Tignor and H.L. Miller (Eds.)]. Cambridge University Press, Cambridge, United Kingdom and New York, NY, USA.

IPCC (Intergovernmental Panel on Climate Change). 2010. Statement on the melting of Himalayan glaciers. A statement from the Chair and Vice-Chairs of the IPCC, and the Co-Chairs of the IPCC Working Groups.

IPCC (Intergovernmental Panel on Climate Change). 2011. *Managing the risks of extreme events and disasters to advance climate Change adaptation*. In: A Special Report of Working Group I and II of the Intergovernmental Panel on Climate Change (eds C.B Field, V Barros, TF Stocker et al.), Cambridge University Press, United Kingdom.

IPCC (Inter governmental panel on climate change). 2013. The Physical Science Basis. Contribution of Working Group I to the Fifth Assessment Report on IPCC [Stocker, T.F., D. Qin, G.-K. Plattner, M. Tignor, S.K. Allen, J. Boschung)]. Cambridge University Press, Cambridge, United Kingdom and New York, NY, USA, 1535 pp.

Jacob D., Elizalde A, Haensler A, Hagemann S, Kumar P, Podzun R, Rechid D, Remedio AR, Saeed F, Sieck K, Teichmann C, and Wilhelm. C. 2012. Assessing the transferability of the regional climate model REMO to different coordinated regional climate downscaling experiment (CORDEX) regions. Atmosphere 3:181–199. Doi: 10.3390/atmos3010181.

Jakob Theme, M., Gobiet, A., and Leuprecht, A. 2011. Empirical-statistical downscaling and error correction of daily precipitation from regional climate models. International Journal of Climatology, 31(10), 1530–1544. doi:10.1002/joc.2168.

Jembere, A. A. 2004. Information theory and artificial intelligence to management uncertainty in hydrodynamics and hydrological models. PhD thesis, UNESCO-IHE, The Netherlands.

Jiang, C., Edmeades, G.O., Armstead, I., Lafitte, H.R., Hayward, M.D. and Hoisington, D. 2009. Genetic analysis of adaptation differences between highland and lowland tropical maize using molecular markers. *Theoretical and Applied Genetics,* 99: 1106-1119.

Jones, R., S. Westra, and A. Sharma. 2010. Observed relationships between extreme sub-daily precipitations, surface temperature, and relative humidity, Geophysical Research Letters, 37, doi: 10.1029/2010GL045081.

Jones C, Giorgi F, and Asrar G. 2011. The Coordinated Regional Downscaling Experiment: CORDEX An international downscaling link to CMIP5. CLIVAR Exchanges 16: 34–40.

Kassa Girmay. 2003. GIS based analysis of land use and land cover, land degradation and population changes: A study of BoruMetero area of south Wello, Amhara Region. Unpublished Master's thesis, Addis Ababa University, Ehtopia.

Kassam, A., and Smith, M. 2011. FAO Methodologies on Crop Water Use and Crop Water Productivity. Water, 18, 1–18.

Kassie B., Rötter, R.P., Hengsdijk, H., Asseng, S., Van Ittersum, M. K., Kahiluoto, and Van Keulen, H. 2013. Climate variability and change in the Central Rift Valley of Ethiopia *Journal of Agricultural Science*, Page 1 of 17. © Cambridge University .doi:10.1017/S00218.

Kiersch, B. 2001. Land use impacts on water resources: A literature review. Land-water linkages in rural watersheds, Electronic Workshop (Discussion Paper 1). FAO, Rome, Italy.

Kim, U. and J. J. Kaluarachchi. 2009. Climate change impacts on water resources in the upper Blue Nile river basin, Ethiopia. J. America. Wat. Res. Assoc., 45, 6, 1361-1378.

Kleinn J., Frei, C., Gurtz, J., Luthi, D., Vidale, P., and Schar. C. 2005. Hydrologic simulations in the Rhine basin driven by a regional climate model

Lambin, E. F., Geist H. J., and Lepers E. 2006. Dynamics of land use and land cover change in tropical regions. Annual Review of Environment and Resources 28: pp. 205–241.

Laprise, R. 2008. Regional climate modeling. Journal of Computational Physics, 227(7), 3641-3666. doi:10.1016/j.jcp.2006.10.024.

Leander R, and Buishand T. 2007. Resembling of regional climate model output for the simulation of Extreme River flows. J Hydro, 332: 487-496.

Legesse Degife, Vallet-Coulomb, C. and Gasse, F. 2003. Hydrological response of a catchment to climate and land use changes in tropical Africa: case study South Central Ethiopia. Journal of Hydrology 275(1–2): pp. 67–85.

Leggett J., Pepper W.J., and Swart R.J. 1992. Emissions Scenarios for IPCC: an update. In Climate Change 1992. The Supplementary Report to the IPCC Scientific Assessment [Houghton, J.T., B.A. Callander & S.K. Varney, (eds)]. Cambridge University Press, Cambridge, UK. 69-95.

Matamoros, D., Guzman, E., Bonni, J. and varolleghem, P.A. 2005. AGNPS and SWAT Model calibration for hydrological Modeling of an Ecuadorian River Basin under Data scarcity, IWA publishing, London, UK, ISBN: 184339510X.

Meehl G, Tebaldi C, Walton G, Easter ling D, and McDaniel L. 2009. Relative increase of record high maximum temperatures compared to record low minimum temperatures in the US. Geophys Res Lett 36:L23701.doi:10.1029/2009GL040736.

Mekonnnen K and Tadele K. 2012. Analyzing the impact of land use and climate changes on soil erosion and stream flow in the Upper Gilgel Abbay Catchment, Ethiopia Ohrid, Republic of Macedonia, pp 1–13.

Ménard R. 2010. Bias Estimation, in: Data Assimilation, edited by: Lahoz, W., Khattatov, B., and Menard, R., 113–135, Springer Berlin Heidelberg, available at: http://dx.doi.org/10.1007/978-3-540-74703-1.

Mengistu K. T. 2009. Watershed Hydrological Response to Changes in Land Use and Land Cover, and Management Practice at Hare Watershed, Ethiopia. PhD thesis, Universität Siegen, Germany.

Mersha Eshete. 2003. Agro-climatic belts of Ethiopia. Potentials and constraints, In: M. Engida (Ed). Proceedings National Sensitization Workshop on Agro-meteorology and GIS, Ethiopian Agricultural Research Organization (EARO) p32-48.

Middelkoop H., Daamen, K., Gellens, D., Grabs, W., Kwadijk, J., Lang, H., Parmet, B., Sch¨adler, B., Schulla, J., and Wilke, K. 2001. Impact of climate change on hydrological regimes and water resources management in the Rhine basin, Clim. Change, 49, 105-128.

Mideksa Torben. 2010. Economic and distributional impacts of climate change: The case of Ethiopia. Global Environmental Change 20, 278-286.

Moriasi, D. N, J. G. Arnold, M. W. Van Liew, R. L. Bingner, R. D. Harem and T. L. Veith. 2007. Model evaluation guidelines for systematic quantification of accuracy in watershed simulations. *Transactions of the ASABE* 50(3): 850-900.

Mosello, B., Calow, R., Tucker, J., Alamirew, T., Kebede, S., Alemseged, T. and Gudina, A. 2015. Building adaptive water resources management in Ethiopia, (May 2015).

Moss, R. H. 2010. The next generation of scenarios for climate change research and assessment. Nature, 463, 747–756.

MoWIE. 2013. Initial National Communication of Ethiopia to the United Nations Frame work convention on Climate Change (UNFCCC). Addis Ababa, Ethiopia 127p.

Mutenyo.I, Nejadhashemi, A.p., woznicki, A. and Giri, S. 2013. Evaluation of SWAT performance on mountainous watershed in tropical Africa, Hydrol Current Res14:001,doi:10.4172 /2157.S14.001.

Nakicenovic, N. and Swart R. 2000. IPCC Special Report on Emissions Scenarios, 599 pp., Cambridge Univ. Press, New York.

Neitsch, S.L., Arnold, J.G., Kiniry, J.R., and Williams, J.R. 2005. Soil and Water Assessment Tool, Theoretical Documentation: Version 2005. Temple, TX. USDA Agricultural Research Service and Texas A & M Black land Research Centre.

Neitsch, S. L., J. G. Arnold, J. R. Kiniry and J. R. Williams. 2009. Soil and Water Assessment Tool theoretical documentation version 2009.

Nikulin G, Jones C, Giorgi F, Asrar G, Büchner M, Cerezo-Mota R, Christensen OB, Déqué M, Fernandez J, Hänsler A, van Meijgaard E, Samuelsson P, Sylla MB, and Sushama L. 2012. Precipitation climatology in an ensemble of CORDEX-Africa regional climate simulations. J.Clim. 25: 6057–6078, DOI: 10.1175/JCLI-D-11-00375.1.

National Metrological Agency (NMA). 2012. Climate Change National Adaptation Programme of Ethiopia (NAPA). Addis Ababa, Ethiopia 96p.

NRC (National Research Council). 2010. Advancing the Science of Climate Change: National Research Council. The National Academy Press, Washington, DC, USA.

OmotoshoJ.Bayo, Balogun, A.A and Ogunjobi, K.O. 2000. Predicting monthly and seasonal rainfall, onset and cessation of the raining season in West Africa using only surface data. International journal of climatology 20:865-880.

Pontius, R.G., Jr.; and Malanson, J. 2005. Comparison of the structure and accuracy of two land change models. *Int. J. George. Inf. Sci.* 2005, *19*, 243–265.

Price, R. K. 2001. Mathematical modeling reference book. Unpublished reference book for MSc students. UNESCO-IHE, the Netherlands.

Rao, V. U. M., Rao, A. V. M. S., Rao, G.G.S. N., and Satyanarayana.T. 2011. Impact of Climate Change on Crop Water Requirements and Adaptation Strategies, 311–319. https: //doi.org /10.1007/978-3-642-19360-6

Ravazzani, G., Corbari, C., Morella, and Mancini.M. 2012. Modified Hargreaves Samani equation for the assessment of reference evapotranspiration in alpine river basins. *J. Irrigation and Drainage. Engineering, 138*(7), 592-599.http://dx.doi.org/10.1061/(ASCE)IR.1943-4774. 0000 453

Refsgaard, J. C., and Storm, B. 1996. MIKESHE. In Computer Models in Watershed Hydrology, 809-846. [(ed.) Singh, V. J.], Highland Ranch, Colo.: Water Resources Publications.

Riahi.K, Gruebler.A, and Nakicenovic.N. 2007. Scenarios of long-term socio-economic and environmental development under climate stabilization. In: Technological Forecasting and Social Change 74, 7, 887-935.

Richard H and McCuen. 1989. Hydrologic analyses and Design Englewood Cliffs. New Jersey.

Ridolfi L, D'Odoricoc P, Porporato A, and Rodriguez II. 2003. Stochastic soil moisture dynamics along a hill slope. J Hydrol 272:264–275.

Rizwan Nawaz, Timothy Beller by, Mohamed Sayed and Mohamed Elshamy. 2010. Blue Nile Runoff Sensitivity to Climate Change. *Open Hydrology Journal*, 2010, 4, 137-151.

Rowell. D.P. 2012. Sources of uncertainty in future changes in local precipitation. Clim Dyn 39:29-50.

Sahilu Geremew and Nigussie Agizew. 2015. Climate Modeling of the Impact of Climate Change on Sugarcane and Cotton for Project on 'a Climate Resilient Production of Cotton and Sugar in Ethiopia' Climate Change and Modeling. EDRI Research Report 21. Addis Ababa: Ethiopian Development Research Institute.

Sahlemedin Sertsu and Taye Bekele. 2000. Procedures for Soil and Plant Analysis; National Soil Research Center Ethiopian Agricultural Research Organization, Technical Addis Ababa, Ethiopia. P. 74.

Saleh, A., Arnold, J. G., Gassman, P. W., Hauck, L. M., Rosenthal, W. D., Williams, J. R. and McFarland. A.M. S. 2000. Application of SWAT for the Upper North Bosque River Watershed. Transactions of the American Society of Agricultural and Biological Engineers 43(5): pp. 1077–1087.

Samani, Z. A., and M. Pessarakli. 1986. Estimating Potential Crop Evapotranspiration with Minimum Data in Arizona. Transactions of the ASAE, 29 (2): 522-524.

Santer, B.D. 2011. Separating signal and noise in atmospheric temperature changes: the importance of timescale. J Geophys Res 116:D22105. doi: 10.1029/2011JD016263.

Santhi, C., Arnold, J.G., Williams, J.R., Dugas, W.A., Srinivasan, R., and Hauck, L.M. 2001. Validation of the SWAT Model on a Large River Basin with Point and Non point Sources, Journal of the American Water Resources Association, Vol. 37, No. 5, 1169-1188pp.

Shabalova M. V., van Deursen, W. P., and Buishand T. A. 2003. Assessing future discharge of the river Rhine using regional climate model integrations and a hydrological model, Clim. Res., 23, 233–246, doi: 10.3354/cr023233.

Sharma B, R. 2006. Crop water requirements and water productivity: concepts and practices. Groundwater governance in Asia. http://www.waterand food.org/gga/Lecture 20% Material/ B.R. Sharma_CWR & WP.pdf.

Shimelis Berhanu, Tena Alamirew, T., Merkel, B. J., and Assefa Mokennin Melesse. 2016. Land Use and Land Cover Change Impact on Groundwater Recharge: The Case of Lake Haramaya Watershed , Ethiopia. https://doi.org/10.1007/978-3-319-18787-7.

Shimelis Gebriye, Ragahavan S and Bijan D. 2008. Stream flow Calibration and Validation of SWAT2005/Arc SWAT in Anjeni Gauged Watershed, Northern Highlands of Ethiopia. In the proceedings of the 4th International SWAT Conference, July 02-06, UNESCO-IHE, Delft, The Netherlands. On press.

Smith M, Kivumbi D and Heng L.K. 2006. Use of the FAO CROPWAT model in deficit irrigation studies. Water Report No. 22, FAO (Food and Agriculture Organization), Rome, Italy.

Spruill. C.A. and S. R. Workman. 2000. Simulation of daily and monthly stream discharge from small watersheds using the SWAT model. *Transactions of the ASAE* 43(6): 1431-1439.

Stern, R., Knock, J., Rijks, D. and Dale, I. 2003. INSTAT Climatic Guide. Pp 398. http://www.reading.ac.uk/ssc/software/instat/climatic.pdf.

Subramanya, K. 2008. Engineering Hydrology 3rd edition, Tata McGraw Hill, New Delhi, India, 155-162.

S.Jemery. 2007. Regional climate modeling for the developing world. American Meteorological Society DOI: 10.1175/BAMS-88-9-1395.

Tarekegn. D and Tadege. A. 2006. Assessing the impact of climate change on water resource of Lake Tana sub-basin using WAtBAL model. American Water Resource. Assoc. 39(2): 413-426.

Tekleab S., Y. Mohamed, and S. Uhlen Brook. 2013. Hydro-climatic trends in the Abay /Upper Blue Nile basin, Ethiopia, Physics and Chemistry of the Earth, 61-62, 32-42.

Terink W. 2010. Evaluation of a bias correction method applied to downscaled precipitation and temperature reanalysis data for the Rhine basin: Hydrology and Quantitative Water Management Group, Wageningen University, Wageningen, The Netherlands now at: Bristol Glaciology Centre, School of Geographical Sciences, University of Bristol, Bristol, UK.

Teshome Seyoum and Koch, M. 2013. SWAT – Hydrologic Modeling & Simulation of Inflow to Cascade Reservoirs of the Semi-Unguaged Omo-Gibe River Basin, Ethiopia, 6th International Conference on Water Resources and Environment Research proceedings, pp 439-461.

Tiruneh, Y., Berhanu, B., Ayalew, S., Tamrat, I., and Tesfaye, Y. 2013. Synthesis report: Awash River Basin Water Audit**.**

Trenberth K.E. 2011. Changes in precipitation with climate change. Clim Res 47:123–138. doi: 10.3354/cr00953.

Trenberth. K.E and Fasullo. J.T. 2012. Climate extremes and climate change: the Russian heat wave and other climate extremes of 2010. J Climate, submitted.

Thornton. P.K, Jones, P.G., Alagarswamy, G. and Andresen. J. 2009. Spatial variation of crop yield response to climate change in East Africa. *Global Environmental Change,* 19: 54-65.

Thornton, P.K., Jones, P.G., Owiyo, T., Kruska, R., Herrero, M., Kristjanson, P., Notenbaert, A., Bekele, N. and Omolo, A. 2006. Mapping climate vulnerability and poverty in Africa. International Livestock Research Institute, Nairobi, Kenya.

UNFCCC (United Nations Framework Convention on Climate Change). 2007. Climate Change Impact, Vulnerabilities and Adaptation in Developing Countries. UNFCCC Secretariat, Martin Luther-King-Straat 8 53175 Bonn, Germany.

USDA-SCS. 1985. National Engineering Handbook, Section 4-Hydrology. USDA-SCS, Washg. DC.

Van Griensven, A., A. Francos and W. Bauwens. 2005. Sensitivity analysis and auto calibration of an integral dynamic model for river water quality. *Water Sci. Technol*. 45: 325- 332.

Van Vuuren D.P., Edmonds J., Thomson A., Riahi K., Kainuma M., Matsui T., Hurtt G.C., Lamarque J-F., Meinshausen M., and Smith S. 2011. Representative concentration pathways: an overview. In: Climatic Change, 109, 5-31.

Van Wambeke, A., 2011. Properties and management of soils of the tropics. FAO Land and Water Digital Media Series No. 56, FAO, Rome.

Vera C, Barange M, Dube O.P, Goddard L, Griggs D, Kobysheva N, Odada E, Parey S, Polovina J, Poveda G, Seguin B, and Trenberth K. 2009. Needs assessment for climate information on decadal timescales and longer. Procedia Environ Sci 1(1):275–286

Verburg P.H, Veldkamp T, and Bouma J. 1999. Land use change under conditions of high population pressure: the case of Java. Glob Environ Change 9(4):303–312.

Verburg P.H, Soepboer W, Veldkamp A, Limpiada R, Espaldon V, and Mastura S. 2002. Modeling the spatial dynamics of regional land use: the CLUE-S model. Environ Manage 30(3):391–405.

Verburg, P.H.; Eickhout, B.; and Meijl, H.V. 2008. A multi-scale, multi-model approach for analyzing the future dynamics of European land use. *Ann. Regional. Sci.* 2008, *42*, 57–77.

WARC (Werer Agricultural Research Center). 2016. Annual research report, Werer, Ethiopia.

Wendroth O, Pohla W, Koszinski S, Rogasik H, Ritsema CJ, and Nielsen DR. 1999. Spatial-temporal patterns and covariance structures of soil water status in two northeast-German field sites. J Hydrol 215:38–58.

White, K. and Chaubey I. 2005. Sensitivity analysis, calibration, and validations for a multisite and multivariable SWAT model. *J. Am. Water Resources. Assoc.* 41(5):1077-1089.

Williams, J. R. 1995. The EPIC model. P. 909-1000. In V. P. Singh (ed). Computer models of watershed hydrology. *Water resources Publications*, Highlands Ranch, CO.

Winchell. M, Willis, C.M. and Griggs, G.B. 2009. Arc SWAT 2.3.4 Interface for SWAT 2005. User's Guide. Texas Agricultural Experiment Station.

World Bank. 2015. Regional dashboard: poverty and equity, Sub-Saharan Africa. http://poverty data.world bank.org/poverty/region/SSA.

Wood, A.W. 2004. Hydrologic implications of dynamical and statistical approaches to downscaling climate outputs. Clim Change 62(1–3):189–216.

You, G. J.Y and Ringler, C. 2010. Climate Change Impacts in Ethiopia Hydro-Economic Modeling Projections. IFPRI research Brief 15-19.

Zheng X, Zhao L, Xiang W, Li N, Lv L, and Yang X. 2012. A coupled model for simulating spatio-temporal dynamics of land-use change: a case study in Changing, Jinan, China. Landscape Urban Plann 106:51-61.

Zeleke Gete and Hurni, H. 2001. Implications of Land Use and Land Cover Dynamics for Mountain Resource Degradation in the Northwestern Ethiopian Highlands. Mountain Research and Development 21: pp. 184-191.

7. APPENDICES

7.1. Appendix Tables

Appendix I. Soil in SWAT data base for each soil layer in the subbasin

Appendix Table 1. Soil parameter in SWAT database for each soil layer in Kesem sub basin

Soil Name	Soil Type					
	ECMB	VCMB	LLEPT	CHLUV	EULEP	EUVET
Soil hydraulic group	B	C	D	D	C	B
Maximum rooting depth(mm)	1700.00	1651.00	1524.00	2300.00	2000.00	2000.00
Texture	LS-LS-LS-LS-LS	C-C-C-C	SICL-C-C	C-C-C-C	C-C	L-C-C
No. Layers	5.00	7.00	1.00	6.00	2.00	3.00
Depth(mm)	200.00	152.40	203.20	180.00	200.00	260.00
Bulky density moist(g/cm^3)	1.10	1.40	1.17	1.10	1.10	1.17
SOL_AWC(mm/mm)	0.15	0.18	0.21	0.11	0.11	0.12
SOL_CBN (weight %)	2.00	2.33	3.49	1.47	2.00	1.15
SOL_K (mm/hr)	25.00	0.90	1.50	4.34	25.00	1.29
Clay (weight %)	50.00	58.50	38.50	60.60	50.00	72.2
Silt (weight %)	34.00	25.65	54.15	23.30	34.00	20.2
Sand (weight %)	17.00	15.85	7.35	16.10	17.00	7.1
Rock Fragments (weight %)	5.00	0.00	0.00	0.00	5.00	40.0
Soil Albedo(fraction)	0.13	0.01	0.01	0.09	0.13	0.13
USLE_K	0.22	0.49	0.49	0.20	0.22	0.2
SOL_EC (ds/m)	0.00	0.00	0.00	0.00	0.13	0.09

where

VCMB - Vertic Cambislos
LLEPT - Lithic Leptosols
EULEP - Eutric Leptosols
SOL_AWC - Available water content in the soil
USLE_K - Universal Soil loss equation soil factor
EUVET - Eutric Vertisols
CHLUV – Chromic luvisols
LC – Clay loam
SL - Loamy Sand soil
SICL - Silty clay loam soil

Appendix II. Weather generator statistic and probability values

Appendix Table 2. Statistical values for Shola gebeya station (1984-1998)

Description	Jan	Feb	Mar	Apr	May	Jun	Jul	Aug	Sep	Oct	Nov	Dec
TMPMX	20.30	21.26	22.56	22.37	23.03	22.42	18.88	19.37	21.27	21.08	20.70	20.10
TMPMN	4.40	6.21	6.81	7.57	7.59	10.92	11.14	10.30	7.62	3.71	2.50	2.79
TMPSTDX	1.76	1.97	1.86	2.06	2.13	2.62	2.76	2.26	1.64	1.29	1.21	1.36
TMPSTDMN	3.44	3.54	2.89	2.35	2.37	1.34	0.83	1.02	2.13	2.75	2.38	2.70
PCP_MM	15.57	22.00	47.05	79.42	38.66	91.76	253.14	216.08	56.40	9.19	1.74	1.62
PCPSTD	1.70	2.26	4.11	5.87	4.14	6.16	7.58	6.73	3.72	2.34	0.46	0.23
PCPSKW	6.01	4.36	3.75	3.48	4.51	3.32	1.41	1.67	3.42	16.68	16.39	9.21
PR_W1	0.14	0.17	0.14	0.21	0.13	0.28	0.75	0.68	0.29	0.09	0.06	0.12
PR_W2	0.77	0.73	0.77	0.75	0.64	0.82	0.97	0.94	0.76	0.55	0.50	0.59
PCPD	10.80	11.53	11.73	13.87	8.33	17.00	29.67	28.53	17.40	5.67	3.73	6.40
RAINHHMX	0.00	0.00	0.00	0.00	0.00	0.00	0.00	0.00	0.00	0.00	0.00	0.00
SOLARAV	23.32	24.38	25.98	25.51	26.34	22.24	15.88	18.78	23.70	25.49	25.11	24.06
DEWPT	0.63	0.61	0.61	0.65	0.57	0.59	0.78	0.80	0.69	0.62	0.59	0.61
WNDAV	2.57	2.61	2.69	2.57	2.75	2.63	2.26	2.18	2.41	2.60	2.58	2.57

Appendix Table 3. Statistical values for Aleltu Agriculture station (1984-1998)

Description	Jan	Feb	Mar	Apr	May	Jun	Jul	Aug	Sep	Oct	Nov	Dec
TMPMX	20.30	21.26	22.56	22.37	23.03	22.42	18.88	19.37	21.27	21.08	20.70	20.07

TMPMN	4.16	5.68	6.27	7.04	6.97	10.16	10.03	9.76	6.99	3.45	2.35	2.70
TMPSTDX	1.76	1.97	1.86	2.06	2.13	2.63	2.76	2.26	1.64	1.29	1.21	1.38
TMPSTDMN	5.28	3.75	3.34	2.86	3.28	3.71	3.26	4.50	3.03	2.79	2.37	2.76
PCP_MM	16.13	25.27	56.53	83.00	53.93	98.00	293.47	278.07	120.20	32.40	12.73	8.00
PCPSTD	2.87	2.99	6.35	6.80	6.03	7.83	10.37	11.02	7.28	3.70	2.16	1.39
PCPSKW	7.37	4.28	5.69	3.92	6.33	4.78	1.65	2.14	3.03	6.40	5.83	7.35
PR_W1	0.03	0.09	0.14	0.19	0.16	0.21	0.65	0.65	0.29	0.09	0.03	0.04
PR_W2	0.44	0.50	0.43	0.53	0.33	0.64	0.81	0.75	0.58	0.50	0.41	0.35
PCPD	1.80	4.27	5.80	9.20	5.80	10.53	23.73	22.33	13.20	4.93	1.47	1.73
RAINHHMX	0.00	0.00	0.00	0.00	0.00	0.00	0.00	0.00	0.00	0.00	0.00	0.00
SOLARAV	24.91	27.09	28.83	28.73	28.69	27.02	23.86	26.05	28.06	27.74	25.89	24.80
DEWPT	0.55	0.52	0.52	0.56	0.50	0.49	0.61	0.63	0.59	0.54	0.51	0.53
WNDAV	2.22	2.20	2.30	2.31	2.49	2.58	2.45	2.24	2.23	2.34	2.28	2.27

Appendix Table 4. Statistical values for Shola gebeya station (1999-2013)

Description	Jan	Feb	Mar	Apr	May	Jun	Jul	Aug	Sep	Oct	Nov	Dec
TMPMX	21.09	22.73	23.02	22.83	23.99	23.96	20.34	20.05	21.70	21.56	20.90	20.43
TMPMN	4.51	5.15	6.77	8.26	8.80	11.17	11.49	10.68	7.86	4.52	3.58	3.33
TMPSTDX	1.69	1.74	2.18	2.47	2.49	2.57	3.16	2.94	2.35	1.85	1.80	1.57
TMPSTDMN	3.23	3.08	3.21	2.47	2.34	1.41	0.98	1.42	1.97	2.11	2.40	2.96
PCP_MM	12.57	12.09	59.85	103.56	50.10	63.33	293.96	307.69	81.31	14.38	11.84	6.58

PCPSTD	1.65	1.91	5.78	6.75	5.39	5.62	11.98	11.25	5.21	3.14	2.80	1.17
PCPSKW	5.53	6.00	4.70	2.65	4.90	4.22	2.31	2.00	3.10	11.25	11.95	9.31
PR_W1	0.15	0.08	0.15	0.16	0.12	0.21	0.54	0.50	0.23	0.10	0.09	0.12
PR_W2	0.69	0.71	0.76	0.83	0.72	0.78	0.94	0.94	0.77	0.52	0.59	0.59
PCPD	9.87	6.00	11.80	14.60	9.73	13.80	27.40	27.93	15.67	5.93	5.27	6.87
RAINHHMX	0.00	0.00	0.00	0.00	0.00	0.00	0.00	0.00	0.00	0.00	0.00	0.00
SOLARAV	23.64	26.76	25.93	25.24	25.61	23.32	17.66	18.67	23.41	25.52	24.57	23.51
DEWPT	0.59	0.51	0.54	0.60	0.52	0.53	0.74	0.79	0.69	0.59	0.58	0.60
WNDAV	2.49	2.70	2.63	2.54	2.63	2.63	2.23	2.09	2.30	2.62	2.63	2.51

Appendix Table 5. Statistical values for Aleltu Agriculture station (1999-2013)

Description	Jan	Feb	Mar	Apr	May	Jun	Jul	Aug	Sep	Oct	Nov	Dec
TMPMX	21.02	22.52	23.17	23.28	24.38	24.34	21.01	20.57	22.28	21.68	21.09	20.51
TMPMN	4.21	5.50	6.74	7.67	8.24	10.90	10.93	10.10	7.35	4.05	3.18	3.03
TMPSTDX	1.76	1.91	1.94	2.07	1.98	1.97	2.66	2.48	1.55	1.79	1.52	1.51
TMPSTDMN	3.53	3.38	3.48	4.29	3.46	4.35	2.69	5.09	2.85	2.40	2.42	3.02
PCP_MM	39.33	30.20	84.73	85.07	70.13	102.53	278.53	285.27	102.53	32.60	19.07	16.80
PCPSTD	3.69	3.13	6.46	6.23	4.82	5.77	10.35	11.08	6.08	3.17	2.19	2.27
PCPSKW	3.79	4.29	3.68	3.72	2.93	2.50	1.91	2.23	2.18	4.48	3.82	5.33
PR_W1	0.07	0.11	0.21	0.22	0.15	0.27	0.64	0.68	0.26	0.10	0.06	0.06
PR_W2	0.65	0.49	0.53	0.56	0.64	0.73	0.80	0.81	0.58	0.52	0.52	0.45
PCPD	5.33	5.00	9.67	9.80	9.60	14.07	23.47	24.33	12.13	5.53	3.07	2.67
RAINHHMX	0.00	0.00	0.00	0.00	0.00	0.00	0.00	0.00	0.00	0.00	0.00	0.00

SOLARAV	23.56	25.84	26.18	26.35	26.33	24.24	18.74	19.79	24.28	25.30	25.09	23.66
DEWPT	0.60	0.55	0.56	0.59	0.51	0.51	0.71	0.77	0.67	0.60	0.58	0.60
WNDAV	2.61	2.76	2.75	2.72	2.79	2.82	2.36	2.26	2.49	2.68	2.74	2.62

where:-

TMPMX: Average or mean daily maximum air temperature for month (ºC).

TMPMN: Average or mean daily minimum air temperature for month (ºC).

TMPSTDMX: Standard deviation for daily maximum air temperature in month (ºC).

TMPSTDMN: Standard deviation for daily minimum air temperature in month (ºC).

PCP_MM: Average or mean total monthly precipitation (mm H2O).

PCPSTD: Standard deviation for daily precipitation in month (mm H2O/day).

PCPSKW: Skew coefficient for daily precipitation in month.

PR_W1: Probability of a wet day following a dry day in the month.

PR_W2: Probability of a wet day following a wet day in the month.

PCPD: Average number of days of precipitation in month.

RAINHHMX: Maximum 0.5 hour rainfall in entire period of record for month (mm H2O).

DEWPT; Average daily dew point temperature in month (ºC)

Appendix III. Metrological and hydrological data tables

Appendix Table 6. Average monthly climate data of Aware melka station (1984-2013)

Parameters	Jan	Feb	Mar	Apr	May	Jun	Jul	Aug	Sep	Oct	Nov	Dec
Tmax(°c)	29.75	31.70	33.70	34.20	35.17	36.27	35.31	35.94	34.92	32.05	32.05	30.27
Tmin(°c)	12.58	13.99	15.79	17.44	18.63	20.33	20.05	19.52	18.69	15.27	12.92	11.88
Rainfall(mm)	35.51	14.27	89.51	67.63	32.34	25.00	127.27	118.48	47.80	30.01	18.94	10.06

Appendix Table 7. Average monthly climate data of Arerti station (1984-2013)

Parameters	Jan	Feb	Mar	Apr	May	Jun	Jul	Aug	Sep	Oct	Nov	Dec
Tmax(°c)	24.71	26.24	27.51	27.58	28.22	29.30	27.45	27.40	27.49	25.78	24.71	24.04
Tmin(°c)	7.37	8.41	9.15	10.35	11.54	14.11	14.11	13.01	9.93	6.94	6.18	6.27
Rainfall(mm)	17.37	11.41	39.15	43.35	15.54	24.11	114.11	86.01	29.30	16.94	15.18	24.27

Appendix Table 8. Average monthly stream flow data of Kesem sub basin (Aware melka) (1984-1998)

Parameters	Jan	Feb	Mar	Apr	May	Jun	Jul	Aug	Sep	Oct	Nov	Dec
Observed(m^3/sec)	2.06	2.82	2.48	3.04	3.27	4.36	30.68	65.50	27.35	6.34	2.90	2.17
Simulated(m^3/sec)	1.21	2.77	2.65	0.89	2.85	4.32	27.35	45.98	23.41	3.21	2.13	2.11

Appendix Table 9. Average monthly stream flow data of Kesem sub basin (Aware melka) (1999-2013)

Parameters	Jan	Feb	Mar	Apr	May	Jun	Jul	Aug	Sep	Oct	Nov	Dec
Observed(m^3/sec)	0.90	1.96	1.21	4.04	5.32	9.93	43.72	63.24	41.16	10.20	4.22	3.71
Simulated(m^3/sec)	0.00	1.25	0.00	3.65	3.22	6.95	30.15	48.97	43.25	7.34	2.35	3.59

Appendix Table 11. Average annual water balance simulated (mm) for a base periods of 1984-1998.

Months	PREC	SURQ	LATQ	GWQ	PER	SWC	ET	PET	WYLD
Jan	15.88	0.12	0.09	0.00	0.11	77.27	10.12	132.16	0.54
Feb	12.85	0.09	0.08	0.05	0.13	79.23	13.77	138.78	0.45
Mar	29.85	0.86	0.27	0.06	1.21	96.60	26.43	170.13	1.37
Apr	39.62	1.17	0.42	0.33	1.44	92.55	41.19	167.42	2.07
May	16.02	0.37	0.16	0.53	0.15	78.05	42.47	188.25	1.18
Jun	72.83	2.49	0.67	0.18	1.79	98.07	41.48	162.00	3.43

Jul	197.33	29.87	6.18	2.20	28.13	114.12	53.56	116.97	38.36
Aug	118.89	21.85	7.42	17.67	34.03	141.57	51.03	137.01	47.45
Sep	15.13	0.45	1.64	24.51	2.91	128.36	34.01	162.57	27.34
Oct	9.17	0.71	0.37	15.54	0.46	104.01	21.34	151.33	17.38
Nov	1.72	0.00	0.12	5.58	0.00	90.52	17.04	134.11	6.32
Dec	2.29	0.00	0.05	0.47	0.00	79.04	12.76	130.18	0.98
Belg	98.34	2.48	0.94	0.96	2.93	346.43	123.86	664.58	5.07
Kiremt	404.18	54.67	15.91	44.56	66.85	482.12	180.08	578.55	116.58
Bega	29.05	0.84	0.62	21.59	0.57	350.84	61.26	547.78	25.23
Annual	531.57	57.99	17.46	67.12	70.35	1179.39	365.21	1790.91	146.88

Appendix Table 12. Average annual water balance simulated (mm) for a base periods of 1999-2013.

Months	PREC	SURQ	LATQ	GWQ	PER	SWC	ET	PET	WYLD
Jan	18.99	3.20	0.26	2.13	2.01	66.50	8.15	81.12	6.20
Feb	16.71	2.47	0.22	1.59	2.38	65.28	9.89	87.42	4.73
Mar	54.20	11.36	0.31	2.06	4.83	66.31	20.38	127.81	14.07
Apr	83.72	18.28	0.66	4.23	14.04	61.70	34.74	115.69	23.56
May	48.27	11.92	0.57	7.98	8.69	64.61	41.92	131.48	20.90
Jun	62.04	10.79	0.45	7.16	6.01	80.79	44.99	136.04	18.76
Jul	225.63	89.01	12.56	9.40	35.79	127.93	52.67	108.26	100.13
Aug	215.80	101.27	13.23	22.97	57.52	123.40	47.00	103.90	127.11
Sep	74.43	25.33	4.56	34.74	31.11	100.91	40.19	107.58	62.82
Oct	18.29	5.03	0.84	31.25	6.42	67.42	31.14	112.47	38.37
Nov	14.45	2.94	0.52	17.11	2.47	72.10	22.52	92.58	21.68
Dec	8.10	1.32	0.36	7.30	1.53	61.62	16.76	80.61	9.93
Belg	202.90	44.03	1.76	15.86	29.94	257.90	106.93	462.40	63.26
Kiremt	577.91	226.39	30.80	74.26	130.43	433.04	184.85	455.78	308.82
Bega	59.83	12.49	1.99	57.79	12.43	267.63	78.58	366.78	76.18
Annual	840.64	282.92	34.54	147.91	172.80	958.56	370.36	1284.96	448.26

Appendix Table 13. Average annual water balance simulated (mm) for future periods of RCP4.5 (2014-2028)

Months	PREC	SURQ	LATQ	GWQ	PER	SW	ET	PET	WYLD
Jan	1.22	0.02	0.04	2.64	0.07	64.92	6.62	106.39	3.30
Feb	5.19	1.00	0.25	0.49	0.36	63.46	5.29	100.47	2.15
Mar	19.16	4.75	0.42	0.18	0.41	61.69	11.70	127.97	5.62

Apr	41.69	9.44	1.23	0.24	1.07	66.58	28.16	135.77	11.24
May	42.84	12.25	1.55	0.68	2.80	57.13	30.86	143.10	14.66
Jun	77.15	23.27	2.48	1.91	13.81	97.46	32.40	148.57	29.69
Jul	221.38	93.39	10.13	10.96	43.91	101.32	63.63	169.01	120.74
Aug	247.62	103.49	11.34	25.00	33.67	98.52	93.10	200.82	143.40
Sep	179.49	46.20	5.12	29.33	30.57	109.68	66.08	157.10	108.69
Oct	57.87	22.33	3.01	26.68	7.09	77.80	29.04	121.01	53.13
Nov	68.68	24.61	2.48	15.57	4.46	55.00	30.08	109.76	43.70
Dec	3.96	0.33	0.28	8.43	0.53	64.07	14.11	103.66	9.81
Belg	108.88	27.42	3.45	1.59	4.64	248.86	76.01	507.30	33.68
Kiremt	725.64	266.36	29.07	67.20	121.96	406.98	255.22	675.50	402.52
Bega	131.72	47.29	5.81	53.31	12.15	261.80	79.85	440.82	109.94
Annual	966.23	341.07	38.34	122.10	138.74	917.64	411.08	1623.62	546.14

Appendix Table 14. Average annual water balance simulated for future periods of RCP4.5 (2029-20243)

Months	PREC	SURQ	LATQ	GWQ	PER	SW	ET	PET	WYLD
Jan	4.21	1.00	0.09	1.58	0.26	67.41	5.15	105.11	3.30
Feb	7.71	1.45	0.24	0.17	0.41	62.75	5.63	100.96	2.31
Mar	50.05	14.04	1.73	0.46	3.97	65.88	22.74	135.68	16.57
Apr	71.18	23.35	3.13	2.04	7.85	62.57	36.51	138.95	28.81
May	38.71	10.05	1.49	3.53	3.29	61.27	31.45	144.30	15.41
Jun	78.16	25.03	2.48	3.25	13.54	84.56	31.42	151.95	32.85
Jul	228.27	98.29	10.13	11.95	39.11	110.13	62.52	172.15	126.97
Aug	249.15	104.53	11.34	26.15	41.04	111.20	95.72	205.53	146.07
Sep	172.07	56.67	5.12	30.05	36.03	104.53	59.85	154.80	109.79
Oct	59.50	23.75	3.26	27.06	9.82	71.89	28.33	125.83	55.28
Nov	21.30	7.56	0.89	16.02	3.94	56.15	17.29	109.54	25.50
Dec	4.69	0.54	0.13	7.63	0.77	60.74	9.58	105.37	9.13
Belg	167.66	48.89	6.59	6.20	15.53	252.47	96.33	519.90	63.09
Kiremt	727.66	284.50	29.07	71.40	129.71	410.42	249.50	684.43	415.69
Bega	89.71	32.84	4.37	52.30	14.79	256.20	60.35	445.84	93.20

Annual	985.02	366.23	40.03	129.90	160.03	919.09	406.18	1650.17	571.99

Appendix Table 15. Average annual water balance simulated for future periods of RCP8.5 (2014-2028)

Months	PREC	SURQ	LATQ	GWQ	PER	SWC	ET	PET	WYLD
Jan	6.60	2.32	0.21	2.33	0.35	62.31	6.73	95.14	5.93
Feb	18.58	5.05	0.77	0.58	1.64	57.18	10.07	94.28	6.91
Mar	23.25	8.01	0.83	0.97	1.43	74.39	13.72	108.34	10.15
Apr	131.46	53.25	5.14	1.77	11.99	58.09	35.56	116.33	60.60
May	66.92	26.31	3.11	5.30	8.02	63.95	37.93	125.83	35.03
Jun	95.59	31.87	3.48	7.00	13.12	95.60	42.27	130.54	44.28
Jul	236.60	106.91	10.13	15.81	35.68	116.32	71.67	142.39	137.80
Aug	242.81	102.41	11.34	28.76	44.82	121.40	66.40	121.17	149.92
Sep	179.53	61.54	5.12	34.85	34.26	90.17	60.81	124.77	120.55
Oct	60.04	22.57	3.03	30.08	6.87	73.11	29.59	107.55	57.71
Nov	30.21	9.30	1.31	17.35	2.28	63.74	24.88	101.24	29.96
Dec	7.02	1.38	0.26	9.37	0.41	59.61	11.86	87.32	11.59
Belg	240.22	92.62	9.85	8.62	23.09	253.61	97.28	444.78	112.70
kiremt	754.52	302.72	30.07	86.42	127.87	423.49	241.14	518.87	452.55
bega	103.86	35.57	4.81	59.13	9.92	258.77	73.06	391.25	105.20
Annual	1098.60	430.91	44.74	154.17	160.88	935.88	411.49	1354.91	670.46

Appendix Table 16. Average annual water balance simulated for future periods of RCP8.5 (2029-2043)

Months	PREC	SURQ	LATQ	GWQ	PER	SWC	ET	PET	WYLD
Jan	4.03	0.52	0.23	2.68	0.36	65.76	7.33	98.41	4.16
Feb	10.10	2.76	0.50	0.78	1.06	61.24	6.52	94.77	4.55
Mar	39.53	13.36	1.28	0.82	2.55	67.86	15.89	116.21	15.86
Apr	68.69	21.89	3.16	1.93	7.42	63.65	30.58	116.51	27.33
May	65.19	25.03	2.48	4.01	6.19	61.60	34.07	129.36	31.82
Jun	91.08	31.93	3.48	4.71	14.25	93.15	36.16	129.17	42.34
Jul	216.14	95.12	10.13	12.38	33.83	109.64	67.42	144.89	121.68
Aug	253.32	111.36	11.34	26.14	45.53	116.39	64.95	123.80	157.16
Sep	192.09	70.98	5.12	34.42	31.31	103.63	63.74	126.25	129.21
Oct	44.80	17.70	2.62	30.29	5.66	71.17	26.93	108.36	52.06

Nov	20.63	6.28	0.71	16.88	1.13	60.48	18.56	103.52	25.00
Dec	14.54	4.17	0.55	8.04	1.22	66.41	12.86	92.91	13.68
Belg	183.51	63.04	7.43	7.54	17.23	254.35	87.06	456.85	79.56
Kiremt	752.64	309.38	30.07	77.66	124.93	422.82	232.27	524.11	450.39
Bega	84.00	28.67	4.12	57.88	8.37	263.83	65.68	403.19	94.90
Annual	1020.16	401.09	41.61	143.08	150.52	941.00	385.01	1384.15	624.85

Appendix Table 17. Average monthly climate data of observed and future bias corrected of Aware melka station

Parameters	Jan	Feb	Mar	Apr	May	Jun	Jul	Aug	Sep	Oct	Nov	Dec
Tmax observed(1984-2013)	29.75	31.70	33.70	34.20	35.17	36.27	35.31	35.94	34.92	32.05	32.05	30.27
Tmax RCP4.5 (2014 - 2073)	31.44	33.14	35.04	35.81	37.10	37.10	36.67	37.65	36.38	33.00	33.15	31.50
Tmax RCP8.5 (2014 - 2073)	31.90	33.73	35.67	36.94	38.12	38.02	37.19	38.01	37.01	33.51	33.51	32.10
Tmin observed (1984-2013)	12.58	13.99	15.79	17.44	18.63	20.33	20.05	19.52	18.69	15.27	12.92	11.88
Tmin RCP4.5 (2014 - 2073)	14.07	15.42	16.53	18.93	20.09	21.52	21.18	20.69	19.91	16.45	14.25	13.17
Tmin RCP8.5 (2014 - 2073)	13.78	14.61	16.42	18.41	19.77	21.27	20.74	20.43	19.46	16.19	13.79	12.85
Prec observed(1984-2013)	35.51	14.27	89.51	67.63	32.34	25.00	127.27	118.48	47.80	30.01	18.94	10.06
Prec RCP4.5 (2014 - 2073)	74.30	29.95	82.35	62.05	35.09	35.04	132.69	124.67	46.62	32.68	21.35	4.26
Prec RCP8.5(2014 - 2073)	76.65	15.02	64.92	55.45	21.11	39.23	149.54	143.48	48.31	38.62	28.94	7.50

Appendix Table 18. Average monthly climate data of observed and future bias corrected of Shola gebeya station

Parameters	Jan	Feb	Mar	Apr	May	Jun	Jul	Aug	Sep	Oct	Nov	Dec
Tmax observed(1984-2013)	20.57	21.78	22.89	22.76	23.63	23.54	20.17	19.84	21.71	21.42	20.95	20.44
Tmax RCP4.5(2014 - 2073)	21.96	22.87	24.02	24.31	25.29	24.46	21.60	21.09	22.88	22.30	21.74	21.67
Tmax RCP8.5(2014 - 2073)	22.87	24.08	25.56	25.71	27.07	25.66	22.92	22.29	23.96	23.19	22.80	22.59
Tmin observed(1984-2013)	4.11	5.47	6.38	7.48	7.52	10.32	10.51	10.03	7.47	3.94	2.86	2.71
Tmin RCP4.5(2014 - 2073)	5.50	6.92	6.95	8.95	8.78	11.30	11.70	11.17	8.62	5.02	4.27	3.91

Tmin RCP8.5(2014 - 2073)	6.93	8.41	8.18	10.27	10.61	12.67	12.71	12.10	9.90	6.67	5.94	5.37
Prec observed(1984-2013)	27.60	27.97	63.90	88.70	59.63	63.93	302.97	288.93	3.78	27.47	16.67	12.03
Prec RCP4.5(2014 - 2073)	34.63	41.65	53.19	79.24	58.67	78.21	288.16	281.00	3.55	27.67	19.93	4.48
Prec RCP8.5(2014 - 2073)	49.86	25.03	37.57	70.61	39.12	83.82	284.88	282.34	3.61	30.83	26.56	5.04

Appendix Table 19. Average monthly climate data of observed and future bias corrected of Aleltu Agriculture station

Parameters	Jan	Feb	Mar	Apr	May	Jun	Jul	Aug	Sep	Oct	Nov	Dec
Tmax observed(1984-2013)	24.71	26.24	27.51	27.58	28.22	29.30	27.45	27.40	27.49	25.78	24.71	24.04
Tmax RCP4.5(2014 - 2073)	25.61	26.60	27.68	28.40	29.00	28.86	26.72	26.70	27.64	26.05	25.19	24.86
Tmax RCP8.5(2014 - 2073)	26.20	27.33	28.49	29.10	29.83	29.48	27.39	27.46	28.39	26.68	25.89	25.41
Tmin observed(1984-2013)	7.37	8.41	9.15	10.35	11.54	14.11	14.11	13.01	9.93	6.94	6.18	6.27
Tmin RCP4.5(2014 - 2073)	7.85	8.77	9.15	11.65	12.92	14.84	14.90	14.13	11.78	8.02	6.81	6.55
Tmin RCP8.5(2014 - 2073)	8.66	9.82	9.75	12.51	13.88	15.66	15.62	14.72	12.61	8.94	7.82	7.38
Prec observed(1984-2013)	17.78	21.37	53.02	93.84	189.93	95.30	297.68	260.46	60.52	11.18	7.23	5.82
Prec RCP4.5(2014 - 2073)	39.41	37.02	44.76	83.07	189.32	111.93	284.59	271.35	64.47	11.82	9.78	2.76

Prec RCP8.5(2014 - 2073)	40.65	18.58	35.28	74.24	173.99	125.31	320.72	312.28	66.80	13.97	13.26	4.86

Appendix Table 20. Average monthly climate data of observed and future bias corrected of Arerti station

Parameters	Jan	Feb	Mar	Apr	May	Jun	Jul	Aug	Sep	Oct	Nov	Dec
Tmax observed(1984-2013)	24.71	26.24	27.51	27.58	28.22	29.30	27.45	27.40	27.49	25.78	24.71	24.04
Tmax RCP4.5(2014 - 2073)	26.02	27.14	28.38	29.08	29.57	30.59	29.05	28.49	28.51	26.63	25.70	25.26
Tmax RCP8.5(2014 - 2073)	26.65	27.93	29.13	29.73	30.37	31.19	29.70	29.24	29.25	27.27	26.41	25.85
Tmin observed(1984-2013)	7.37	8.41	9.15	10.35	11.54	14.11	14.11	13.01	9.93	6.94	6.18	6.27
Tmin RCP4.5(2014 - 2073)	8.94	9.99	9.95	12.04	13.13	15.42	15.40	14.33	11.25	7.88	7.48	7.67
Tmin RCP8.5(2014 - 2073)	9.83	11.14	10.54	12.93	14.05	16.24	16.15	15.02	12.13	8.87	8.55	8.57
Prec observed(1984-2013)	17.37	11.41	39.15	43.35	15.54	24.11	114.11	86.01	29.30	16.94	15.18	24.27
Prec RCP4.5(2014 - 2073)	11.29	1.26	23.61	22.40	4.73	11.52	62.83	36.52	10.56	3.96	9.16	6.86
Prec RCP8.5(2014 - 2073)	2.95	1.02	22.77	26.53	8.75	12.09	75.91	58.91	15.54	7.57	12.93	7.28

Appendix IV. Soil physiochemical data tables

Appendix Table 21. Soil sample analysis of Kesem sub basin (Berehet woreda).

Sample code	Kesem sub basin (Berehet woreda) soil sample analysis during *kiremt* with respect to depth							
	0-30							
	Textural class				Fc	Pwp	P_d	Mc
	Clay	Silt	Sand	Class				
HA	11.80	81.00	7.20	Silt	31.50	6.33	1.52	16.74
HB	12.00	62.50	25.50	Silt loam	35.60	13.70	1.43	21.40
HC	11.85	81.02	7.03	Silt	29.80	6.38	1.55	18.74
HD	11.00	79.00	9.00	Silt	31.60	6.90	1.57	16.74
HE	10.00	82.00	8.00	Silt	30.00	6.34	1.52	16.81
MA	39.00	43.00	8.00	Silt clay	41.60	24.20	1.46	18.64
MB	45.00	46.00	9.00	Silt clay	40.60	27.80	1.45	11.84
MC	50.00	23.00	31.00	Clay	42.00	29.90	1.36	19.30
MD	51.00	22.00	27.00	Clay	41.60	30.10	1.35	23.60
ME	49.00	24.00	29.00	Clay	42.00	29.90	1.36	19.30
LA	46.00	45.00	9.00	Silt clay	41.60	27.80	1.45	12.78
LB	34.00	34.00	32.00	Clay loam	35.00	21.30	1.47	22.60
LC	46.00	45.00	9.00	Silt clay	40.60	27.90	1.45	12.78
LD	31.00	32.00	37.00	Clay loa	35.00	21.30	1.40	21.60
LE	50.00	23.00	27.00	Clay	42.20	28.90	1.36	19.30

Sample code	30-60							
	Textural class				F_c	Pwp	p_d	Mc
	Clay	Silt	Sand	Class				
HA	16.00	61.00	23.00	Silt loam	32.10	13.70	1.45	20.33
HB	16.00	59.00	23.00	Silt loam	29.10	15.70	1.44	21.25
HC	13.00	77.00	10.00	Silt	30.50	6.13	1.54	20.74
HD	16.00	61.00	23.00	Silt loam	32.60	14.70	1.42	20.33
HE	16.00	64.00	23.00	Silt loam	30.10	11.70	1.40	20.33
MA	11.00	79.00	9.00	Silt	30.70	6.43	1.40	20.74
MB	41.00	46.00	13.00	Silt clay	40.70	26.60	1.44	17.83
MC	31.00	32.00	37.00	Clay loam	35.00	21.30	1.42	21.60
MD	50.00	23.00	27.00	Clay	42.00	29.90	1.38	25.40
ME	33.00	33.00	35.00	Clay loam	36.20	20.90	1.43	20.30
LA	46.00	43.00	11.00	Silt clay	39.60	25.63	1.39	13.56
LB	36.00	34.00	30.00	Clay loam	36.00	20.10	1.50	24.10
LC	46.00	43.00	11.00	Silt clay	39.60	23.63	1.35	13.56
LD	33.00	33.00	35.00	Clay loam	36.20	20.90	1.42	20.30

LE	30.00	32.00	38.00	Clay loam	35.00	21.30	1.45	21.60

Sample code	60-90							
	Textural class				F_c	Pwp	p_d	Mc
	Clay	silt	Sand	Class				
HA	14.00	62.00	24.00	Silt loam	30.10	13.70	1.46	20.33
HB	15.00	60.00	23.00	Silt loam	30.10	15.70	1.45	21.25
HC	13.00	75.00	12.00	Silt	30.30	6.13	1.51	20.74
HD	13.00	64.00	23.00	Silt loam	31.60	14.70	1.45	20.33
HE	18.00	63.00	22.00	Silt loam	29.10	11.70	1.46	20.33
MA	13.00	78.00	10.00	Silt	30.45	6.43	1.42	20.74
MB	43.00	45.00	12.00	Silt clay	40.44	26.60	1.43	17.83
MC	32.00	31.00	37.00	Clay loam	35.00	21.30	1.42	21.60
MD	50.00	23.00	27.00	Clay	42.00	29.90	1.40	25.40
ME	32.00	33.00	36.00	Clay loam	36.20	20.90	1.43	20.30
LA	47.00	42.00	11.00	Silt clay	38.60	25.63	1.38	13.56
LB	36.00	33.00	31.00	Clay loam	36.00	20.10	1.50	24.10
LC	45.00	44.00	11.00	Silt clay	39.60	23.63	1.34	13.56
LD	33.00	34.00	34.00	Clay loam	36.20	20.90	1.42	20.30
LE	32.00	32.00	36.00	Clay loam	35.00	21.30	1.45	21.60

HA-HE = Higher class; MA-ME = Middle class HA-HE = Higher class; MA-ME = Middle class; LA-LE = Lower class

Appendix Table 22. Infiltration rate of Kesem sub basin (Berehet woreda).

Station		Higher class				Middle class				Lower class			
Time interval (min)	Cumulative Time (min)	Infiltration Depth (cm)	Cumulative Depth(cm)	Infiltration Rate (cm/min)	Infiltration Rate (mm/hr)	Infiltration Depth (cm)	Cumulative Depth(cm)	Infiltration Rate (cm/min)	Infiltration Rate (mm/hr)	Infiltration Depth(cm)	Cumulative Depth(cm)	Infiltration Rate (cm/min)	Infiltration Rate (mm/hr)
0	0	0	0	0.00	0	0	0		0	0	0	0.00	0
5	5	7	7	1.40	840	2.5	2.5	0.5	300	4.5	4.5	0.90	540
5	10	6.8	13.8	1.36	816	4	6.5	0.8	480	5	9.5	1.00	600
5	15	6.5	20.3	1.30	780	5	11.5	1	600	5.7	15.2	1.14	684
10	25	10.1	30.4	1.01	606	7	18.5	0.7	420	5.4	20.6	0.54	324
10	20	8.9	39.3	0.89	534	4	22.5	0.4	240	3.1	23.7	0.31	186
10	30	8.3	47.6	0.83	498	3	25.5	0.3	180	4.2	27.9	0.42	252
10	40	8	55.6	0.80	480	2	27.5	0.2	120	2.5	30.4	0.25	150
10	50	7.2	62.8	0.72	432	1.9	29.4	0.19	114	2.2	32.6	0.22	132
10	60	6.3	69.1	0.63	378	1.5	30.9	0.15	90	2	34.6	0.20	120
10	70	5	74.1	0.50	300	1.1	32	0.11	66	1.8	36.4	0.18	108
10	80	3.3	77.4	0.33	198	0.7	32.7	0.07	42	1.6	38	0.16	96
10	90	2.4	79.8	0.24	144	0.5	33.2	0.05	30	1.3	39.3	0.13	78
10	100	1.7	81.5	0.17	102	0.3	33.5	0.03	18	1.1	40.4	0.11	66
10	110	1.1	82.6	0.11	66	0.3	33.8	0.03	18	0.7	41.1	0.07	42
20	130	0.6	83.2	0.03	18	0.3	34.1	0.015	9	0.4	41.5	0.03	12
20	150	0.5	83.7	0.023	12	0.2	34.3	0.01	6	0.4	41.9	0.015	6
40	190	0.5	84.2	0.023	12	0.2	34.5	0.01	6	0.4	42.3	0.015	6

Appendix V. Metrological weather parameters and reference ET_O at Shola gebeya data tables

Appendix Table 23. The monthly and seasonal average weather parameters and reference ETo under baseline climate (1984-2013)

Month	Tmin (°C)	Tmax (°C)	RH (%)	Wind (m/s)	Sun (Hr)	Rad (MJ/m²/day)	ETo (mm/day)
Jan	4.60	20.80	60.00	2.60	9.50	21.40	3.95
Feb	5.90	22.10	57.00	2.70	10.30	24.00	4.60
Mar	6.80	22.90	58.00	2.70	10.50	25.50	4.93
Apr	7.90	22.60	61.00	2.60	10.30	25.30	4.87
May	8.50	23.60	52.00	2.80	10.30	24.80	5.18
Jun	11.30	22.90	61.00	2.60	8.70	21.90	4.55
Jul	11.20	19.30	79.00	2.20	6.50	18.80	3.39
Aug	10.30	20.00	77.00	2.20	8.30	22.00	3.84
Sep	7.20	21.50	66.00	2.50	9.60	24.10	4.45
Oct	3.80	21.30	59.00	2.70	10.30	24.10	4.53
Nov	3.00	20.70	59.00	2.60	9.80	22.10	4.09
Dec	3.20	20.30	60.00	2.50	9.40	20.80	3.81
Kiremt	10.00	20.93	70.75	2.38	8.28	21.70	4.06
Belg	7.28	22.80	57.00	2.70	10.35	24.90	4.90
Bega	3.65	20.78	59.50	2.60	9.75	22.10	4.10

Appendix Table 24: The monthly and seasonal average weather parameters and reference ET_O under future climate (2014-2043)

Month	Tmin (°C)		Tmax (°C)		RH (%)		Wind (m/s)		ETo (mm/day)	
	4.5	8.5	4.5	8.5	4.5	8.5	4.5	8.5	4.5	8.5
Jan	7.50	8.60	22.10	22.60	49.00	51.00	2.52	2.60	3.52	5.38
Feb	9.70	9.60	23.60	24.10	47.00	42.00	2.63	2.70	3.98	6.38
Mar	10.90	11.00	25.60	26.20	38.00	38.00	2.71	2.70	4.56	7.31
Apr	12.30	12.70	25.90	27.10	44.00	43.00	2.32	2.50	4.65	7.24
May	12.80	13.70	26.90	28.40	49.00	41.00	2.76	2.00	4.68	7.30
Jun	15.30	16.30	26.90	27.90	52.00	46.00	2.29	2.60	4.63	6.75
Jul	15.20	15.60	22.90	24.50	71.00	69.00	3.81	2.40	3.90	4.95
Aug	14.30	15.10	23.50	22.80	76.00	75.00	3.13	3.40	4.18	4.27
Sept	13.30	13.60	23.60	23.90	76.00	74.00	3.09	3.20	4.30	4.64
Oct	9.90	10.50	23.20	24.00	59.00	54.00	3.95	2.00	4.28	5.79
Nov	9.40	10.40	21.20	21.30	61.00	63.00	2.09	2.10	3.57	4.53
Dec	8.40	8.70	21.00	21.10	58.00	61.00	2.30	2.30	3.31	4.54
Kiremt	14.53	15.15	24.23	24.78	68.75	66.00	3.33	3.40	4.25	5.15
Belg	11.43	11.75	25.50	26.45	44.50	41.00	2.35	2.48	4.47	7.06
Bega	8.80	9.55	21.88	22.25	56.75	57.25	2.89	2.65	3.67	5.06

7.2. Appendix Figure

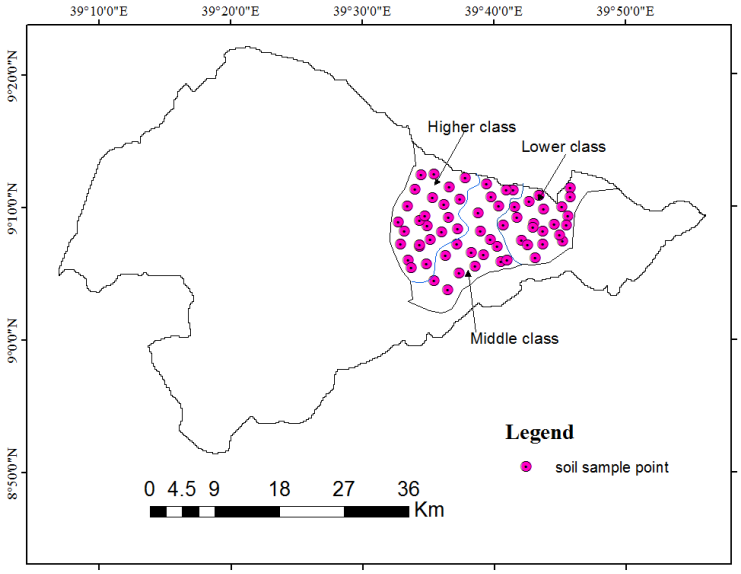

Appendix Figure 1. Soil sample location of Kesem sub basin (Berehet woreda)

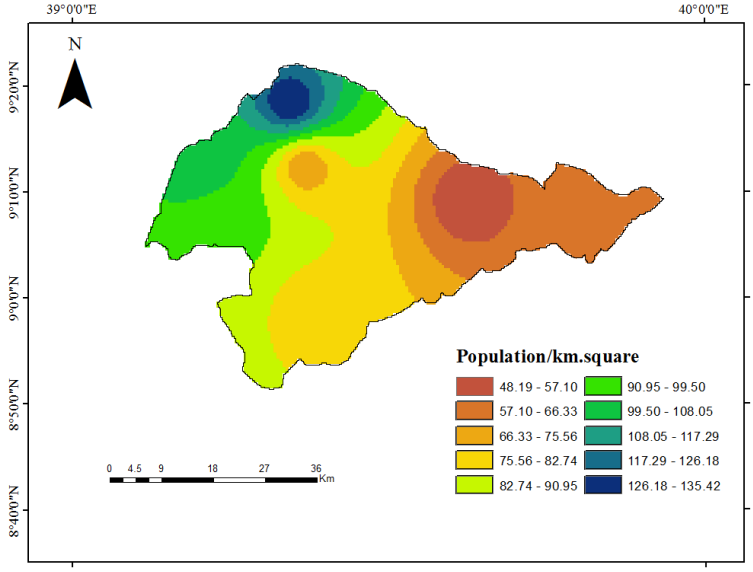

Appendix Figure 2. Population density of Kesem sub basin